ISTANBUL TECHNICAL UNIVERSITY ★ GRADUATE SCHOOL

BIOMEDICAL APPLICATION OF AN ENZYMATICALLY SYNTHESIZED BIOPOLYESTER

M.Sc. THESIS

ŞENOL BEYAZ

Department of Chemical Engineering

Chemical Engineering Programme

JUNE 2024

ISTANBUL TECHNICAL UNIVERSITY ★ GRADUATE SCHOOL

BIOMEDICAL APPLICATION OF AN ENZYMATICALLY SYNTHESIZED BIOPOLYESTER

M.Sc. THESIS

Şenol BEYAZ
(506211027)

Department of Chemical Engineering

Chemical Engineering Programme

Thesis Advisor: Prof. Dr. F. Yüksel GÜVENİLİR

JUNE 2024

İSTANBUL TEKNİK ÜNİVERSİTESİ ★ LİSANSÜSTÜ EĞİTİM ENSTİTÜSÜ

ENZİMATİK OLARAK SENTEZLENMİŞ BİR BİYOPOLİESTERİN BİYOMEDİKAL UYGULAMASI

YÜKSEK LİSANS TEZİ

Şenol BEYAZ
(506211027)

Kimya Mühendisliği Anabilim Dalı

Kimya Mühendisliği Programı

Tez Danışmanı: Prof. Dr. F. Yüksel GÜVENİLİR

HAZİRAN 2024

Şenol BEYAZ, a M.Sc. student of ITU Graduate School student ID 506211027, successfully defended the thesis/dissertation entitled "BIOMEDICAL APPLICATION OF AN ENZYMATICALLY SYNTHESIZED BIOPOLYESTER", which he prepared after fulfilling the requirements specified in the associated legislations, before the jury whose signatures are below.

Thesis Advisor :	**Prof. Dr. F. Yüksel GÜVENİLİR** Istanbul Technical University	.....
Jury Members :	**Prof. Dr. Didem SALOĞLU DERTLİ** Istanbul Technical University	.....
	Asst. Prof. Dr. Yasemin KAPTAN Beykent University	.....

Date of Submission : 20 May 2024
Date of Defense : 26 June 2024

To my beloved wife and precious family,

FOREWORD

I would like to express my gratitude and huge respect to my esteemed thesis advisor, Prof. Dr. Fatoş Yüksel GÜVENİLİR, who gave me both academic and life discipline with her mentorship, supported me in every times and kept my motivation and interest alive.

I would like to thank and appreciate Dr. Cansu ÜLKER TURAN, who helped me in every way possible with the problems I encountered, both laboratory experiments and methods of the thesis and during my studies. Her valuable comments and evaluations played a major role in determining the roadmap of this study.

Also, I would like to express my gratitude and appreciation to Dr. Yasemin KAPTAN for giving me every information that she already knew and for always helping my experiments with pleasure.

I will always be indebted to my dear wife İrem GÜVEN BEYAZ, who were always with me in the struggle with the problems I faced during my study and every moments in my life.

I am deeply thankful to my dear friend Mete DERVİŞCEMALOĞLU for his kind support.

Finally, I would like to thank my entire family, who encouraged me to continue my graduate education and supported me throughout my graduate studies.

This study was financially supported by the Istanbul Technical University Research Projects Coordination Department. Grant number : MYL-2022-44072.

May 2024

Şenol BEYAZ
(Chemical Engineer)

TABLE OF CONTENTS

Page

ABBREVIATIONS

^{1}H-NMR **:** Proton Nuclear Magnetic Resonance
3-APTES **:** (3-Aminopropyltriethoxysilane
3-APTMS **:** (3-Aminopropyl)trimethoxysilane
3-GPTMS **:** (3-Glycidyloxypropyl)trimethoxysilane
CALB **:** *Candida antarctica* Lipase B
DLS **:** Dynamic Light Scattering
DNA **:** Deoxyribonucleic acid
DSC **:** :Differential Scanning Calorimetry
DTG **:** Derivative of weight loss
FT-IR **:** Fourier Transform Infrared Spectroscopy
GPC **:** Gel Permeation Chromatography
Olu **:** Oleuropein
PBS **:** Phosphate Buffered Saline
PCL **:** Poly(ε-caprolactone)
PGA **:** Polyglycolic acid
PHB **:** Polybutylene terephthalate
PHBV **:** Poly(3-hydroxybutyrate-co-3-hydroxyvalerate)
PLA **:** Poly(lactic acid)
PLGA **:** Poly(lactic-co-glycolic acid)
PPL **:** Porcine pancreatic lipase
PVA **:** Polyvinyl alcohol
RHA **:** Rice Husk Ash
RNA **:** Ribonucleic acid
ROCOP **:** Ring Openning Copolymerization
ROP **:** Ring Openning Polymerization
ROS **:** Reactive Oxygen Species
SEM **:** Scanning Electron Microscope
TC **:** Trans-chalcone
TGA **:** Thermo Gravimetric Analysis
XRD **:** X-Ray diffraction analysis

δ-VL **:** δ-Valerolactone

ε-CL **:** ε-Caprolactone

ω-PDL **:** ω-Pentadecalactone

SYMBOLS

ΔH_m	**:** Melting Enthalpy
$I_{1.26}$	**:** Integral of Peak at 1.26 ppm in 1H-NMR Spectrum
$I_{1.64}$	**:** Integral of Peak at 1.64 ppm in 1H-NMR Spectrum
$I_{3.65}$	**:** Integral of Peak at 3.65 ppm in 1H-NMR Spectrum
$I_{4.06}$	**:** Integral of Peak at 4.06 ppm in 1H-NMR Spectrum
$I_{4.16}$	**:** Integral of Peak at 4.16 ppm in 1H-NMR Spectrum
K_H	**:** Higuchi Dissolution Constant
K_{KP}	**:** Korsmeyer-Peppas Release Rate Constant
m	**:** Number of δ-Valerolactone Units
M_n	**:** Number Average Molecular Weight
n	**:** Number of ω-Pentadecalactone Units
n	**:** Release Exponent
OD	**:** Optical density
R^2	**:** Coefficient of determination
Q_0	**:** Initial Concentration of Drug
Q_t	**:** Cumulative % Drug Release at Any Time
Q_t / Q_∞	**:** Fraction of Drug Released at Any Time
t	**:** Time
T_g	**:** Glass Transition Temperature
T_m	**:** Melting Temperature
v/v	**:** Volume to volume ratio
W_0	**:** Initial Weight
W_t	**:** Dry Weight at Any Time

LIST OF TABLES

Page

LIST OF FIGURES

Page

BIOMEDICAL APPLICATION OF AN ENZYMATICALLY SYNTHESIZED BIOPOLYESTER

SUMMARY

Polymers have played an integral role in advancing drug delivery technology by providing controlled release of therapeutic agents at fixed doses over long periods of time, cyclic dosing, and adjustable release of both hydrophilic and hydrophobic drugs. Modern advances in drug delivery are now based on the rational design of polymers designed to exert different biological functions. Enzyme-based biopolymer syntheses are needed in order to reduce the toxic accumulations caused by these drug systems in the human body, to minimize their side effects, and their effects on the environment. Unlike synthetic polymers, biopolymers produced naturally using enzymes; They are suitable for medical applications due to their biocompatibility, biodegradability, non-toxicity and ability to adsorb bioactive molecules. The use of these biopolymers in drug delivery systems is possible by turning them into materials such as cast films, microspheres, nanoparticles and nanofibers. Various proteins, drugs and proteins can be easily loaded into microspheres. Therefore, in this study, microspheres consisting of biopolymers loaded with antibacterial agents and drugs will be produced. In this study, polypentadelactone-co-valerolactone copolymer synthesized by the immobilized enzyme.

In this study, Candida antarctica B lipase was immobilized to rice husk ash, on which surface modifications were applied using the immobilization methods used in previous studies, primarily to be used in enzymatic polymerization reactions. ω-pentadecalactone-co-δ-valerolactone copolymer was produced by ring-opening polymerization using immobilized enzyme from ω-pentadecalactone and δ-valerolactone at different reaction times and temperatures, using monomer ratios of 75-25%. During support preparation and immobilization, RHA was produced by burning rice husks at 600-650°C for 6 hours. The surface of RHA was then modified using a silanization chemical called 3-aminopropyl triethoxysilane (3-APTES), and functional amine (-NH_2) groups were added to the surface. Lipase immobilization was achieved by physical adsorption. Previous scientific investigations attempted to optimize novel immobilized lipases using various 3-APTES concentrations and enzyme loading ratios. These research studies are used as references. After copolymers is produced, they will be formed into microspheres and added with oleuropein as an antibacterial agent and loaded with trans-Chalcone as a drug for use in biomedical fields. A drug delivery system with strong mechanical properties, biocompatible, biodegradable, harmless to the environment and living things will be developed by incorporating the copolymer into the polymer-containing microspheres of the drug and antibacterial agent.

ω-Pentadecalactone, or pentadecanolide, is a cyclic ester having a 15-carbon backbone. ω-pentadecalactone may have antibacterial and antioxidant properties. Its potential pharmacological qualities make it an attractive candidate for the development

of pharmaceutical formulations and nutraceuticals. δ-valerolactone, a lactone, is employed as a chemical intermediate in several processes, such as polyester manufacturing. Polyvalerolactone is a semi-crystalline aliphatic polyester that is hydrophobic. PVL is a well-known biopolymer that has several applications in medication formulation and delivery systems. PVL-based polymers have been employed as antifungal carriers as well as a hydrophobic block in amphiphilic block copolymers for the in vivo administration of chemotherapeutic medications such as daunorubicin (DNR), doxorubicin (DOX), and others.

Microspheres are spherically shaped particles that can vary in size from one to a thousand meters. Microspheres are biodegradable, free-flowing particles made up of proteins or synthetic polymers. They are capable of encapsulating small molecules, proteins, peptides, and nucleic acids. They have various advantages over traditional dosage forms, including increased solubility of poorly soluble pharmaceuticals, protection against enzymatic and photolytic degradation, reduced dosing frequency, greater bioavailability, controlled release profile, dose reduction, and drug toxicities.

Oleuropein appears to be an effective antibacterial agent. Oleuropein, the major phenolic component of the olive tree, is a chemical found in the fruit in the early stages of ripening, and its level diminishes as the fruit ripens as it is digested. Recent research indicates that oleuropein possesses anticancer, antiviral, antioxidant, and anti-inflammatory properties. Oleuropein will be employed as an addition in this investigation since it is considered to improve antibacterial activity and cell proliferation. Chalcones are open-chain chemicals found naturally in plants. The chemical structure is composed of two aromatic rings separated by a three-carbon α,β-unsaturated carbonyl system.. Trans-chalcone (TC) has grown in popularity in recent years for its biological properties due to its abundance in nature, simplicity of synthesis, and simple structure. TC has been demonstrated to have anticancer effects against a variety of types. TC is also anti-inflammatory, working by reducing the oxidative stress caused by a variety of inflammatory diseases. Many additional compounds are metabolically activated by TC. It has been demonstrated that these substances have estrogenic action. Due to the estrogenic action of xenobiotic chemicals, animals may experience a variety of negative health impacts, including obesity, accelerated female puberty, a decrease in sperm count, altered sexual behavior and reproductive organs, and an increased risk of certain cancers. Controlling the amount of TC treatment and preventing the buildup of TC molecules in the body are therefore crucial.

The aim of this study is to develop a new drug delivery system by loading drug and adding antibacterial agent into the bio-based polymeric structure. Microspheres will be obtained by synthesizing a biocompatible, non-toxic and high molecular weight copolymer by using naturally immobilized enzyme to be compatible with the environment and human body. Controlled drug delivery will be carried out by loading a drug and adding an antibacterial agent to this product. Thus, the side effects of the drug will be reduced and its therapeutic properties will be increased. The lack of research in the literature on the use of oleuropein and transchalcone with microspheres for medical reasons adds to the scientific value of the study. The study's uniqueness stems from the lack of literature on the poly(ω-pentadecalactone-co-δ-valerolactone) copolymer produced by enzymatic polymerization. The copolymer synthesized using a biocatalyst will be loaded with oleuropein and trans-chalcone while microspheres are produced and it will be used as medicine. With this mixture, cell biological compatibility will be ensured and the drug will be ensured to reach the desired area at

the desired time. As a result, a new drug delivery system will be created by using natural and synthetic polymers, drugs and antibacterial agents.

In the second stage, a ω-pentadecalactone-co-δ-valerolactone copolymer was produced enzymatically using the monomer ratios from earlier research as a reference. The highest molecular weighted sample (M_n = 23722 g/mol) was obtained at 80°C and 24 hour reaction duration with 75% ω-pentadecalactone feed weight ratio and selected for microsphere formation. Therefore, in this work, ω-pentadecalactone-co-δ-valerolactone is synthesized utilizing these values. In the third stage of the study, oleuropein added and transchalcone loaded PDL-VL microspheres was tried to be produced via O/W emulsion method. In order to determine the highest encapsulation efficiency and drug release behavior, combinations of 10, 20 and 40 percent TC, as well as 42.5, 75 and 100 Olu, in proportion to the copolymer mass were examined. It was determined that microspheres produced at 100% Olu:PDL-VL ratio and 20% TC:PDL-VL ratio had the highest Encapsulation Efficiency (%) which it was 81.7 ± 0.5 (%). After microspheres are made, several characterization analysis were applied such as SEM, DSC, TGA, FTIR and XRD in order to understand thermal, mechanical and morphological properties of microspheres. DSC analysis was applied to observe the thermochemical changes of the copolymer and microspheres samples. Melting temperatures and enthalpy values of microspheres were examined according to the previous scientific studies. The fact that no melting peak was observed in both oleuropein and transchalcone samples indicates that PDL-VL/Olu and TC-loaded PDL-VL/Olu microspheres are properly dispersed into the structure as stated in the literature. TGA analyzes were applied in order to analyze the thermal degradation behavior of microspheres and compare with PDL-VL. FT-IR was used as a characterization method to observe the chemical groups indicating the presence of Olu, TC and microspheres. All the characteristic peaks were examined and explained. It was concluded that Olu and TC were encapsulated in the microspheres. In addition to all other analyses, the influence of TC loading on crystallinity and crystalline structures of microspheres was examined using XRD analysis. The X_c values were determined, and distinctive crystalline peaks were investigated. The results were similar with those obtained from the DSC. It can be seen from the SEM images that spherical geometry was found in all microsphere formulations. Antibacterial acitivty tests were also examined and it led to the conclusion that PDL-VL/Olu and TC-loaded PDL-VL/Olu microspheres have antibacterial properties. As a results of cytotoxicity anaylsis, it leads to a reduction in the viability of human breast cancer cell lines (MCF-7), and therefore it is effective and promising for human breast cancer therapy. In this study, pH dependent drug release experiments were performed with two pH values which was 5.6 and 7.4 in order to see drug release behaviour of microspheres produced with different environments. The microsphere formulations improved the total cumulative release of TC, which reached 91.18 % in pH 5.6 media and 85.89 % in pH 7.4 media. The behavior of microspheres' release was based on pH; the more acidic the release medium, the greater the release. In all cases, TC release was carried out for up to 964 hours. Lastly, the release kinetics of the design points were investigated. When the release rate constants were assessed, it was discovered that the release suited the Korsmeyer-Peppas kinetic model, which had the highest correlation coefficient. After all characterization analysis and drug release behaviour were obtained, it can be concluded that the the results of this study point to a potential use for microspheres in the long-term therapy of disease. And, undoubtedly, much more study will be required to assess cytotoxicity, cell survival, and in vivo pharmacokinetics.

ENZİMATİK OLARAK SENTEZLENMİŞ BİR BİYOPOLİESTERİN BİYOMEDİKAL UYGULAMASI

ÖZET

Polimerler, terapötik ajanların uzun süreler boyunca sabit dozlarda kontrollü salınımını, döngüsel dozlamayı ve hem hidrofilik hem de hidrofobik ilaçların ayarlanabilir salınımını sağlayarak ilaç dağıtım teknolojisinin geliştirilmesinde bütünleyici bir rol oynamıştır. İlaç dağıtımındaki modern gelişmeler artık farklı biyolojik işlevler gerçekleştirmek üzere tasarlanmış polimerlerin rasyonel tasarımına dayanmaktadır. Bu ilaç sistemlerinin insan vücudunda oluşturduğu toksik birikimlerin azaltılması, yan etkilerinin ve çevreye etkilerinin en aza indirilmesi için enzim bazlı biyopolimer sentezlerine ihtiyaç duyulmaktadır. Sentetik polimerlerden farklı olarak enzimler kullanılarak doğal olarak üretilen biyopolimerler; Biyouyumlulukları, biyolojik olarak parçalanabilirlikleri, toksik olmamaları ve biyoaktif molekülleri adsorbe edebilmeleri nedeniyle tıbbi uygulamalara uygundurlar. Bu biyopolimerlerin ilaç taşıyıcı sistemlerde kullanımı cast film, mikroküre, nanopartikül ve nanolif gibi malzemelere dönüştürülmesiyle mümkündür. Çeşitli proteinler, ilaçlar ve proteinler mikrokürelere kolaylıkla yüklenebilmektedir. Bu nedenle bu çalışmada antibakteriyel madde ve ilaçlarla yüklü biyopolimerlerden oluşan mikroküreler üretilecektir. Bu çalışmada immobilize enzim ile polipentadelakton-ko-valerolakton kopolimeri sentezlendi.

Bu çalışmada, öncelikle enzimatik polimerizasyon reaksiyonlarında kullanılmak üzere, önceki çalışmalarda kullanılan immobilizasyon yöntemleri kullanılarak yüzey modifikasyonları uygulanan pirinç kabuğu külüne Candida antarctica B lipazı immobilize edilmiştir. ω-pentadekalakton-ko-δ-valerolakton kopolimeri, %75-25 monomer oranları kullanılarak, farklı reaksiyon süreleri ve sıcaklıklarda, ω-pentadekalakton ve δ-valerolaktondan immobilize edilmiş enzim kullanılarak halka açılması polimerizasyonuyla üretilmiştir. Desteğin hazırlanması ve immobilizasyonu sırasında, pirinç kabuklarının 600-650°C'de 6 saat yakılmasıyla RHA üretilmiştir. Daha sonra RHA'nın yüzeyi, 3-aminopropil trietoksisilan (3-APTES) adı verilen bir silanizasyon kimyasalı kullanılarak değiştirildi ve yüzeye fonksiyonel amin ($-NH_2$) grupları eklenmiştir. Lipaz immobilizasyonu fiziksel adsorpsiyonla sağlandı. Önceki bilimsel araştırmalar, çeşitli 3-APTES konsantrasyonlarını ve enzim yükleme oranlarını kullanarak yeni immobilize lipazları optimize etmeye çalışmıştır. Bu araştırma çalışmaları referans olarak kullanılmaktadır. Kopolimerler üretildikten sonra mikroküreler haline getirilecek ve biyomedikal alanlarda kullanılmak üzere üzerine antibakteriyel madde olarak oleuropein eklenecek ve bu mikroküreler ilaç olarak trans-kalkon ile yüklenecektir. İlacın polimer içeren mikroküreleri ve antibakteriyel ajanın içine kopolimer katılarak güçlü mekanik özelliklere sahip, biyouyumlu, biyolojik olarak parçalanabilen, çevreye ve canlılara zararsız bir ilaç dağıtım sistemi geliştirilecektir.

ω-Pentadekalakton veya pentadekanolid, 15 karbonlu bir omurgaya sahip siklik bir esterdir. ω-pentadekalakton antibakteriyel ve antioksidan özelliklere sahip olabilir. Potansiyel farmakolojik nitelikleri, onu farmasötik formülasyonların ve nutrasötiklerin geliştirilmesi için çekici bir aday haline getirmektedir. Bir lakton olan δ-valerolakton, polyester üretimi gibi çeşitli işlemlerde kimyasal bir ara madde olarak kullanılır. Polivalerolakton, hidrofobik olan yarı kristalli alifatik bir polyesterdir. δ-valerolakton monomerinin polimerleştirilmesiyle üretilir. PVL, ilaç formülasyonu ve dağıtım sistemlerinde çeşitli uygulamalara sahip, iyi bilinen bir biyopolimerdir. PVL bazlı polimerler, daunorubisin (DNR), doksorubisin (DOX) ve diğerleri gibi kemoterapötik ilaçların in vivo uygulanması için amfifilik blok kopolimerlerde hidrofobik bir blokun yanı sıra antifungal taşıyıcılar olarak da kullanılmıştır.

Mikroküreler, boyutları bir metreden bin metreye kadar değişebilen küresel şekilli parçacıklardır. Mikroküreler, proteinlerden veya sentetik polimerlerden oluşan biyolojik olarak parçalanabilen, serbest akışlı parçacıklardır. Küçük molekülleri, proteinleri, peptitleri ve nükleik asitleri kapsülleme yeteneğine sahiptirler. Zayıf çözünen farmasötiklerin artan çözünürlüğü, enzimatik ve fotolitik bozunmaya karşı koruma, azaltılmış dozlama sıklığı, daha yüksek biyoyararlanım, kontrollü salım profili, doz azaltımı ve ilaç toksisiteleri dahil olmak üzere geleneksel dozaj formlarına göre çeşitli avantajlara sahiptirler.

Oleuropein etkili bir antibakteriyel madde gibi görünmektedir. Zeytin ağacının ana fenolik bileşeni olan oleuropein, olgunlaşmanın erken aşamalarında meyvede bulunan bir kimyasaldır ve meyve olgunlaştıkça sindirildikçe seviyesi azalır. Zeytin meyvelerinin kendine özgü acı tadından sorumludur. Son araştırmalar, oleuropeinin antikanser, antiviral, antioksidan ve antiinflamatuar özelliklere sahip olduğunu göstermektedir. Oleuropein, antibakteriyel aktiviteyi ve hücre proliferasyonunu iyileştirdiği düşünüldüğü için bu araştırmada ilave olarak kullanılacaktır.

Kalkonlar bitkilerde doğal olarak bulunan açık zincirli kimyasallardır. Kimyasal yapı, üç karbonlu a,β-doymamış karbonil sistemi ile ayrılan iki aromatik halkadan oluşur. Trans-kalkon (TC), doğada bol miktarda bulunması, sentezinin basitliği ve basit yapısı nedeniyle biyolojik özellikleri nedeniyle son yıllarda popülerlik kazanmıştır. TC'nin çeşitli türlere karşı antikanser etkileri olduğu gösterilmiştir. Trans-kalkonun anti-leishmanial aktivitesi geniş çapta incelenmiştir. TC ayrıca antiinflamatuardır ve çeşitli inflamatuar hastalıkların neden olduğu oksidatif stresi azaltarak çalışır. Birçok ilave bileşik TC tarafından metabolik olarak aktive edilir. Bu maddelerin östrojenik etkiye sahip olduğu kanıtlanmıştır. Ksenobiyotik kimyasalların östrojenik etkisi nedeniyle hayvanlar, obezite, kadınlarda ergenliğin hızlanması, sperm sayısında azalma, cinsel davranışta ve üreme organlarında değişiklik ve bazı kanser risklerinde artış gibi çeşitli olumsuz sağlık etkileriyle karşılaşabilir. TC tedavisi miktarının kontrol edilmesi ve vücutta TC moleküllerinin birikmesinin önlenmesi bu nedenle çok önemlidir.

Bu çalışmanın amacı biyo bazlı polimerik yapıya ilaç ve antibakteriyel ajan eklenerek yeni bir ilaç taşıyıcı sistem geliştirmektir. Çevreye ve insan vücuduna uyumlu olacak şekilde doğal olarak immobilize edilmiş enzim kullanılarak biyouyumlu, toksik olmayan ve yüksek molekül ağırlıklı kopolimer sentezlenerek mikroküreler elde edilecektir. Bu ürüne ilaç ve antibakteriyel madde eklenerek kontrollü ilaç dağıtımı gerçekleştirilecek. Böylece ilacın yan etkileri azalacak ve tedavi edici özelliği artacaktır. Oleuropein ve transkalkonun mikrokürelerle tıbbi amaçlarla kullanımına ilişkin literatürde araştırma bulunmaması, çalışmanın bilimsel değerini artırmaktadır. Taşıma sistemi verimliliğini artırmak için doğal ve biyo bazlı sentetik polimerler

birleştirildi. Çalışmanın benzersizliği, enzimatik polimerizasyonla üretilen poli(ω-pentadekalakton-ko-δ-valerolakton) kopolimeriyle ilgili literatür eksikliğinden kaynaklanmaktadır. Biyokatalizör kullanılarak sentezlenecek kopolimer, oleuropein ve trans-kalkon ile yüklenerek mikroküreler üretilecek ve ilaç olarak kullanılacaktır. Bu oluşan karışım ile hücre biyolojik uyumu sağlanacak ve ilacın istenilen zamanda istenilen bölgeye ulaşması sağlanacaktır. Sonuç olarak doğal ve sentetik polimerler, ilaçlar ve antibakteriyel ajanlar kullanılarak yeni bir ilaç dağıtım sistemi oluşturulacaktır.

Çalışmanın ikinci aşamasında, daha önceki araştırmalardan elde edilen monomer oranları referans olarak kullanılarak enzimatik olarak bir ω-pentadekalakton-ko-δ-valerolakton kopolimeri üretilmiştir. En yüksek moleküler ağırlıklı numune (Mn = 23722 g/mol) 80°C'de ve 24 saatlik reaksiyon süresinde %75 ω-pentadekalakton besleme ağırlık oranıyla elde edilmiştir ve mikroküre oluşumu için seçilmiştir. Dolayısıyla bu çalışmada bu değerler kullanılarak ω-pentadekalakton-ko-δ-valerolakton sentezlenmiştir. Daha sonra numunenin mikroküre üretiminde kullanılacağı belirlenmiştir. Çalışmanın üçüncü aşamasında oleuropein/transkalkon yüklü PDL-VL mikroküreleri O/W emülsiyon yöntemiyle üretilmilmiştir. En yüksek enkapsülasyon verimliliğini ve ilaç salım davranışını belirlemek amacıyla kopolimer kütlesine orantılı olarak yüzde 10, 20 ve 40 TC'nin yanı sıra 42,5, 75 ve 100 Olu'luk kombinasyonlar incelenmiştir. %100 Olu:PDL-VL oranında ve %20 TC:PDL-VL oranında üretilen mikrokürelerin en yüksek enkapsülasyon verimine (%) sahip olduğu ve 81,7 ± 0,5% olduğu belirlenmiştir. Mikroküreler sentezlendikten sonra PDL-VL, PDL-VL/Olu ve TC yüklü PDL-VL/Olu mikrokürelerinin, termal, mekanik ve morfolojik özelliklerini anlamak amacıyla SEM, DSC, TGA, FTIR ve XRD gibi çeşitli karakterizasyon analizleri uygulanmıştır. Kopolimer ve mikroküre örneklerinin termokimyasal değişimlerini gözlemlemek için DSC analizi uygulanmıştır. PDL-VL, PDL-VL/Olu ve TC yüklü PDL-VL/Olu mikrokürelerinin erime sıcaklıkları ve entalpi değerleri daha önce yapılan bilimsel çalışmalara göre incelenmiştir. Hem oleuropein hem de transkalkon numunelerinde herhangi bir erime zirvesinin gözlenmemesi, PDL-VL/Olu ve TC yüklü PDL-VL/Olu mikrokürelerinin literatürde belirtildiği gibi yapıya düzgün bir şekilde dağıldığını göstermektedir. TC yüklü PDL-VL/Olu ve PDL-VL/Olu mikrokürelerinin termal bozunma davranışını analiz etmek ve PDL-VL ile karşılaştırmak için TGA analizleri uygulanmıştır. FT-IR analizleri, Olu, TC, PDL-VL, PDL-VL/Olu ve TC yüklü PDL-VL/Olu mikrokürelerinin varlığını gösteren kimyasal grupları gözlemlemek için bir karakterizasyon yöntemi olarak kullanılmıştır. Tüm karakteristik zirveler incelenmiştir ve açıklanmıştır. Olu ve TC'nin mikroküreler içerisinde enkapsüle olduğu sonucuna varılmıştır. Diğer tüm analizlere ek olarak, TC yüklemesinin mikrokürelerin kristalliği ve kristal yapıları üzerindeki etkisi XRD analizi kullanılarak incelenmiştir. X_c değerleri belirlenmiştir ve ayırt edici kristal tepe noktaları araştırılmıştır. Sonuçlar DSC'den elde edilenlerle benzer olarak belirlenmiştir. SEM görüntülerinden tüm mikroküre formülasyonlarında küresel geometrinin bulunduğu görülmektedir. Antibakteriyel aktivite testleri de incelenmiştir ve TC yüklü PDL-VL/Olu ve PDL-VL/Olu mikrokürelerinin antibakteriyel özelliklere sahip olduğu sonucuna varılmıştır. Sitotoksisite analizi sonucunda, elde edilen maddenin insan meme kanseri hücre hatlarının (MCF-7) canlılığında azalmaya yol açmakta olduğu görülmüştür ve bu nedenle insan meme kanseri tedavisinde etkili ve umut verici olduğu söylenebilir.

Bu çalışmada, farklı ortamlarda üretilen mikrokürelerin ilaç salım davranışlarını görmek amacıyla 5,6 ve 7,4 olmak üzere iki pH değerinde pH'a bağlı ilaç salım

deneyleri yapılmıştır. Mikroküre formülasyonları, pH 5.6 ortamda %91.18'e ve pH 7.4 ortamda %85.89'a ulaşan toplam TC kümülatif salınımını iyileştirmiştir. Mikroküreciklerin salınma davranışı pH'a dayanmaktadır; Salım ortamı ne kadar asidik olursa, salınım da o kadar fazla olur sonucuna varılmıştır. Tüm durumlarda TC salımı 964 saate kadar gerçekleştirilmiştir. Son olarak tasarım noktalarının salınım kinetiği araştırılmıştır. Salınım hızı sabitleri değerlendirildiğinde salınımın en yüksek korelasyon katsayısına sahip olan Korsmeyer-Peppas kinetik modeline uygun olduğu keşfedilmiştir. Tüm karakterizasyon analizleri ve ilaç salınım davranışı elde edildikten sonra, bu çalışmanın sonuçlarının, mikrokürelerin hastalıkların uzun vadeli tedavisinde potansiyel bir kullanıma işaret ettiği sonucuna varılabilir. Ve hiç şüphesiz sitotoksisiteyi, hücre sağkalımını ve in vivo farmakokinetiği değerlendirmek için çok daha fazla çalışmaya ihtiyaç duyulacaktır.

1. INTRODUCTION

As the environment becomes more polluted, there is a growing interest in developing biodegradable polymers. Aliphatic polyesters are particularly interesting due to their versatile characteristics and diverse synthesis techniques. There are two methods for producing biodegradable polyesters. The first method involves polycondensation of a hydroxyl acid or diol with a diacid, which often results in low molecular weight polymers (<30 kDa). To achieve greater molecular weight polymers, ring-opening polymerization (ROP) is typically used as a second technique. Lactone monomers used in this reaction include ε-caprolactone (ε-CL), ω-pentadecalactone (ω-PDL), and lactide. Polylactones and PLAs have biocompatibility, mechanical resilience, and biodegradability, making them suitable for biomedical applications such vascular implants, suture materials, and tissue engineering scaffolds. Biodegradable polymers are being studied for their potential to carry and release drugs in the body. Biodegradability allows for regulated drug release over time. Extensive research on enzymatic ROP (eROP) has emerged in response to the increased need for ecologically benign and heavy metal-free goods. Enzymes are not only non-toxic, but also capable of catalyzing specific reactions. This eliminates the need to protect or deprotect functional groups, allowing for selective synthesis of polymers from chiral monomers [1].

Lipases (glycerol ester hydrolase, E.C. 3.1.1.3) catalyze esterification, hydrolysis, and transesterification, producing a variety of useful chemicals under moderate circumstances. These enzymes have unique interfacial kinetics, resulting in strong catalytic activity at the water-oil interface that decreases dramatically in bulk water or oil phases. Uppenberg, Hansen, Patkar, and Jones (1994) initially identified the three-dimensional structure and amino acid sequence of Candida antarctica lipase B. CALB has excellent catalytic activity for both water-soluble and insoluble compounds. CALB's regioselectivity and chiral selectivity enable it to catalyze reactions in the organic phase while maintaining excellent stability [2].

Novel drug delivery technologies have several advantages over standard multi-dose treatment. According to recent trends, micro particulate drug delivery systems are particularly well suited to controlled release and delayed-release oral formulations with low dose dumping, blending flexibility to achieve different release patterns, and reproducible and short gastric residence time [3]. Drugs delivery techniques have advanced, especially those that allow the medicine to work in the intended effect area for a longer period of time under regulated conditions. These cutting-edge drug delivery methods can deliver drugs to a particular place, alter the rate at which they are supplied, and/or extend the therapeutic impact [4]. One of the most advanced techniques for maintaining and regulating pharmacological activity in a particular place is the use of microspheres as drug carriers. To offer temporary embolization, microspheres composed of biodegradable components are used. Theoretically, after serving their therapeutic purpose, they ought should be eliminated from the body without affecting the functionality of other organs [5].

The European Medicines Agency (EMA) has linked the phenolic acid oleeuropein, which is found in large quantities in the leaves and fruits of the Olea europaea plant, to a number of health benefits for people [6]. Because of its well-established anti-inflammatory and antioxidant characteristics, oleeuropein may also have antiviral, antimicrobial, and neuroprotective qualities [7]. When loaded onto microspheres, it can be utilized as an antibacterial agent and in the treatment of diseases [8].

Trans-chalcone (TC), also known as 1,3-diphenyl-2-propen-1-one, is a flavonoid found in plants and a primary precursor to other flavonoids. Depending on the illness model, TC has anti-inflammatory and antioxidant properties. [9] They exhibit many biological activities, including antibacterial, antihelmintic, anticancer, antifungal, antidiabetic and amoebic properties. Previous research indicates that chalcones have potent antileishmanial and antimalarial properties These medications disrupt the parasite's mitochondrial structure and function. Recent research indicates that chalcones reduce parasite respiration and mitochondrial dehydrogenase activity [10].

In this study, it was aimed to produce biocompatible drug loaded and antibacterial agent added microspheres. Oleuropein will be used as an antibacterial agent and trans-chalcone will be used as an drug. Initially, the surface of the support material was silanized with the agent 3-APTES, as reported in earlier investigations. Following that, CALB was immobilized on surface-modified RHA using a physical adsorption

method, as previously described [11]. In the second stage of the study, ω-pentadecalactone-co-δ-valerolactone copolymer was effectively synthesized from ω-pentadecalactone and δ-valerolactone with CALB immobilized to RHA, using the techniques and parameters in earlier studies. [11]. In the third stage of the study, oleuropein/transchalcone loaded PDL-VL microspheres was tried to be produced via O/W emulsion method. Microspheres with the highest encapsulation efficiency were identified and used to study drug release behavior. After microspheres are made, several characterization analysis were applied such as scanning electron microscope (SEM), differential scanning calorimetry (DSC), thermal gravimetric analysis (TGA), fourier transform infrared spectroscopy (FTIR) and X-Ray diffraction analysis (XRD) in order to understand thermal, mechanical and morphological properties of PDL-VL, PDL-VL/Olu and TC-loaded PDL-VL/Olu microspheres. Antibacterial tests of PDL-VL, PDL-VL/Olu and TC-loaded PDL-VL/Olu microspheres were performed on gram positive *Staphylococcus aureus*, and gram negative *Escherichia coli* bacteria. Antibacterial activities (%) for all the samples were determined. The human breast cancer cell (MCF-7) and microspheres loaded with oleuropein at 1:1 (wt%) with copolymer concentrations and TC at 1:5 (wt%) with copolymer concentrations were used for in vitro cytotoxicity tests (WST), where the highest cytotoxicity was observed at these concentrations. In addition, a drug release study was conducted for TC-loaded PDL-VL/Olu microspheres and The drug release profiles were fitted to several kinetic models to better understand the process of drug release. After all characterization analysis and drug release behaviour were obtained, it can be concluded that the the results of this study point to a potential use for microspheres in the long-term therapy of disease.

2. LITERATURE REVIEW

2.1 Biopolymers

Biopolymers are biologically produced polymers as opposed to synthetic ones. Because of their non-toxicity, biocompatibility, biodegradability, and capacity to adsorb bioactive compounds, they are well-suited for use in medical applications. The need for biomaterials and, consequently, biopolymers has grown steadily as a result of the environmental and usage issues associated with the use of synthetic polymers. New approaches have also been developed to produce biomaterials that are even more efficient. Because of this tremendous interest, biopolymers have become increasingly popular as it has become apparent that they have a wide range of uses in the medical industry, including tissue engineering and drug delivery systems [12]. Furthermore, increasing evidence shows that enzyme-mediated catalytic bioprocesses exhibit numerous advantages over traditional synthetic approaches. Additionally, biocatalysts are environmentally friendly as they require minimal use of chemicals and do not produce any toxic byproducts during the reaction. Because, unlike traditional chemical synthesis and physical modification, enzymatic polymerization is an emerging biologically based alternative approach for producing polymeric products [13].

Biopolymers, which are essential to modern sustainable material science, have their origins in prehistoric societies that used natural materials such as plant fibers, animal skins, and resins for a variety of uses. Since the development of contemporary biotechnology and the increased awareness of the need for a sustainable environment, attention has turned to biopolymers made from biomass sources that are renewable, such as microbes, plants, and animals as it can be seen from Figure 2.1. These biopolymers are a varied range of materials with special qualities and uses, generally divided into polysaccharides, proteins, nucleic acids, and biopolyesters [14].

Long chains of sugar molecules called polysaccharides are widely found in nature and play a crucial role in the functioning of living things. One of the prominent polysaccharides is cellulose, which is known to contribute to the strength and stiffness

of plant cell walls by serving as their structural basis. Another well-known member of this group is starch, which is used extensively as a staple food by both humans and animals. It is the main energy storage form in plants. Chitin provides these creatures with structural support and defense. It is mostly present in the cell walls of fungi and the exoskeletons of arthropods. Alginate is mainly produced from seaweed and has a variety of uses in the food and pharmaceutical industries. It can be used as a thickening and gelling agent in many kinds of formulations. These polysaccharides, distinguished by their diverse structures and functionalities, play integral roles across a spectrum of applications spanning biomedicine, food science, agriculture, and materials engineering [15].

Proteins, such as collagen, gelatin, and silk fibroin, are made up of amino acids and are useful in medical applications like tissue engineering and drug delivery systems due to their biocompatibility [16]. Nucleic acids, such as DNA and RNA, serve as the blueprint for life and are being researched for utilization in biotechnology and drug delivery.

Furthermore, polyhydroxyalkanoates (PHA) and biopolyesters such as poly(lactic aci d) (PLA) provide fascinating alternatives to traditional plastics, providing biodegrada bility and renewability while maintaining mechanical qualities suited for a variety of applications [17].

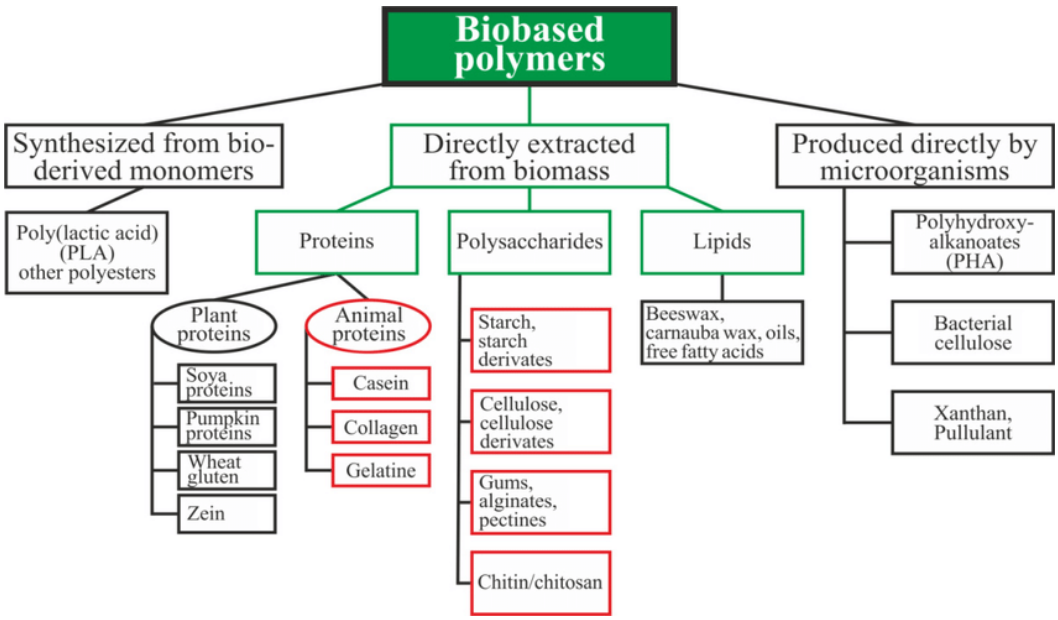

Figure 2.1 : Classification of biobased polymers [18].

Polyesters, a type of biopolymer, have major applications due to their versatility and eco-friendliness. Poly(lactic acid) (PLA) is a widespread example, generated from renewable resources such as cornstarch or sugarcane [19]. PLA has qualities similar to typical petroleum-based polymers, but it is also biodegradable and compostable under the right conditions, making it ideal for packaging, biomedical applications, and 3D printing [19]. Moreover, Polyhydroxyalkanoates (PHA), a further significant class of biodegradable polyesters, are produced through microbial fermentation of renewable carbon sources such as sugars or lipids [20]. PHA polymers have mechanical characteristics similar to regular plastics, but they can be broken down by microorganisms in a variety of environments, making them interesting candidates for biomedical applications [20].

2.2 Lipase Enzyme

Lipases (EC 3.1.1.3) are triacylglycerol acylhydrolases that break down carboxylic ester linkages and belong to the hydrolase family. These enzymes are classified as serine hydrolases and don't require a cofactor [20]. Lipases primarily hydrolyze triglycerides into fatty acids and glycerol, but can also catalyze esterifications and interesterifications in non-aqueous environments. Lipases have a unique mode of activation at the interface. Lipases typically have an α-helical oligopeptide structure that covers the active site (lid or flap) and prevents substrates from reaching it [21]. When there is no hydrophobic interface, the enzyme's active site remains concealed from the reaction media. This enzyme shape is known as the "closed conformation". In contrast, when a hydrophobic interface occurs, the enzyme undergoes a conformational shift to expose its catalytic triad to the hydrophobic phase. This enzyme conformation shift occurs in the "open conformation". Thus, the activation mechanism of lipase is referred to as "interfacial activation" [21]. These forms are given in Figure 2.2. Lipases catalyze the hydrolysis of ester bonds at the interface of an insoluble substrate and an aqueous phase, where the enzymes remain liquefied under normal circumstances. Pseudomonas aeruginosa, Candida Antarctica B, and Burkholderia glumae had a lid but did not exhibit interfacial activation. Lipases perform several conversion reactions, including esterification, transesterification, interesterification, acidolysis, alcoholysis, and aminolysis [20].

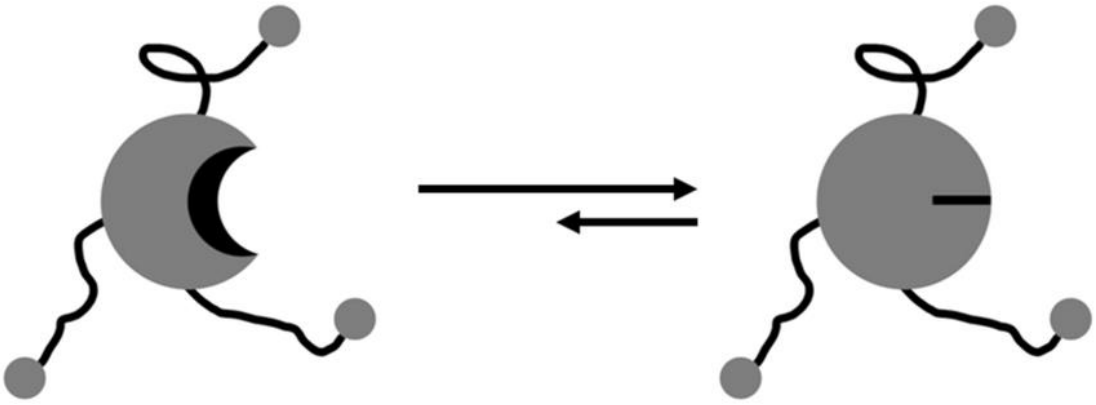

Figure 2.2 : Free lipase open and closed form [22].

Lipase possesses significant selectivity (regio-, enantio-, stereo-, and chemo-selectivity), can catalyze at the interface of aqueous and organic phases, and interacts with a wide range of substrates. Lipase's unique behavior allows for the development of lipase-catalyzed polymerization processes. Lipase-catalyzed ROP of lactones, lactides, and cyclic carbonates can yield aliphatic polyesters or polycarbonates [23]. Lipases are commonly utilized in industry due to their ability to catalyze a wide range of reactions. These unusual catalysts may catalyze reactions across immiscible organic and aqueous phases and maintain catalytic activity in organic solvents. Immobilization can improve the activity, selectivity, and operational stability of enzymes in both aqueous and non-aqueous solvents, allowing for more efficient utilization [11]. Candida antarctica lipase B (CALB) is an efficient and selective lipase capable of catalyzing esterification and transesterification processes [11]. It is immobilized on macroporous acrylic resin and marketed as Novozyme 435®. In this study, free CALB was immobilized on a new support to produce an alternative to Novozyme 435® [23].

2.3 Enzyme Immobilization

Lipases' commercial usage has been limited because to their expensive cost. However, immobilization methods using solid supports may overcome this. Immobilization improves product separation and allows for more flexible enzyme/substrate interactions in different reactor setups. Furthermore, immobilizing enzymes on solid substrates can enhance stability and selectivity [21]. There are several techniques for immobilizing enzymes. As it is shown in Figure 2.3, the most frequent methods are adsorption, trapping, and cross-linking to a support. Adsorption is the process of physically adsorbing an enzyme onto a support material, such as a polymer matrix or

inorganic support. Enzyme entrapment occurs when it becomes trapped within a material's lattice structure or polymer ns. While this reduces enzyme leaching and enhances stability, it can also restrict substrate delivery to the active site. Enzymes can be immobilized by cross-linking them to an insoluble support or covalently attaching them to a functionalized support [11]. Immobilization of enzymes on supports (carriers) is a process used to improve the activity, selectivity, and stability of biocatalysts. Furthermore, the usage of solid supports can substantially aid in the extraction of an enzyme from the reaction solution [24]. The activity of immobilized lipase is substantially determined by the enzyme molecules, the immobilization process, the reaction media, and the kind of support. It has been shown that the intensity of enzyme-support, enzyme-substrate (in the reaction media), and support-substrate interactions influences the stability and specificity of biocatalysts. It has also been demonstrated that the reaction media can influence the enzyme-substrate molecular recognition mechanism. Interestingly, a good material for enzyme immobilization can trap substrates by hydrophobic or electrostatic coupling, so contributing to a favorable partition effect of the substrate in the reaction media [24].

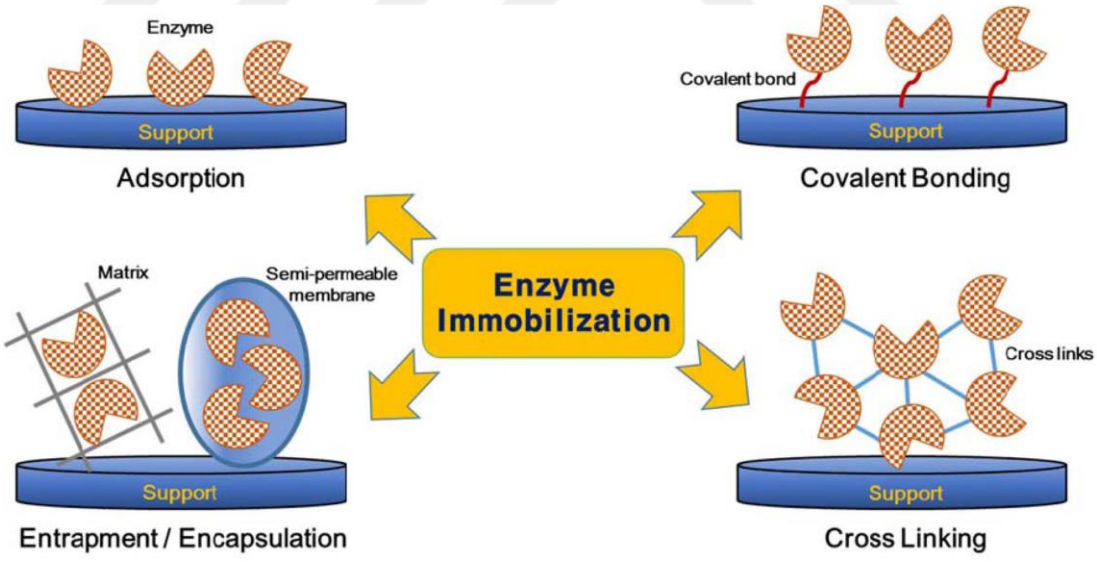

Figure 2.3 : Immobilization methods of enzymes [25].

To achieve physical adsorption, immerse the support in an enzyme solution and incubate for several hours. Enzymes are absorbed into the matrix via weak non-specific forces such hydrogen bonding, Van der Waals forces, and hydrophobic interactions. However, mild nonspecific forces can cause reversible enzyme leakage from the matrix by altering the parameters that affect contact strength, such as pH,

ionic strength, temperature, or solvent polarity [25]. Covalent binding is a common approach for immobilizing enzymes. It involves creating stable complexes between enzyme functional groups and a support matrix. Enzyme functional groups suitable for covalent coupling include amino, carboxylic, phenolic, sulfhydryl, thiol, imidazole, indole, and hydroxyl groups. Enzyme binding to solid supports involves two stages: activating the surface using linker molecules like glutaraldehyde or carbodiimide, and then covalently attaching the enzyme to the activated support [25]. Cross-linking immobilization involves covalent connection between enzymes without the need of carriers. Cross-linking immobilization strengthens the linkage between enzymes, resulting in improved stability [26]. Entrapment is an irreversible immobilizing process. This approach prevents enzyme leakage by regulating the pore size of the polymeric network, allowing for unrestricted diffusion of reaction contents (substrates or products). This technique prevents denaturation by not allowing enzymes to react with polymers. The entrapment process has several benefits, including increased enzyme loading capacity, cheaper manufacturing costs, improved mechanical stability, and less mass transfer. The encapsulating material may be modified to create an appropriate microenvironment with desired pH, polarity, or amphilicity [26]. Encapsulation is similar to entrapment in that enzymes are enclosed in a polymer matrix. However, the polymer support matrix comprises "pockets" or "pores" to immobilize enzymes. Encapsulated enzymes enhance enzymatic activity by altering hydrophobic interactions, increasing reaction surface area, and boosting intermediate concentration. They are more stable in a range of conditions. They are frequently used in fields including biocatalysis, biosensing, enzyme therapy, biomedicine, and bioremediation [27].

Lipases are often immobilized on supports through adsorption via hydrophobic interactions because it is inexpensive and increases enzyme activity. For example, the most widely used commercial enzyme, Novozyme 435®, is produced by physical adsorption of CALB on porous acrylic resin [23].

2.3.1 Support materials for enzyme immobilization

The immobilized enzyme system's performance relies heavily on the matrix's properties. Ideal support features include compression resistance, hydrophilicity, enzyme inertness, ease of derivatization, biocompatibility, microbiological resistance,

and cost-effectiveness [28]. Furthermore, it should have the potential to enhance enzyme activity and specificity [23]. As it can be seen from Table 2.1, supports can be classified as inorganic or organic based on their chemical structure. Organic supports can be separated into natural and synthetic polymers [28].

Table 2.1 : Classification of supports used for enzyme immobilization [23].

Chemical Composition	Example
Organic	**Natural polymers:**
	Polysaccharides (cellulose, dextrans, agar, agarose, chitin, chitosan, alginate), proteins (collagen, albumin)
	Synthetic polymers:
	Polystyrene, polyacrylate, polymethacrylates, polyacrylamide, polyamides, vinyl, and allyl-polymers
	Polysaccharides (cellulose, dextrans, agar, agarose, chitin, chitosan, alginate), proteins (collagen, albumin)
Inorganic	Zeolites, ceramics, celite, silica, bentonite, clay, alumina, glass, activated carbon

Among the support materials which is used for enzyme immobilization, silica is the most extensively utilized support material for lipase immobilization due to its large specific surface area, biocompatibility, and inexpensive cost. Furthermore, the surface could be simply adjusted [23].

As it is written before, the most widely used immobilized lipase is Novozyme 435®, a commercially available immobilized version of CALB. This catalyst is efficient and adaptable, using a porous acrylic resin as the enzyme carrier [29].

Rice beneficiation produces rice husk as a byproduct, accounting for around 23% of the original weight. Rice husk's high silicon concentration makes it a valuable source for producing elementary silicon and other silicon compounds, including silica, silicon carbide, and silicon nitride [30]. Rice husk is a composite substance composed from lignin, cellulose, hemicellulose, and silicon dioxide [31]. Rice husks include 80% organic and 20% inorganic materials. RH's primary elemental components are C (37.05 wt.%), H (8.80 wt.%), N (11.06%), Si (9.01 wt.%), and O (35.03%). RH

contains 24.3% hemicellulose, 34.4% cellulose, 19.2% lignin, 18.85% ash, and 3.25 percent other substances [32]. Rice husk is a desirable material for industrial applications due to its high silica concentration (87-97 wt.% SiO_2), high porosity, lightweight nature, and large exterior surface area [32]. Figure 2.4 shows the applications of rice husk for lipase enzyme. Rice husk ash is typically formed during the calcination process of rice husks. Rice husk ash is a cost-effective way to immobilize enzymes. It is more efficient, renewable, and includes 91.43% SiO_2 [31]. As a result of molecule adsorption, the silica compound in the amorphous state has a tiny particle size and a large surface area. One kind of amorphous silica is silica gel, which may be manufactured via sol-gel. Silica gel is commonly employed as a precursor because of its excellent thermal stability, inability to expand, inertness, and transparency. Silica sol-gel matrices can be utilized to encapsulate enzymes without affecting their structure. Enzymes are stabilized by silica matrix encapsulation, which forms a scaffolding around them to prevent aggregation, dissociation, and destruction [31].

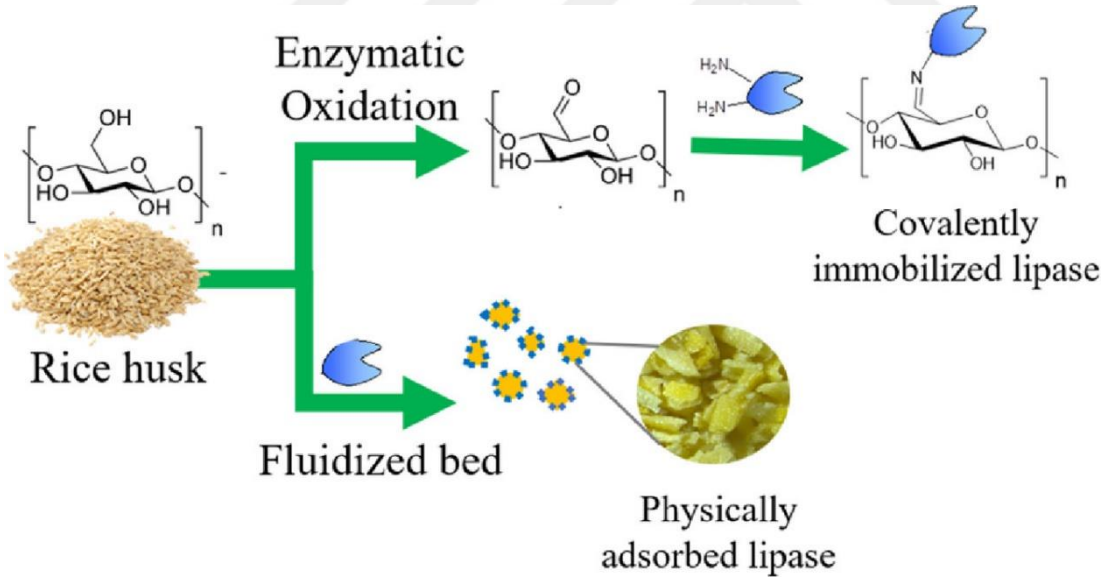

Figure 2.4 : Applications of rice husk for lipase enzyme [33].

As it is shown in Figure 2.5, Silica consists of siloxane (Si-O-Si) and silanol (Si-OH) groups. Silanol groups are scattered on the surface, whereas siloxane groups are found within. Chemical changes are made to the silanol groups on the surface. Organosilane agents modify surfaces by silanization [23]. Among the efficient silanization coupling agents are 3-aminopropyl triethoxysilane (APTES) and 3-glycidyloxypropyl trimethoxysilane (GPTMS); their effective performance is ascribed to the distinct

qualities supplied by their bifunctional features [34]. APTES is the most widely used organosilane for functionalizing oxide surfaces. Oxide surfaces include hydroxyl groups (-OH) with high surface energy, allowing for fast interaction and covalent bonding with silane molecules [35]. Density functional theory (DFT) analysis indicates that the protonated amines ($-NH_3+$) in APTES interact strongly with Si surface silanols (-55.2 kcal/mol). The amine head of APTES binds strongly to the silica surface, making its silanols available for covalent condensation with neighboring SiNPs or self-condensation with unreacted APTES molecules. This promotes particle agglomeration at high APTES loading [34]. After activation of silica particles with organosilane agents, enzyme can be covalently immobilized on these particles [23].

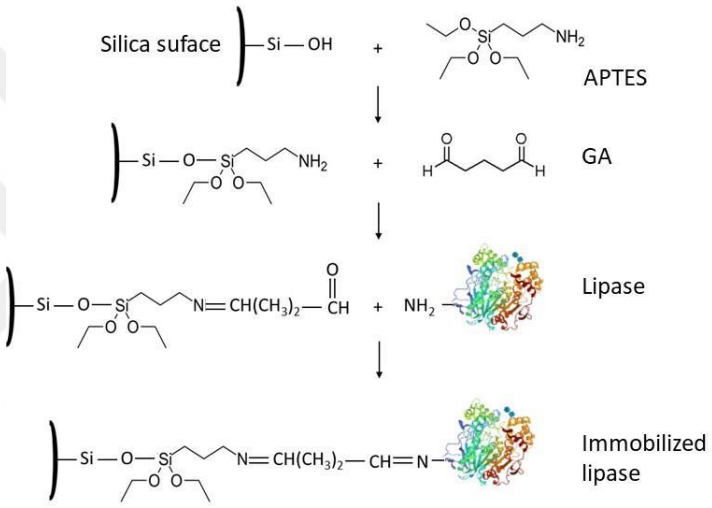

Figure 2.5 : Immobilization of lipase on APTES/GA-activated silica surface [36].

2.4 Biopolymer Production

The biopolymer production process is divided into four categories based on the intended outcome and the material utilized. These techniques include chemical synthesis, bacterial synthesis, biopolymer blends, and gathering from renewable resources [37]. Ring-opening polymerization (ROP) of cyclic esters has resulted in biodegradable polyesters, providing a sustainable alternative to standard polyester materials [38]. The ring-opening polymerization (ROP) technique is used to produce large-scale biopolymers such as PLA, PHA polyesters, and cyclic polyesters via chemical processes. This polymerization is selected because it allows exact control of polymer molar mass. A catalyst, such as a metal ion, is required to initiate the polymerization reaction. Ring-opening polymerization often employs metal catalysts such as tin (II) octoate [Sn(Oct)2] or tin(II) butoxide, as well as lithium, magnesium,

zinc, and zirconium [37]. Polymers like polycaprolactone and polylactide have been used in many applications. The limited commercial availability of cyclic esters limits the microstructure and characteristics of the resultant polymers. In recent years, ring-opening copolymerization (ROCOP) of epoxides and cyclic anhydrides has arisen as an alternative to ROP of cyclic esters to generate a wider range of polyester materials with different microstructures, characteristics, and uses [38].

Due to the scarcity of group 1A metals such as lithuim and the development of hazardous organometallic intermediates as a result of the reaction, the application of the produced compounds in medical domains has been limited, and several catalysis approaches have been attempted. Using bioresorbable salts, devoid of harmful metallic residues, for the ROP of cyclic lactones is an alternative method for producing aliphatic polyester. These catalysts contain cations such as Na+, K+, Mg^{+2}, Ca^{+2}, Zn^{+2}, and Fe^{+2}. These metals are referred to as "friendly metals". These cations have been examined using a variety of counter ions, including chloride, ionide, oxide, hydroxide, carbonate, acetate, lactate, tartrate, and citrate [23]. Although some chemical catalysts efficiently polymerize lactones and can be employed in food applications, they are unsuitable for biomedical applications. Therefore, it is vital to enhance enzymatic polymerization [23].

Since it does not produce harmful organometallic intermediates and lowers the reaction conditions to a more ideal level, enzymatic ring-opening polymerization has been an effective polymerization technique [23]. Enzymatic ROP (eROP) has been the subject of much research due to the increased interest in ecologically friendly processes and products free of heavy metals. In addition to their non-toxic nature, enzymes are also capable of catalyzing stereoselective and regioselective reactions. Thus, polymers from chiral monomers may be produced selectively and functional groups do not need to be protected or deprotected. Figure 2.6 shows the synthesis of polyester materials via ROP and it can be seen from the Figure 2.7 that which type of materials are used for lipase-catalyzed ROP. While many of the heavy metal catalysts used in ROP cannot be recycled, a variety of enzyme immobilization techniques allow for the recycling of enzymes, particularly lipases, which are the primary biocatalysts utilized in eROP as it be seen from Figure 2.8 [39].

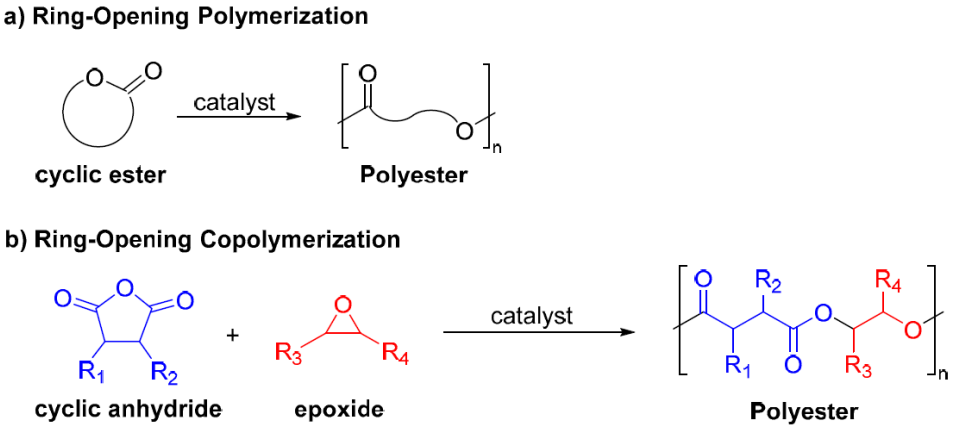

Figure 2.6 : Synthesis of polyester materials via (a) ROP of cyclic esters; (b) ROCOP of epoxides and cyclic anhydrides [38].

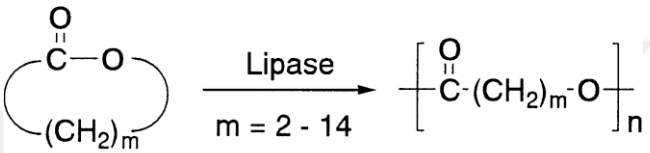

m=2: β-PL	m=2: poly(3HP)
m=3: γ-BL	m=3: poly(4HB)
m=4: δ-VL	m=4: poly(5HV)
m=5: ε-CL	m=5: PCL
m=10: UDL	m=10: poly(UDL)
m=11: DDL	m=11: poly(DDL)
m=14: PDL	m=14: poly(PDL)

Figure 2.7 : Lipase-catalyzed ring-opening polymerization [40].

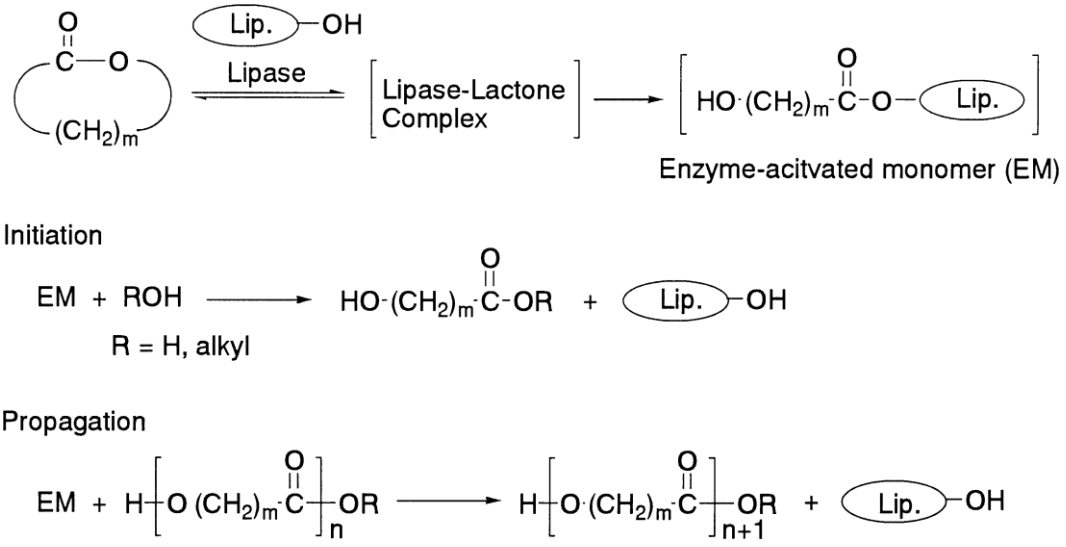

Figure 2.8 : Mechanism of lipase-catalyzed ring-opening polymerization of lactones [40].

Lipase has been used to accelerate the polymerization of lactides in organic solvents like toluene. In enzymatic polymerization studies, it is preferable to use enzymes like

Candida antarctica lipase B (CALB) either in free form or immobilized on acrylic resin (Novozyme 435®). It has been noted that at temperatures where the polymerization reaction occurs, lipase becomes more durable and active when immobilized on organic or inorganic surfaces. Because of these benefits, the immobilization procedure of the enzyme—which also directly boosts efficiency—has become a widely utilized scientific approach for producing biopolymers at a lower cost [37].

2.4.1 Poly (ω-Pentadecalactone -co-Valerolactone)

Aliphatic polyesters are a class of biocompatible and biodegradable polymers with applications in medicine, pharmacology, and the environment. Hence, they have drawn a lot of research interest. [Chang]. According to the research studies, ω-pentadecalactone (ω-PDL), ε-decalactone, δ-valerolactone (δ-VL), and ε-caprolactone (ε-CL) are the most famous and studied ones in order to their properties [41]. The polymerization reactions of macrolactones are primarily driven by entropy due to their low ring strain and bigger size. Traditional chemical techniques struggle to polymerize macrolactones, leaving only a few efficient catalysts [42]. Typically, macrolactones are converted to aliphatic polyesters using organometallic catalysts like stannous octoate and zinc lactate [41]. As a result of using metallic catalysts in the polymerization of these products, some unwanted toxic products would be produced [43]. Using enzymes to catalyze ring-opening polymerization instead of organometallic catalysts eliminates the possibility of hazardous metal contaminants in the final product, making it suitable for biomedical applications [41]. Lipases are commonly utilized in industry due to their ability to catalyze a wide range of reactions. These unusual catalysts may catalyze reactions across immiscible organic and aqueous phases and maintain catalytic activity in organic solvents. Immobilization can improve the activity, selectivity, and operational stability of enzymes in both aqueous and non-aqueous solvents, allowing for more efficient utilization [11]. Candida antarctica lipase B (CALB) has strong catalytic activity for both water-soluble and insoluble compounds. CALB's regioselectivity and chiral selectivity make it an efficient catalyst for organic reactions with high stability. It can be seen from the studies that CALB immobilization on a carrier improved its stability, increased the number of uses, and made separation from the reaction system easier, all of which contributed to a decrease in processing costs [44].

2.4.1.1 ω-Pentadecalactone

ω-Pentadecalactone is a fragrance component used in decorative cosmetics, fine scents, shampoos, toilet soaps, face cream, fragrance cream, various toiletries, and non-cosmetic items including home cleansers and detergents [45]. ω-Pentadecalactone, also known as pentadecanolide, is a cyclic ester with a 15-carbon backbone. ω-pentadecalactone may have biological actions including antibacterial and antioxidant effects. Molecular structure of ω-Pentadecalactone is given in Figure 2.9. Its potential pharmacological properties make it a suitable option for the development of pharmaceutical formulations and nutraceutical products. In polymer chemistry, ω-pentadecalactone serves as a monomer for the synthesis of biodegradable polyesters, particularly poly(ω-pentadecalactone) (PPDL). Poly(ω-pentadecalactone) (PPDL) is a semicrystalline polymer derived from pentadecanolide or ω-pentadecalactone (Poly(ω-pentadecalactone), a commercially available macrolactone commonly utilized in the fragrance industry [42]. PPDL, an important poly(ω-hydroxy fatty acid), is a crystalline polymer with 14 methylene groups and in-chain ester group linkage in each repeating unit. It has a high melting point of around 100 °C. Furthermore, PPDL has mechanical qualities similar to linear high-density polyethylene (HDPE). PPDL research is gaining popularity due to its potential for industrial-scale manufacturing, including biodegradability, thermal stability, and mechanical characteristics [46]. Before recent studies with lipase-catalyzed polymerizations, only low molecular weight poly(PDL) was accessible, leading to limited interest in its characteristics and uses. Recently, high molecular weight poly(PDL) was made available using lipase catalysis, prompting a review of its characteristics [47].

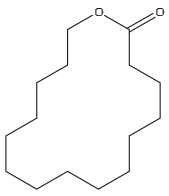

Figure 2.9 : Molecular structure of ω-Pentadecalactone [45].

2.4.1.2 δ-Valerolactone

A lactone called δ-valerolactone is used as a chemical intermediary in several processes, including the manufacture of polyesters. When polymerized, this monomer—which is derived from sugars—has characteristics similar to rubber [48, 49]. δ-valerolactone is a renewable monomer that is highly soluble in water.

Polyvalerolactone is a semi-crystalline aliphatic polyester that is hydrophobic. It is created by polymerizing δ-valerolactone monomer that the molecular structure is given in Figure 2.10. PVL is a well-established biopolymer with several uses in drug formulation and delivery systems. PVL-based polymers have been used as carriers for antifungal medicines and as a hydrophobic block in amphiphilic block copolymers for in vivo delivery of chemotherapy drugs like daunorubicin (DNR), doxorubicin (DOX), and others [50]. PVL's features include hydrophobicity, crystal structure, low melting point, and minimal cytotoxicity. PVL is also compatible with other polymers. New research and experimental results are required to achieve the best outcomes from the synthesis of these polymers. For this objective, fresh and novel copolymerization syntheses are being tried [51].

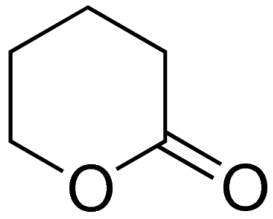

Figure 2.10 : Molecular structure of δ-Valerolactone [52].

2.5 Applications of Biopolymers

Recent research has shown that biopolymers have potential applications as materials for medical device manufacture. These biomaterials are best identified by their molecular weight, lubricity, material chemistry, water absorption degradation, form and structure, solubility, hydrophilicity/hydrophobicity, erosion process, and surface energy. Biopolymers are used in a variety of industries, including pharmaceutical encapsulation, food packaging, agriculture, cosmetics, water treatment, biosensors, and data storage (see Figure 2.11). Polysaccharide-based materials are used in several sectors, including films, membranes, fibers, hydrogels, food packaging, sponges, and air gels [53]. Biopolymers are a diverse class of materials obtained from natural sources that provide a wide range of biomedical applications due to their inherent biocompatibility and biodegradability. These polymers have received a lot of interest in drug delivery systems, with chitosan, alginate, gelatin, and hyaluronic acid standing out as promising options for encapsulating and delivering pharmaceuticals precisely and efficiently [54]. Furthermore, biopolymers play an important part in tissue engineering, where scaffolds made of collagen, fibrin, gelatin, and alginate produce a

biomimetic milieu that promotes cell proliferation and tissue regeneration [55]. Such scaffolds are useful for the repair and regeneration of a variety of tissues, including bone, cartilage, skin, and heart tissue, opening up new possibilities for regenerative medicine [56]. Furthermore, biopolymer-based wound dressings, which incorporate ingredients like chitosan, alginate, collagen, and hyaluronic acid, assist in wound healing by providing moisture retention, antibacterial activity, and encouraging hemostasis. These dressings treat various wound types while promoting tissue healing and regeneration. [57]. Biopolymers can also be used as absorbable sutures and staples in surgical procedures that need precise tissue approximation. Materials like polyglycolic acid (PGA), and polylactic acid (PLA), and their copolymers provide mechanical strength for wound closure while gradually being reabsorbed by the body, eliminating the need for suture removal operations [58]. Furthermore, biopolymers show promise in orthopedic implants, dental materials, and a wide range of other biomedical applications, demonstrating their versatility and potential to advance medical technologies and treatments [59].

Figure 2.11 : Applications of biopolymers [53].

2.6 Drug Delivery Systems

Drug delivery systems (DDS) are used to make and store drug molecules into tablets or liquids for administration [60]. Traditional dosage forms have a high dose and limited availability, inconsistency, first-pass effect, variation of plasma drug levels, and rapid release of medicinal compounds. Drug delivery systems will tackle the issues

through improved performance, protection, patient compliance, and product shelf life [61]. They speed up the delivery of drugs to the precise intended spot in the body, enhancing therapeutic efficacy while decreasing off-target accumulation [60]. Smart drug delivery systems (SDDS) direct the release of active molecules to the target location of action in response to biological or physical stimulation. These systems aim to regulate release kinetics and minimize negative effects. Systems built of stimuli-responsive polymers can alter characteristics based on environmental variables. Minor environmental changes can significantly impact polymer properties, including physical state, shape, solubility, solvent interactions, and hydrophilic/lipophilic balance. Polymers that respond to light, temperature, pH, or redox can be used to create these systems [62]. Drugs can be administered by numerous routes, including oral, buccal, sublingual, nasal, ocular, transdermal, subcutaneous, anal, transvaginal, and intravenous [60]. Figure 2.12 shows the concentration as a function of time after administration for the controlled release. Targeted drug delivery transports therapeutic agents to specified regions without affecting other parts of the body. This method targets specific parts of the body for drug delivery. This improves therapy efficacy while reducing negative effects [63]. Advancements in drug delivery technology impact bioavailability, absorption, and pharmacokinetics. Drug targeting involves four principles: loading the drug, avoiding degradation by bodily fluids, reaching the target region, and releasing the drug at a preset time [63].

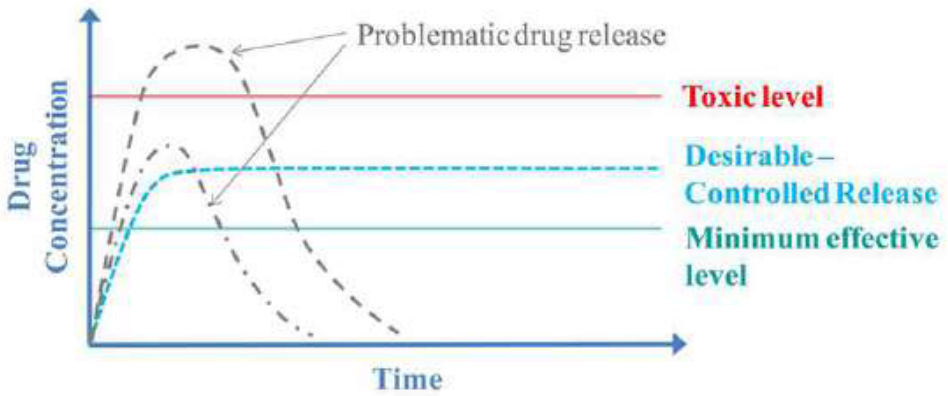

Figure 2.12 : Concentration as a function of time after administration [64].

Biodegradable and bioerodible polymers play a significant role in drug delivery [66]. Over the past 30 years, biodegradable polymeric drug delivery systems (DDS) based on aliphatic polyesters, polylactic acid (PLA), polyglycolic acid (PGA), and poly(D,L-lactide-co-glycolide) (PLGA) microspheres have been extensively studied as a

formulation approach to protect encapsulated drugs from degradation, enhance bioavailability, and sustain drug release [67]. These classes offer several benefits and are generally well-tolerated in living systems without causing harm. They are non-toxic and physiologically inert. Controlled drug delivery may be achieved using both natural and synthetic polymers, however, synthetic polymers are preferred. Controlled polymerization allows for extremely repeatable structure-function relationships. Some polymers are biodegradable, reducing the risk of accumulating in the body. However, this only applies if the breakdown by-products are non-toxic, do not trigger an immune response, and are below the renal threshold [65].

The most often utilized biodegradable synthetic polymers in drug delivery systems (DDS) are polyesters which include polyglycolide (PGA), polylactide (PLA), and copolymers with specified architecture and chemical composition (lactide to glycolide ratio). The rate of drug release might vary depending on the lactide-to-glycolide ratio. Lactide-rich polymers are very hydrophobic, resulting in delayed degradation and reduced water absorption [64]. There are three main categories of polymeric drug delivery systems; colloidal carriers (micro, nanoparticles, micelles, micro/nano gels), implantable networks or hydrogels, and polymer-drug conjugates as it can be seen from Figure 2.13. Depending on the administration model and desired release method, multiple methods of distribution can be chosen [64].

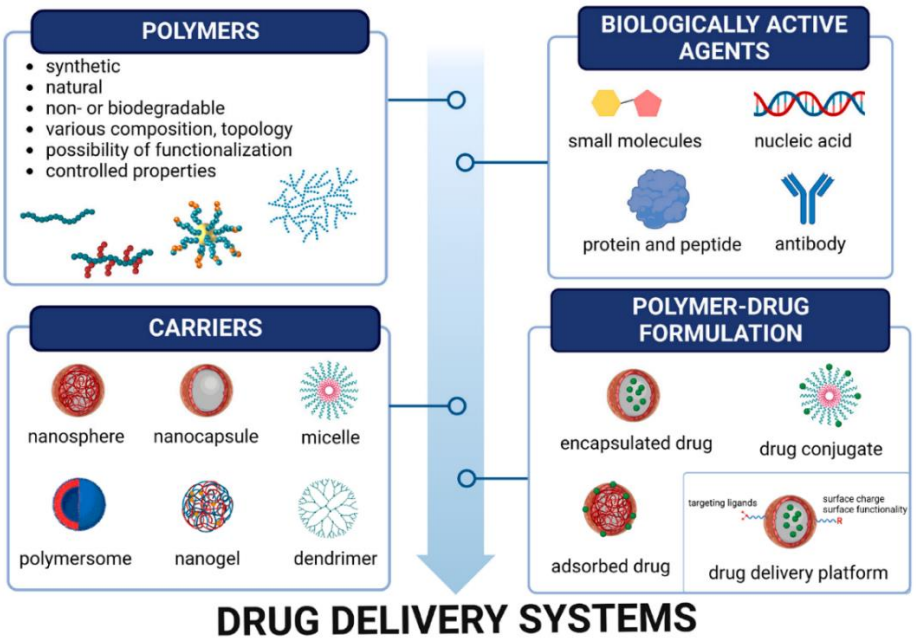

Figure 2.13 : A diagram of the formulation of polymeric carriers for biomedical delivery systems [65].

Drug release from these systems follows three broad pathways, as it can be seen in Figure 2.14. The therapeutic agent is evenly distributed in all polymer matrices, but drug release is regulated by diffusion, polymer surface erosion, or a combination of both [68]. Achieving continuous release (zero-order release) is challenging due to the decreased concentration and chemical activity of the drug. As the drug is released from the polymer matrix (i) and (iii) in Figure 2.15, its chemical activity or concentration decreases with time, resulting in first-order release rather than zero-order release. Currently, most monolithic biodegradable devices adopt either mechanism (i) or (iii), as indicated in Figure 2.15 [68].

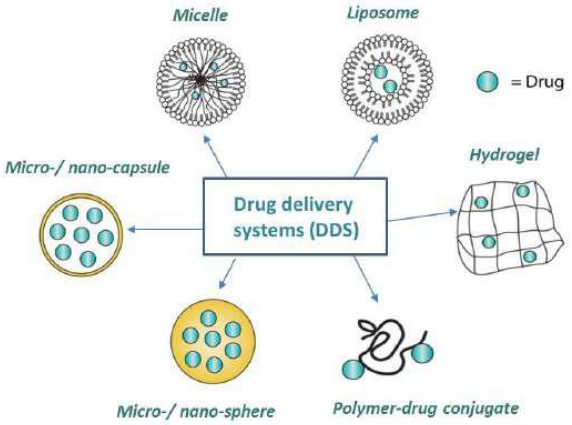

Figure 2.14 : Overview of polymeric-based drug delivery systems [64].

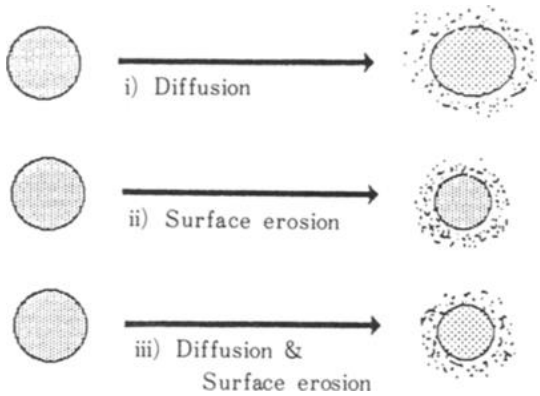

Figure 2.15 : Release mechanisms of biodegradable polymeric drug delivery systems [68].

2.7 Microspheres

Microspheres are spherically shaped particles that range in size from one to a thousand meters and their structures can be seen from Figure 2.16. The term microsphere refers to particles that might be solid or hollow [69]. Microspheres are biodegradable, free-flowing particles composed of proteins or synthetic polymers. A polymer matrix

includes distributed drug molecules, and controlled drug release can be achieved by diffusing through the matrix or by degrading the matrix itself [70]. They can encapsulate tiny compounds, proteins, peptides, and nucleic acids. They outperform nanoparticles in terms of translational efficiency and clinical success rate. They provide several advantages over conventional dosage forms, including enhanced solubility of poorly soluble drugs, protection of drugs from enzymatic and photolytic degradation, decreased dosing frequency, improved bioavailability, controlled release profile, dose reduction, and drug toxicities [71]. In terms of efficacy, microspheres have also offer several advantages. The spherical form and tiny particle size facilitate drug administration in the body. Another advantage of small particle sizes is their increased surface area, which works especially well to improve the efficiency of drugs that are not easily soluble in the body. To generate microspheres, various processes can be utilized, including single and double emulsion solvent evaporation, sedimentation polymerization, spray-drying, electrospraying, and phase separation technologies [70].

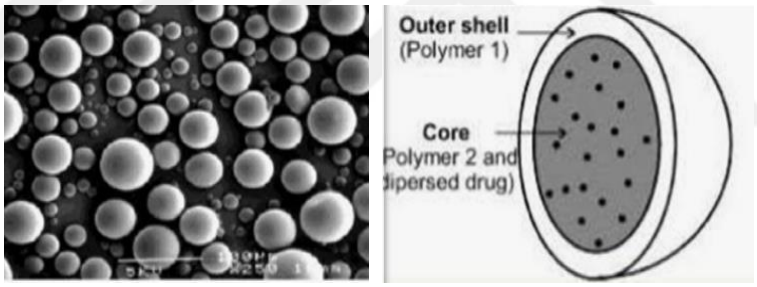

Figure 2.16 : Microspheres [72].

Microspheres are able to be targeted to a specific area using active or passive targeting approaches. Passive targeting is based on the microspheres' size and general surface features, such as hydrophobicity, surface charge, and non-specific adhesion, which lead them to a given organ. Active targeting, on the other hand, is most commonly connected with ligand-receptor recognition, which is known as secondary active targeting. The increasing number of studies in recent years demonstrating the potential use of microspheres as drug delivery carriers for targeted delivery has captured the interest of researchers throughout the world [71].

2.7.1 Emulsion/solvent evaporation method

Microspheres can be produced by evaporating an organic solvent from dispersed oil droplets containing polymers and drugs [73]. Extensive research has been conducted

on the solvent evaporation approach for producing microspheres of biocompatible polymers and copolymers [74]. Microencapsulation using solvent evaporation is commonly utilized in the pharmaceutical industry to create controlled-release formulations. Microencapsulation can be achieved by several solvent evaporation techniques. The hydrophilicity or hydrophobicity of the active molecules determines the most suitable approach for drug encapsulation [75]. The easiest approach for producing drug-loaded microspheres is emulsion/solvent evaporation. The emulsion could either be single or double, depending on the solubility of the polymer and the drug being used. The single O/W (oil-water) emulsion/evaporation process consists of two phases: organic (internal or dispersed) and aqueous (external or continuous) as indicated in Figure 2.17. The organic phase is comprised of polymer and drugs dissolved in an organic solvent, which is then emulsified with water. The aqueous phase is an aqueous solution with high hydrophilic-lipophilic balance (HLB) surfactants; typically, an aqueous polyvinyl alcohol (PVA) solution is employed as the continuous phase [76]. It is waited in the mixing position until the organic solvent evaporates [73].

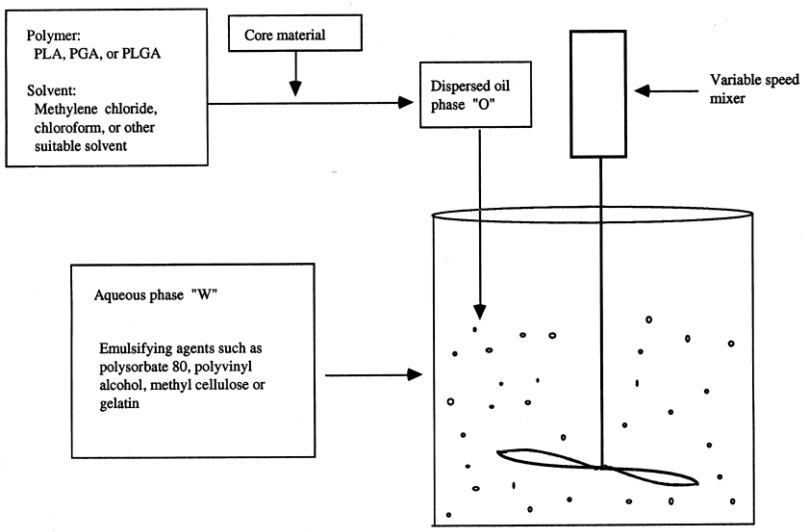

Figure 2.17 : Schematic diagram of O/W emulsion solvent evaporation method [76].

Figure 2.18 shows the formation of microcapsules by single O/W emulsion/solvent evaporation method. However, when the drug that needs to be encapsulated is insoluble in the organic phase, multiple emulsions are required. The double emulsion technique for microspheres creates several emulsions (w/o/w) and is ideal for water-soluble pharmaceuticals, peptides, proteins, and vaccines. This approach works with both natural and synthetic polymers. The aqueous protein solution is distributed in a

lipophilic organic continuous phase. This protein solution may include active components. The continuous phase contains a polymer solution that encapsulates protein from the scattered aqueous phase. The initial emulsion is sonicated before being added to an aqueous solution of polyvinyl alcohol (PVA). This leads to the creation of a double emulsion as it is given in Figure 2.19. The emulsion undergoes solvent removal by either evaporation or extraction [72].

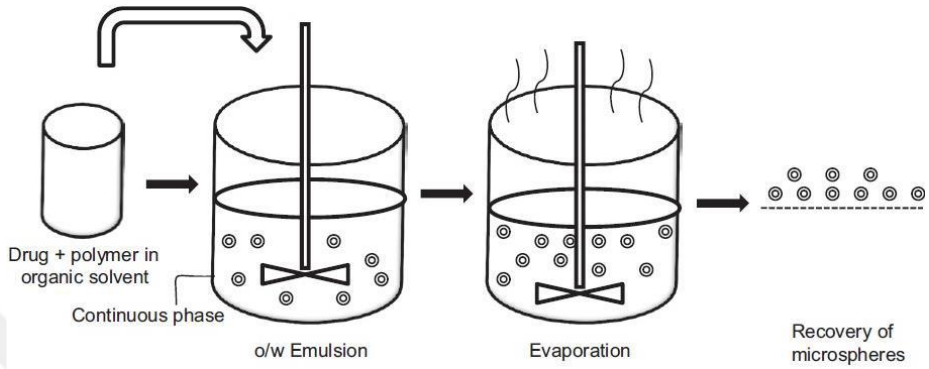

Figure 2.18 : Formation of microcapsules by single O/W emulsion/solvent evaporation method [77].

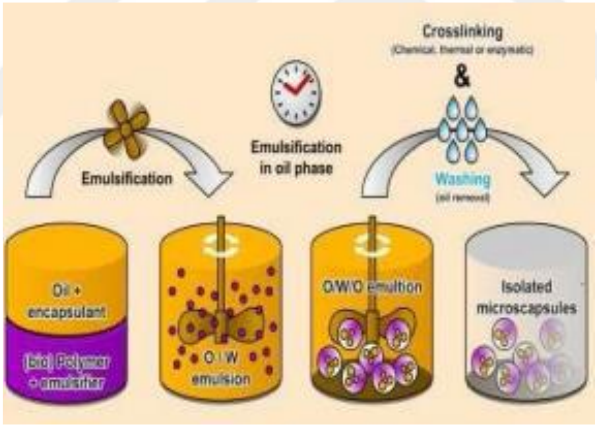

Figure 2.19 : Microspheres created using the Double Emulsion Technique [72].

Emulsion solvent evaporation has many advantages over other preparation processes, including spray drying, sonication, and homogenization. It requires just basic conditions like ambient temperature and steady stirring. This allows for a stable emulsion while maintaining pharmacological activity [78].

2.8 Oleuropein

Oleuropein, the main component of Olea europea, known as the olive tree, belongs to a very special group of coumarin-like compounds called secoiridoids, which are abundant in oleaceae, gentianales, cornales, and many other plants. Figure 2.20

indicates the molecular structer of oleuropein. Oleuropein, the heterosidic ester of elenolic acid and hydroxytyrosol, has many beneficial effects on human health. According to research, it has been observed that oleuropein has various pharmacological properties such as antioxidant, anti-inflammatory, antiatherogenic, anti-cancer, antimicrobial, and antiviral, and for these reasons, it is commercially available as a food supplement in Mediterranean countries. Additionally, research has demonstrated that oleuropein has anti-ischemic, hypolipidemic, and cardioprotective properties against acute adriamycin cardiotoxicity. A study also revealed that oleuropein aids in the prevention of Alzheimer's disease. The phenol components of olive oil, particularly oleuropein, which functions as a free radical scavenger at the skin level, were demonstrated in another study to have a direct antioxidant impact on the skin [79, 80].

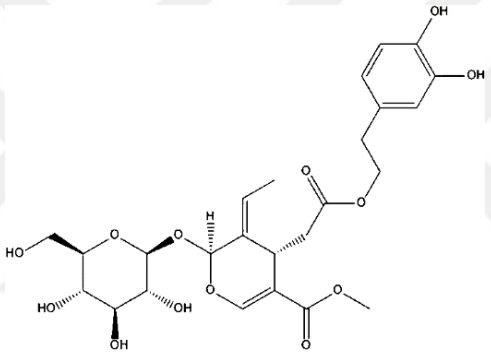

Figure 2.20 : Molecular structure of oleuropein [81].

2.9 Transchalcone

Chalcones are open-chained compounds found naturally in plants. As shown in Figure 2.21, their chemical structure consists of two aromatic rings separated by a three-carbon, -unsaturated carbonyl system [82]. Such structure is the primary distinction between chalcones and other flavonoids [83]. By adding functional groups to the aromatic rings, chalcones' chemical structure can be varied. Chalcone molecules act as pigments in plants due to their characteristic, vivid yellow color. Due to their natural abundance, simplicity in manufacture, and biological activity, chalcones have recently drawn interest in terms of biology. It is known that a number of chalcones and chalcone derivatives show anticancer efficacy against a variety of forms of cancer, including breast, colon, ovarian, bladder, and urinary tract cancers, as well as antifungal, anti-tuberculosis, anti-AIDS, and antidiabetic activities. Chalcones can be chemically

synthesized by Claisen-Schmidt condensation reaction. The reactants are acetophenone and benzaldehyde, and the reaction is catalyzed by a base, generally NaOH or KOH [84].

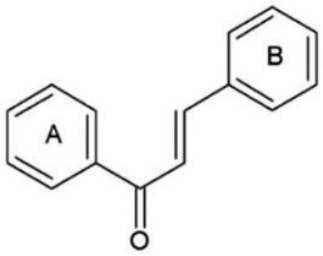

Figure 2.21 : Molecular structure of trans-chalcone [84].

3. MATERIALS AND METHODS

3.1 Materials

Rice husks were kindly supplied by a local rice production facility (Edirne, Turkey) and treated to obtain rice husk ash (RHA). (3-APTES, $C_9H_{23}NO_3Si$, 98 %, Sigma-Aldrich), was used in the experiments for surface modification of RHA. During the preparatory preparation stage, rice husks were rinsed with distilled water to eliminate extraneous contaminants. Dried rice husks were burnt for 6 hours at 600-650 °C to produce RHA, which were then employed as a support material for enzyme immobilization. Reactions were catalyzed by immobilized Candida antarctica Lipase B (CALB) enzyme (E.C. 3.1.1.3, recombinant, expressed in Aspergillus niger, Sigma). CALB in free form purchased from Sigma Aldrich was immobilized onto RHA. Surface modification of RHA was achieved by 3-aminopropyl triethoxysilane (3-APTES) ($C_9H_{23}NO_3Si$) (Merck) treatment. Acetone (C_3H_6O, 100 %, Merck) was used as medium in surface modification of RHA. Sodium dihyrogen phosphate monohydrate (NaH_2PO_4. H_2O) (Carlo Erba) and disodium hydrogen phosphate heptahydrate (Na_2HPO_4. $7H_2O$) (Merck) were used for preparation of 0.015 M, pH = 7 phospate buffer solution. δ-valerolactone (δ-VL) ($C_5H_8O_2$, Sigma-Aldrich) and ω-pentadecalactone (ω-PDL) ($C_{15}H_{28}O_2$, Sigma-Aldrich) was used as monomer in polymerization reactions. Toluene (C_7H_8, 99.8 %, Merck) was used as organic solvent in polymerization reactions. Chloroform ($CHCl_3$, 99 %, Merck) was used to terminate polymerization reactions and as solvent for PPDL-PVL copolymers during microsphere formation. For the termination of polymerization reactions and precipitation of obtained polymers methanol (99% CH_3OH) (Emboy) were also used, was respectively purchased from Merck. Chloroform (99%, $CHCl_3$) (Merck) was used to solubilize polymer samples for ^1H NMR analysis. Transchalcone (TC, $C_{15}H_{12}O$, 97%, Sigma-Aldrich), model drug, was purchased from Sigma-Aldrich. During preparation of TC/Oleuropein-loaded microspheres, dichloromethane (CH_2Cl_2, 99 %, Carlo Erba) was used as solvent of TC, in the internal phase. Poly(vinyl alcohol) $(C_2H_4O)n$, Sigma-Aldrich) was used as an organic solvent during the preparation of

TC/Oleuropein loaded microspheres. Oleuropein, antibacterial agent, was purchased from natural supplier. Methanol (CH_3OH, 99.8 %, Merck) was used in determination of loading efficiency of the microspheres. Potassium di-hydrogen phosphate (KH_2PO_4, 100 %, Carlo Erba) and di-potassium hydrogen phosphate (K_2HPO_4, 100 %, Merck), sodium chloride (NaCl, 99.6 %, Carlo Erba), potassium chloride (KCl, 100 %, Merck), disodium phosphate dihydrate ($Na_2HPO_4.2H_2O$, 100 %, J. T. Baker), sodium dihydrogen phosphate (NaH_2PO_4, 100 %, Merck), acetic acid (CH_3COOH, 99.8 %, Merck), sodium acetate (CH_3COONa, 99 %, GPR) and hydrochloric acid (%37 puriss.) (HCl, Riedel-De Haën) were used to prepare buffer solutions for enzyme immobilization and drug release studies. For the preparation of proton nuclear magnetic resonance (^{1}H-NMR) samples, deuterated chloroform ($CDCl_3$, Merck, 99.8%) was used. In antibacterial test for preparation of liquid and solid media for cultured bacteria were Agar-Agar and Nutrient Broth (Merck) were used. *Staphylococcus aureus* (ATCC 6538) and *Escherichia coli* (ATCC 8739) bacteria were kindly provided by Istanbul Technical University Food Engineering Department. In WST test, MCF-7 human breast cancer cell was used. WST-1 solution was purchased from Sigma-Aldrich, whereas Eagle's minimum essential medium (EMEM), fetal bovine serum (FBS), trypsin-EDTA, and Trypan blue were obtained from Gibco BRL and utilized in cell viability assays. All chemicals and reagents were of analytical grade.

3.2 Methods

3.2.1 Preparation of support material for the enzyme immobilization

First, rice husks were rinsed with distilled water to eliminate any contaminants. After the rinsing, they dried in an oven at 30 °C overnight. After that, the dried rice husks were burned in oven at between 600-650 $^{\circ}$C for 6 hours. The oven's temperature was continually checked and increased by 10°C per minute until the burning temperature was attained. After the burning process was finished, the rice husk ashes (RHA) were transferred to a desiccator to prevent moisture after cooling [11]. Figure 3.1 shows a picture of the processed rice husks.

Figure 3.1 : From left to right: dried rice husk, rice husk ash after combustion.

Before the immobilization process, the surface of the support material was silanized using the agent 3-APTES as it is described in previous studies [11]. 250 mg RHA was combined with 15% (v/v) 3-APTES in 5 mL acetone. The mixture was incubated in a shaking water bath (Julabo SW22) at 50°C and 160 rpm for 2 hours. Figure 3.2 shows the shaking water bath utilized in the studies.

Figure 3.2 : Shaking water bath used in experiments.

After the reaction, surface-modified (activated) RHA was filtered and rinsed with distilled water using a vacuum pump (Sartorius stedim 16612) to remove any unreacted chemical substances. Then, dried in oven at 60°C for 2 hours.

0.015 M, pH 7 phosphate buffer was prepared by mixing 29.25 mL 1M $NaH_2PO_4.H_2O$ and 45.75 mL 1M $NaH_2PO_4.7H_2O$ with distilled water and diluting to 1 L with distilled water. The pH of the buffer was adjusted using a pH meter (Inolab TWT).

3.2.2 Immobilization of CALB

The prepared supports were used for lipase immobilization. CALB was immobilized on surface-modified RHA via a physical adsorption technique, as previously described [11]. CALB and RHA were mixed in 25 mL of 0.015 M pH 7 phosphate buffer with a 2μL/mg enzyme loading ratio for 5 hours at room temperature. At the conclusion of the interval, immobilized lipase was filtered and dried in an oven at 300 °C for 12 hours. Figure 3.3 shows a picture of the filtered enzyme.

Figure 3.3 : Filtered immobilized enzyme after the immobilization via physical adsorption.

3.2.3 Enzymatic synthesis of poly(ω-pentadecalactone-co-δ-valerolactone)

Immobilized CALB was utilized as a biocatalyst for the copolymerization of pentadecalactone and valeractone. The copolymerization technique was the same as the previous work in which poly(ω-pentadecalactone-co-ε-caprolatone) copolymers were produced [41]. Reactions were carried out in 1 g toluene in a nitrogen environment. The weight ratio of toluene to total monomers was 1:2, with an enzyme concentration of 20%. The reaction mixture was agitated at 120 rpm at 80°C. Copolymers with monomer ratios (75%-25% in weight ratios) were manufactured in 24 hours. In the previous study [37], different monomer ratios and polymerization times were tried and it was decided that these were the most ideal ratios. Therefore, this study proceeded directly through these rate and time parameters. At the end of the process, additional chloroform was used to stop the polymerization. The enzyme was then isolated by filtering, and the chloroform was evaporated in an oven set to 500°C. The copolymer was collected by precipitation in cold methanol. The precipitated

copolymer samples were filtered and dried in an oven at 350°C. Figure 3.4 shows pictures of the enzymatic polymerization equipment and glass reactor.

Figure 3.4 : Apparatus used for polymerization.

3.2.4 Preparation of microspheres

Microspheres were prepared by conventional O/W emulsion/solvent evaporation method [85]. Internal phase consisted of TC solution in dichloromethane (DCM) and PPDL-PVL copolymer with/without Oleuropein in chloroform (CH). Amount of PPDL-PVL copolymer system was varied, maintaining the TC:PPDL-PVL ratio at 1:10, 1:5 and 1:2.5. In the previous studies, various PVA solution concentrations (0.1, 0.5 and 1 (w/v) %) was used and it can be seen that 1 (w/v) % was the most suitable concentration for microsphere fabrication [85]. External phase was PVA solution with constant concentration (1 (w/v) %) to be able to observe the effects of different concentrations on TC loading and release. First, TC solution and PPDL-VL solution were well mixed by a vortex mixer. This solution was added to 50 ml of PVA solution under agitation at 1500 rpm for 5 min to form a milky white emulsion. The emulsion was then diluted with 50 mL of distilled water and stirred for 24 hours to allow the solvents to evaporate. After evaporation, the emulsion was centrifuged to remove the PVA and noncapsulated TC, and the microspheres were dried overnight in a 30°C oven. The encapsulation efficiencies (EC) and loading capacities (LC) of the microspheres were determined directly by extracting the drug content with methanol [85]. Methanol dissolves the chalcone contained in the particles but not the polymer, hence the polymer did not interfere with the UV spectrophotometer absorbance measurements [85]. The resultant suspension was filtered, and the absorbance was

measured at 308 nm using a UV spectrophotometer with methanol as the blank solution (a calibration curve is supplied in Appendices A). The formulae used to calculate encapsulation efficiency and loading capacity are as follows.

$$EE\ (\%) = \frac{(weight\ of\ TC\ in\ the\ microspheres)}{weight\ of\ TC\ in\ the\ emulsion} x100 \quad (3.1)$$

$$LC\ (\%) = \frac{(Actual\ weight\ of\ TC\ in\ the\ microspheres)}{Total\ weight\ of\ microspheres} x100 \quad (3.2)$$

3.2.5 In vitro TC release from loaded microspheres

Drug release characteristics from microspheres were investigated. Drug release experiments were carried out using PBS solution (pH 7.4, 0.1 M) as the release medium. 10 mg of loaded microspheres were suspended in PBS solution and shaken in an incubator at 37°C and 120 rpm. At the prescribed time intervals, a 1 ml aliquot was taken and the same volume of fresh PBS solution was added. If necessary, the aliquot was filtered using syringe filters to eliminate any suspended microspheres that were present. The withdrawn sample was diluted to 10 ml with PBS, and the absorbance was measured using a UV spectrophotometer. The pH-responsive release behavior of the loaded microspheres was examined by shifting the release medium to an acetate buffer solution (pH 5.6). All release experiments were conducted under sink conditions. Related calibration curves were presented in the Appendices A.

3.2.6 Kinetic model fitting

The drug release patterns were fitted to kinetic models to better understand the process of drug release in each sample. The data was fitted to the Higuchi and Korsmeyer-Peppas kinetic models using nonlinear regression, and the associated kinetic parameters were determined. The equations used for the kinetic models are shown below.

$$Higuchi: Q_t/Q_\infty = K_H \times t^{0.5} \quad (3.3)$$

$$Korsmeyer - Peppas: Q_t/Q_\infty = K_{KP} \times t^n \quad (3.4)$$

Where Q_t/Q_∞ is the fraction of drug released at time t and n is the release exponent. K_H ($t^{-0.5}$) and K_{KP} (t^{-n}) are the Higuchi and Korsmeyer-Peppas release rate constants, respectively.

3.2.7 Antibacterial activity test of microspheres

Antibacterial activity of PDL-VL, PDL,VL/Olu and TC-loaded PDL-VL/Olu microspheres was investigated by application of turbidimectric method. As it is described in previous studies, Two distinct bacterial species were chosen: gram-negative *Escherichia coli*, and gram-positive *Staphylococcus aureus*. First, the drawing method was used to cultivate bacteria on slant nutrient agars. Slanted agars cultured with bacteria were incubated for one night at 37°C. Following that, liquid media (Nutrient Broth) were inoculated with bacterial samples extracted from the slanted agar and incubated for a full day at 37°C. Figure 3.5 depicts the incubator that was utilized [37].

Figure 3.5 : Incubator that was used for antibacterial activity test.

The MacFarland densiometer was used to set the turbidimeter to 0.5 McFarland for each type of bacteria. In Figure 3.6, the McFarland densitometer picture that was utilized is displayed. For every species of bacterium, the concentration of standardized inoculums was 10^8 CFU/ml. Following the dilution processes for each bacteria in Figure 3.7, the obtained bacterial cultures were diluted first to 10^{-1} (10^7 CFU), then to 10^{-2} (10^6 CFU), and lastly to 10^{-3} (10^5 CFU), at which the antibacterial test was to be applied.

Figure 3.6 : Left to right: McFarland Densitometer and 0.5 MF adjusted bacteria cultures from each type of bacteria.

Microspheres containing different ratios of PDL-VL, PDL,VL/Olu and TC-loaded PDL-VL/Olu and control samples are placed in a 10^{-3} diluted bacterial suspensions to the amount of 3 mg in powder form. Suspensions with and without membrane samples were incubated at 37^{0}C for 24 hours in shaking water bath.

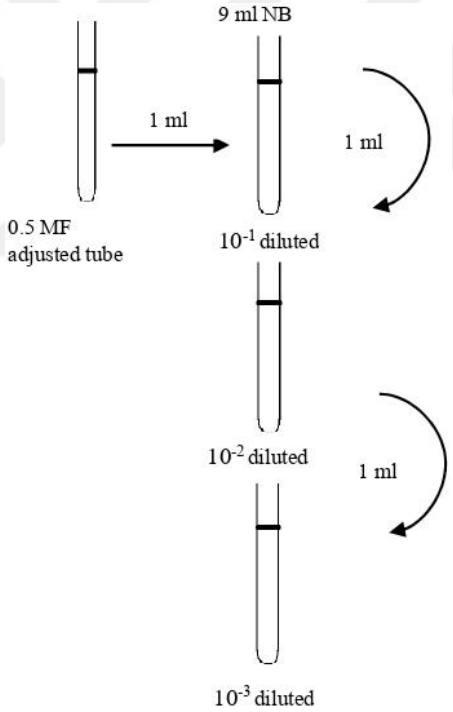

Figure 3.7 : The scheme followed in the dilution step.

Following the incubation period, 200 µl suspension samples were extracted and inserted into the 96-well plate wells. As agreed upon in scientific investigations [86, 87], measurements were made in a microplate reader (BioTek, Synergy HT) at 600 nanometers. Figure 3.8 shows the picture of the wells and the microplate reader that was utilized.

Figure 3.8 : Microplate Reader and 96-Well Plate.

The measured absorbance and antibacterial activity values were calculated using Equation 3.5 [88].

$$Antibacterial\ activity\ (\%) = \left(\frac{OD_1 - OD_2}{OD_1}\right) x\ 100 \qquad (3.5)$$

In this equation, OD_1 represents the absorbance value of bacterial culture without microspheres, and OD_2 represents the absorbance value of bacterial cultures containing microsphere samples of PDL-VL, PDL-VL/Olu and TC-loaded PDL-VL/Olu.

3.2.8 In vitro cytotoxicity (WST) test of microspheres

The MCF-7 (human breast cancer cell) line was chosen as the cells to be tested. WST test was perform with positive and negative control. Positive control was carried out in the presence of a substance with known toxic effects (H_2O_2 was used), and negative control was carried out in the presence of a substance that was not a sample but contained only cell medium. The cells were kept in 25cm^2 flasks with Eagle Minimum Essential Media (EMEM) containing 10% fetal bovine serum after being passaged eighteen times. (FBS; P30-1301, Pan Biotech) It was examined twice a day until a growth rate of at least 70% was attained. (Duplicating duration: 28–32 hours) The samples' DMSO concentrations were set to 20 mg/mL during the preparation of the stock solution. Vibration was used to sonicate samples in the medium. Subsequently, the samples were incubated at room temperature for 24 hours at a speed of 25 rpm. After centrifuging the samples for ten minutes at 2500 rpm, the separated supernatant was employed in the cytotoxicity test.

Cells exhibiting a growth rate of 70% or above were treated with 500µL of Trypsin-EDTA. The cells were treated with 5% CO_2 at 37°C for three to five minutes. As soon

as the cells beneath the inverted microscope started to separate from one another, the media containing 10% FBS was added. (Germany: Zeiss Primovert) To get rid of the medium, the sample was centrifuged for five minutes at 300 x g. After that, 1 mL of EMEM medium was added. Trypan blue was used in conjunction with the Logos Luna II device to count cells. After counting, 104 cells per well in a 96-well plate were introduced to media containing 10% FBS.

The culture media was taken out after 72 hours incubation and measured. A concentration of 500 µg/µl of the active ingredient was used in EMEM medium containing 10% FBS. Three duplicates of the group were administered in three separate wells. The cells were cultured for 22 hours following the administration of the samples. Ten percent of the well capacity was filled with WST-1 solution. (20 microliters) The cell culture plate was incubated for two more hours in the incubator after it had been covered with aluminum foil. After 2 hours of additional incubation, measurements were taken in the cell culture dish at wavelengths of 430 and 650 nm. The percent viability results of the cells were calculated and formulated using Equation 3.6.

$$\%\, Cell\ Viability = \frac{Sample\ well - \ Blank}{Positive\ control - Blank} x100 \qquad (3.6)$$

3.3 Characterization Techniques

3.3.1 Gel permeation chromatography (GPC)

The molecular weights of the produced PDL-VL copolymers were determined using gel permeation chromatography. Measurements were done using an Agilent 1100 type GPC equipment. To prepare the samples, 3 mg of PDL-VL copolymer was dissolved in 1 mL of THF for each. The produced solutions were filtered through a 0.45 µm filter using a syringe before being added to the device for finalization.

3.3.2 Scanning electron microscope (SEM)

Surface structure of the microspheres were observed by using a scanning electron microscope (SEM, TESCAN VEGA 3). Scannings were operated at 15 kV.

3.3.3 Fourier transform infrared spectroscopy (FT-IR)

Perkin Elmer's FT-IR Spectrum One B Spectrometer was used to analyze the chemical structure and content of Olu, PDL-VL, PDL-VL/Olu microspheres, TC-loaded PDL-VL/Olu microspheres and TC samples. The variations in functional groups following each phase of enzyme immobilization can be seen by FT-IR measurement. Furthermore, using FT-IR, the synthesized polymer was identified as PDL-VL by comparing it to the distinctive functional groups and bonds of PDL-VL. Each sample was tested using KBr pellets. The spectra were collected using at least 32 scans with a resolution of 2 cm^{-1}.

3.3.4 Hydrogen nuclear magnetic resonance spectroscopy (^{1}H-NMR)

The conversions of the produced PDL-VL copolymers were determined using hydrogen nuclear magnetic resonance spectroscopy (^{1}H NMR). Prior to analysis, samples were thawed with chloroform. The characteristic choices for ω-PDL and δ-VL are as follows. Investigations were conducted using the calculations in the following section:

m: Number of δ-VL units n: Number of ω-PDL units DP_n: Degree of polymerization

M_n: Number average molecular weight (g/mol)

$I_{4.35}$, $I_{4.06}$, $I_{3.65}$, $I_{1.64}$, $I_{1.26}$: Related peak integrals

Characteristic peaks were assigned to the related protons of ω-PDL and δ-VL homopolymers according to the literature as follows [37]: δ 4.06 (OCH_2), δ 3.65 (HOCH_2), δ 2.30 (COCH_2), 1.64 and 1.26 (all other protons) ppm. Conversion rates are calculated with the following Equation 3.7 and Equation 3.8.

$$\begin{gathered} 2m + 2n = I_{4.06} \\ 4m + 24n = I_{1.64} + I_{1.26} \\ DP_n = \frac{I_{4.06} + I_{3.65}}{I_{3.65}} \end{gathered} \tag{3.7}$$

$$\begin{gathered} M_n = 241.38 + 101.116 + DP_n \times (100.116 \times Molar\ composition\ of \\ \delta - \mathrm{VL} \times 0.01 + 240.38 \times Molar\ composition\ of \\ \omega - \mathrm{PDL} \times 0.01) \end{gathered}$$

$$Total\ conversion = \frac{I_{4.06}}{I_{4.06} + I_{4.35}} \times 100 \quad (3.8)$$

3.3.5 Differential scanning calorimetry (DSC)

Differrential scanning calorimetry (DSC) employing TA instruments Q10 calorimeter utilized to determine thermal characteristics. Measurements were conducted in an inert nitrogen environment at a flow rate of 50 ml min^{-1} and analyzed. Melting temperature (T_m) and glass transition temperature (T_g) were measured using heat-cool-heat thermal cycles on samples ranging from -80 to 20000°C at a rate of 1000°C min^{-1}.

3.3.6 Thermal gravimetric analysis (TGA)

Thermal characterization of surface-modified RHA and PCL samples were carried out by TGA. For this aim, 5-10 mg of samples were heated from room temperature to 1000˚C with a rate of 10˚C/min under air flow. The apparatus used is SEIKO TG/DTA 6300.

3.3.7 X-Ray diffraction analysis (XRD)

For the investigation of crystal structures of PDL-VL samples and microspheres, X-Ray diffraction (XRD) patterns were identified by (XRD, Rigaku MiniFlex) with Cu-Kα radiation over the range from 5° to 70° with a step size of 0.02°. Crystallinity percentage (X_c) was calculated by the following equation.

$$X_c = \frac{Total\ area\ of\ all\ crystalline\ peaks}{Total\ area\ of\ all\ peaks} \times 100 \quad (3.9)$$

3.3.8 Ultraviolet (UV) spectrophotometer

Encapsulation rate of microspheres and the amount of transchalcone released was determined by measuring absorbance on Ultraviolet (UV) spectrophotometer. Solutions containing different transchalcone concentrations were prepared to obtain calibration graph. pH 5.6 acetate buffer, pH 7.4 phospate buffer and methanol were prepared as blank solution.

3.3.9 Dynamic light scattering analysis (DLS)

Particle size measurements were carried out by Dynamic Light Scattering (DLS, Malvern Zetasizer Nano ZS) method. Zeta potential measurements (Malvern Zetasizer Nano ZS) of PDL-VL, PDL-VL/Olu and TC-loaded PDL-VL/Olu samples were carried out in distilled water.

4. RESULTS AND DISCUSSION

4.1 Synthesis of Poly(ω-pentadecalactone-co-δ-valerolactone) with Immobilized Enzyme

Prior research has demonstrated that in toluene medium, ω-PDL and ε-CL exhibited ring-opening polymerization in conjunction with handmade immobilized CALB. A synthetic ω-PDL-co-ε-CL was created, possessing an average molecular weight (M_n) of 20960 g/mol [89]. In contrast to earlier research, this study examined the immobilized CALB's copolymerization performance for δ-VL and ω-PDL in order to choose which ones to use for the creation of microspheres. Previous research used various parameters to investigate the effects of polymerization duration and monomer ratio on the molecular weight of the copolymer. In this study, the ratio of 75:25 (wt.%) was investigated. The temperature was kept constant at 80 ^{0}C, where the highest efficiency was achieved in previous studies [41]. The molecular weight of the PDL-VL copolymer synthesized according to the procedure described in this reference was found to be 23722 $(g/mol)^2$ [41]. During the 24-hour polymerization period at 800°C, the combination with 75% ω-PDL feed ratio produced the highest M_n levels at a conversion rate of 96.6% [41].

4.2 Fabrication of Microspheres

Enzymatically synthesized copolymer (PDL-VL), which was produced to be studied in biomedical applications, was made into a microspheres due to its large surface area and many pharmacokinetic advantages brought with it as it is decribed before. TC-loaded PDL-VL/Olu microsphere structures are produced by emulsion/solvent evaporation method. In the previous studies various microsphere formulations were prepared to investigate the effect of the process parameters [85]. As it is decribed in previous study, the external phase of the microsphere formulations was PVA with varying concentrations (0.1, 0.5 and 1 %) were investigated and summarized. According to the results obtained, 1% PVA concentration in the external phase resulted in greater encapsulation efficiency, which can be attributed to the increased viscosity, which inhibits

drug diffusion into the external phase [85]. Hence, in this study, microspheres are produced with %1 PVA concentration in the external phase. In previous study, the effect of internal phase concentration also examined [85]. In this study, different Olu and TC ratios on PDL-VL were also examined as it can be seen from the Table 4.1.

Table 4.1 : Microsphere formulations, encapsulation efficiencies, mean particle diameters and zeta potentials.

Sample Code	Olu:PDL-VL ratio (%)	TC:PDL-VL ratio (%)	Encapsulation Efficiency (%)[1]	Mean Particle Diameter (μm)[2]	Zeta Potential (mV)[2]
A-1	0	0	-	2.9 ± 1.7	-14.3 ± 0.1
A-2	0	20	39.0 ± 3.4	8.5 ± 4.5	-16.0 ± 2.4
B-1	42.5	0	-	2.0 ± 2.0	-6.3 ± 1.3
B-2	42.5	20	29.3 ± 6.3	9.1 ± 1.7	-3.1 ± 0.6
C-1	75	0	-	0.5 ± 0.2	-20.3 ± 3.1
C-2	75	20	58.4 ± 8.5	0.4 ± 0.03	-19.0 ± 1.0
D-1	100	0	-	2.2 ± 0.4	-7.8 ± 2.4
D-2	100	10	70.3 ± 0.4	0.8 ± 0.2	-5.9 ± 1.1
D-3	100	20	81.7 ± 0.5	3.4 ± 1.9	-6.5 ± 0.6
D-4	100	40	59.2 ± 0.2	1.3 ± 0.7	-1.9 ± 2.2

[1]Calculated from Equation 3.1.
[2]Measured by Malvern Zetasizer Nano ZS.

In general, the copolymer mass was kept constant at 50 mg, and experiments were carried out with 22.5 mg, 37.5 mg and 50 mg Olu amounts. (%42.5 = 22.5 mg, %75 = 37.5 mg and %100 = 50 mg Olu amounts) On the other hand, studies were carried out with TC amounts of 5 mg, 10 mg and 20 mg. (%10 = 5 mg, %20 = 10 mg and %40 = 20 mg TC amounts) At the same time, microsphere productions without the addition of TC or Olu and without both were also produced and examined. As can be seen in Table 4.1, it was determined that microspheres produced at 100% Olu:PDL-VL ratio and 20% TC:PDL-VL ratio (Sample D-3) had the highest encapsulation efficiency (%). Encapulation efficiency was calculated by using Equation 3.1. It was observed that the encapsulation efficiency increased by increasing the Olu ratio from 42.5% to 100%, and at the same time, it was observed that the 100% Olu:PDL-VL ratio was kept constant and the TC:PDL-VL ratio increased the encapsulation efficiency during the transition from 10% to 20%. However, it was observed that there was a decrease in encapsulation efficiency at 40% TC:PDL-VL ratio. As can be seen from the results, when TC and Olu were not present, the mean particle diameter was determined as 2.9±1.7, and in the presence of 20% TC by mass, the mean particle diameter values of the microspheres increased suddenly and were seen as 8.5±4.5. From here, it can be

concluded that TC loading significantly increases the mean particle value. On the contrary, when Olu was added at 42.5% and 75% by mass, the mean particle diameter values were found to be 2.0±2.0 and 0.5±0.2, respectively. From here, it can be concluded that the addition of Olu also reduces the mean particle diameter value. It has been observed that at lower mean particle size values, the encapsulation efficiency is higher. While the internal and external phase parameters do not vary, the stirring rateon different stirrers may have caused variability in the mean particle diameter value. Because, as can be seen in the previous scientific study, increasing the stirring rate has an effect on this value [85]. Having a small particle size is a desired feature in microspheres. The spherical shape and tiny particle size make it simple to use the drug delivery system in the body. Another advantage of tiny particle size is greater surface area, which is especially useful for boosting the action of poorly soluble drugs [70]. Zeta potential values were negative as expected. In particular, it was observed that the absolute Zeta potential value reached the highest level when 75% Olu by mass was added and 20% TC was loaded. The presence of carboxyl groups can be shown as the reason for this.

4.3 Characterization of Microspheres

For the characterization of the chemical and mechanical properties of the produced PDL-VL copolymers and microspheres, PVL-VL/Olu and TC-loaded PDL-VL/Olu microspheres SEM, FT-IR, DSC, TGA and XRD measurement analyzes were applied and investigated.

4.3.1 SEM results of microspheres

Table 4.2 shows the sample codes and Olu and TC ratios which is used for microsphere fabrciations. A series of optical microscope pictures were utilized to observe particle shape and determine particle size as it can be seen from the Figure 4.1. Spherical geometry was found in all microsphere formulations. SEM photographs of individual microspheres were examined. PDL-VL, PDL-VL/Olu, and TC-loaded PDL-VL/Olu microspheres were spherical in shape with a highly porous and rough surface structure, as predicted for an atmospheric solvent evaporation approach [76].

Table 4.2 : Sample codes, Olu and TC ratios in order to PDL-VL copolymers.

Sample Code	Olu:PDL-VL ratio (%)	TC:PDL-VL ratio (%)
A-1	0	0
A-2	0	20
B-1	42.5	0
B-2	42.5	20
C-1	75	0
C-2	75	20
D-1	100	0
D-2	100	10
D-3	100	20
D-4	100	40

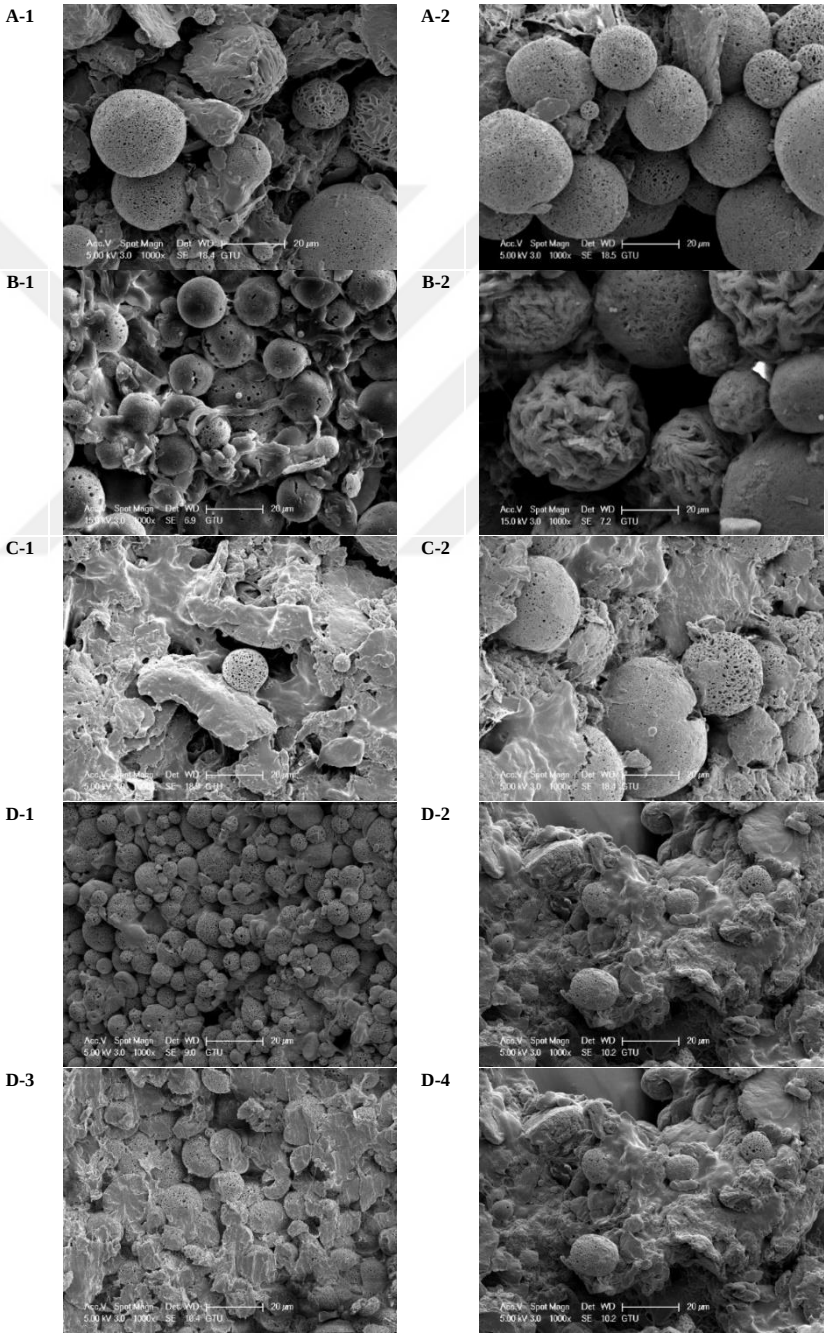

Figure 4.1 : SEM images of : PDL-VL, PDL-VL/Olu and TC-loaded PDL-VL/Olu microspheres (Magnification 1000x).

4.3.2 FT-IR results of microspheres

For further characterization, Olu, PDL-VL, PDL-VL/Olu microspheres, TC-loaded PDL-VL/Olu microspheres and TC were examined by FTIR analysis. Results of FTIR analysis are given in Figure 4.2. The peaks unique to the synthesized PDL-VL copolymers are: 2921 cm-1 and 2845 cm-1 peaks of the asymmetrical and symmetrical CH2 groups in their structures, 1726 cm-1 peaks caused by the C=O groups in the structure of both monomers, and 1290 cm-1 peaks caused by the C-O and C-C bonds in the monomers, 1162 cm-1 peaks caused by symmetrical C-O-C bonds. These peaks align with earlier scientific findings [90].

According to the scientific literature, oleuropein, like copolymers, produces vibration peaks of symmetrical and asymmetrical CH_2 groups at 2922 cm^{-1} and 2850 cm^{-1}, respectively, as well as vibration peaks of the C=O ester group at 1730 cm^{-1} [91]. For this reason, the peaks overlapped and no significant difference was observed. Oleuropein's FTIR spectrum shows a wide band at 3360 cm^{-1}, which indicates O-H stretching. The vibration signals for C-H stretching were seen at 2950 cm^{-1} and 2917 cm^{-1}. The signals at 1698 cm^{-1} and 1622 cm^{-1} indicate the vibration of oleuropein's two carbonyl groups. The signals at 1517 cm^{-1} for stretching and 1440 cm^{-1} for bending vibrations correspond to the functional groups C=C and O-H, respectively. Furthermore, an O-H bending vibration signal was detected at 1376 cm^{-1}. Strong stretching signals of C-O were found at 1256 cm^{-1}, 1192 cm^{-1}, 1158 cm^{-1}, 1068 cm^{-1}, and 1036 cm^{-1}. Signals at 918 cm^{-1} and 855 cm^{-1} showed C-C bending vibrations. Oleuropein has been reported to have FTIR values of 1440, 1575, and 1625 cm-1 [92].

For TC, the specific peaks identified were at 675-900 cm^{-1} (oop C-H bending, aromatic), 1011 cm^{-1} (in-plane C-H bending), 1400-1500 cm^{-1} (C-C stretching, aromatic), 1605 cm^{-1} (C=C), 1663 cm^{-1} (α, β unsaturation in ketones), and several peaks at 3030, 3052, and 3082 cm^{-1} (C-H, aromatic) [85].

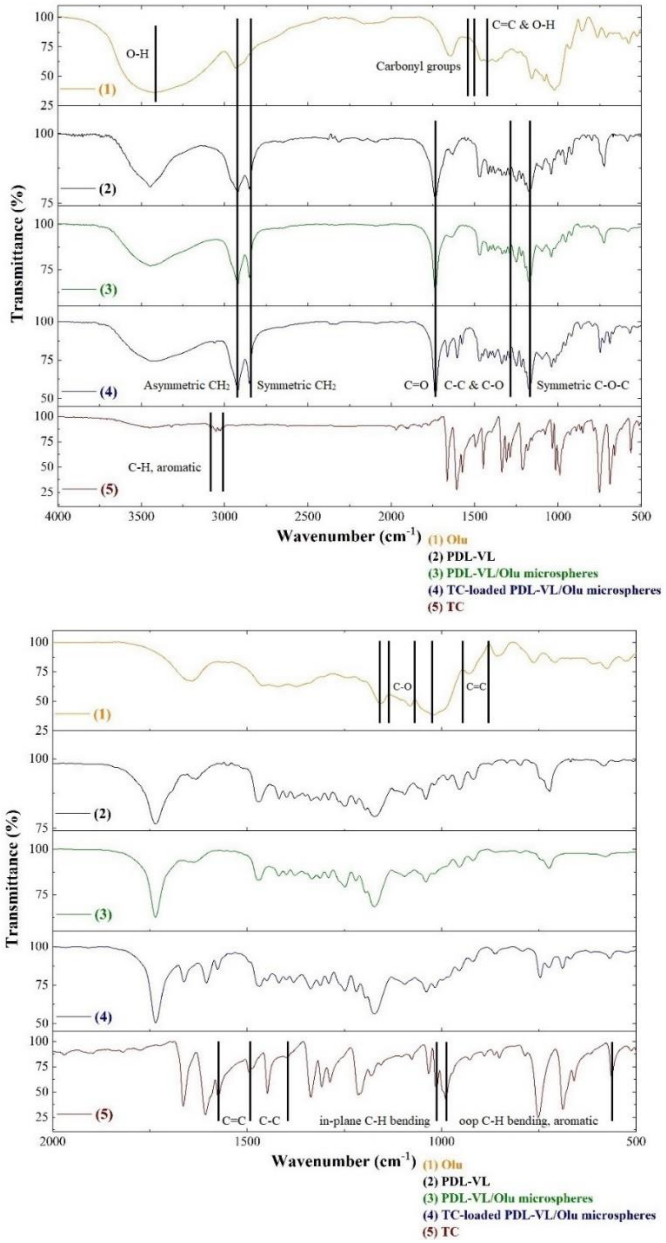

Figure 4.2 : FT-IR spectra of (1) Olu, (2) PDL-VL, (3) PDL-VL/Olu microspheres, (4) TC-loaded PDL-VL/Olu microsphes, (5) TC.

As a result, when looking at the FT-IR spectra results of TC-loaded PDL-VL/Olu microspheres, it was concluded that there was a change in the height of the peaks and therefore they were overlapped. No significant difference was observed. This result supports the findings of FT-IR spectra indicating that Olu added to the microspheres and TC was encapsulated in the microspheres.

4.3.3 DSC results of microspheres

DSC analysis was applied to observe the thermochemical changes in the PDL-VL structure after the addition of Olu and TC. The DSC curves in Figure 4.3 demonstrate

the melting temperatures of the samples. In the scientific literature, the T_m value of VL homopolymers is 53°C [51], whereas the T_m value of PDL homopolymers is 97°C [90]. If the T_m data are examined in this way, the T_m values of the copolymer samples fall between these levels, as predicted. The enthalpy values of PDL-VL powder, PDL-VL/Olu and TC-loaded PDL-VL/Olu microspheres were calculated as 117.3 J/g, 85.2 J/g and 120.6 J/g, respectively, from the areas below the melting peaks. The measured values are given in Table 4.3. It can be said that the T_m and enthalpy value increased with loaded TC. Additionally, it was observed that the addition of Oleuropein reduced the enthalpy value. However, it has increased the melting temperature.

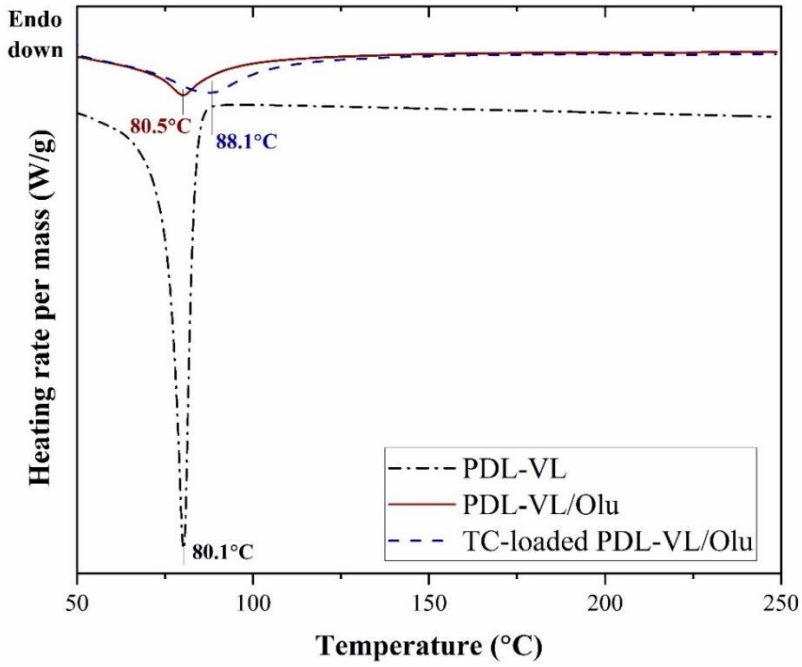

Figure 4.3 : Melting temperatures of samples: DSC second heating curves, PDL,VL, PDL-VL/Olu, TC-loaded PDL-VL/Olu.

Table 4.3 : T_m and enthalpy values of PDL-VL, PDL-VL/Olu and TC-loaded PDL-VL/Olu microspheres.

	T_m (℃)	ΔH_m (J/g)
PDL-VL	80.1	117.3
PDL-VL/Olu	80.5	85.2
TC-loaded PDL-VL/Olu	88.1	120.6

Scientific research revealed that oleuropein also had a crosslinking effect [93]. When DSC data are combined with the current investigation, the rise in melting temperature might be attributed to improved durability and thermal stability as a result of the crosslinking action given by oleuropein. The addition of oleuropein resulted in a

decrease in melting enthalpy, and the literature indicates that additional substances might reduce melting enthalpy and hence crystallinity [94, 95]. Furthermore, there was no extra melting peak associated with oleuropein, indicating that it was well absorbed and disseminated throughout the microspheres and amorphous structure [96]. In a previous study, the melting temperature of commercial TC was observed to be 59°C [85]. At the same time, in another scientific study, it was observed that the addition of TC to the copolymer increased the melting temperature [97]. The same behavior was observed in this study. Furthermore, since there was no extra melting peak associated with transchalone as it can be observed from the DSC analysis, it can be concluded that it was well absorbed and disseminated throughout the microspheres and amorphous structure [96]. Additionally, based on scientific articles, it can be deduced that transchalcon can be used as a thermal stabilizer [97].

4.3.4 TGA results of microspheres

TGA analyzes were applied in order to analyze the thermal degradation behavior of TC-loaded PDL-VL/Olu and PDL-VL/Olu microspheres and compare with PDL-VL. Thermal gravimetric analysis identifies melt-related processes. Weight loss occurs through several mechanisms, including dehydration, sublimation, evaporation, and reduction. Various elements, such as sample preparation, carrier size, furnace atmosphere, pressure, humidity, and temperature mode, might impact thermal analysis results and curve shapes [98]. If the TGA results shown in Figure 4.4 are evaluated, PDL-VL showed a single step degradation at 417.4 ^{0}C which is the main degredation temperature of the polymer, since there is no additional material. PDL-VL/Olu and TC-loaded PDL-VL/Olu samples decompose in 3 steps except water/solvent evaporation period. The loss of -2.7% is approximately the same for all 3 samples and similar scientific research have shown that water evaporation causes a mass change in the first step at these temperatures up to 100°C. [99]. It can be said that the last step is the main degradation step of the polymer. In the TC-loaded PDL-VL/Olu microsphere, a slight decrease was observed due to TC had lower decomposition peak [85]. The first degradation step of the PDL-VL/Olu sample starts earlier than the TC-loaded PDL-VL/Olu sample and occurs in a wider temperature range. However, it can be seen that at this stage, a lower part of it undergoes decomposition. The second decomposition step of this sample is also at a lower temperature, but the decomposed part is almost the same. There may be overlap in the degradation temperatures of the transchalcone

and oleuropein. Since the degradation temperature of the transchalcone is slightly higher, it may have increased the degradation temperatures of Steps 1 and 2, especially Step 1. According to the scientific investigations on oleuropein-doped zein nanofibers, the degradation of oleuropein was evaluated at 180°C, when a significant percentage of mass loss occurred [93]. Also commercial TC had decomposition peak at 227 °C, respectively [85]. Based on these scientific results, the decrease in the second stage degradation temperature following oleuropein addition is assumed to be attributable to oleuropein's lower degradation temperature when compared to the neat sample. According to Paulik and Erdey's scientific investigations [100], degradation happens swiftly when the intensity is high, and this information indicates that quicker degradation happened in the second stage due to the lower second step degradation temperature with the addition of oleuropein. Finally, the polymer degradation temperature of the neat sphere is higher than PDL-VL/Olu and TC-loaded PDL-VL/Olu microspheres because it is undoped. From this it can be concluded that the addition of additives reduces the decomposition temperature [101]. In addition, since higher percentage degradations were observed in the 1st and 2nd steps in the drug-loaded sample (since there is an additional drug additive to oleuropein), the degradation percentage of the main polymer is lower (52%) compared to the PDL-VL/Olu microspheres.

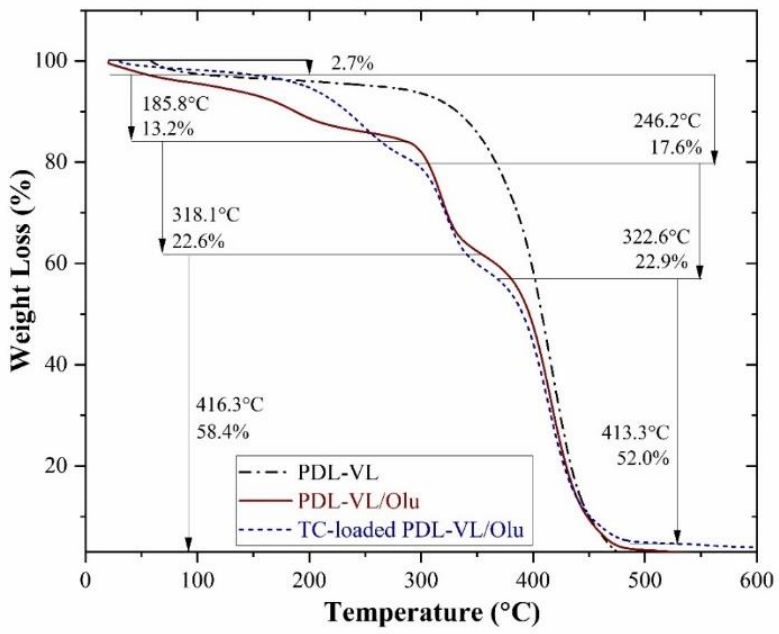

Figure 4.4 : TGA and derivative of weight losses results; PDL-VL (black), PDL-VL/Olu(red), TC-loaded PDL-VL/Olu (blue).

4.3.5 XRD results of microspheres

The effect of TC loading on crystallinity and crystalline structures of microspheres was investigated by XRD analysis. On the XRD analysis, PDL-VL copolymer, PDL-VL/Olu and TC-loaded PDL-VL/Olu microspheres were examined as it can be seen from Figure 4.5. X_c values was calculated according to Equation 3.9 which is given section 3.3.7 as 71.9, 50.3 and 41.3, respectively.

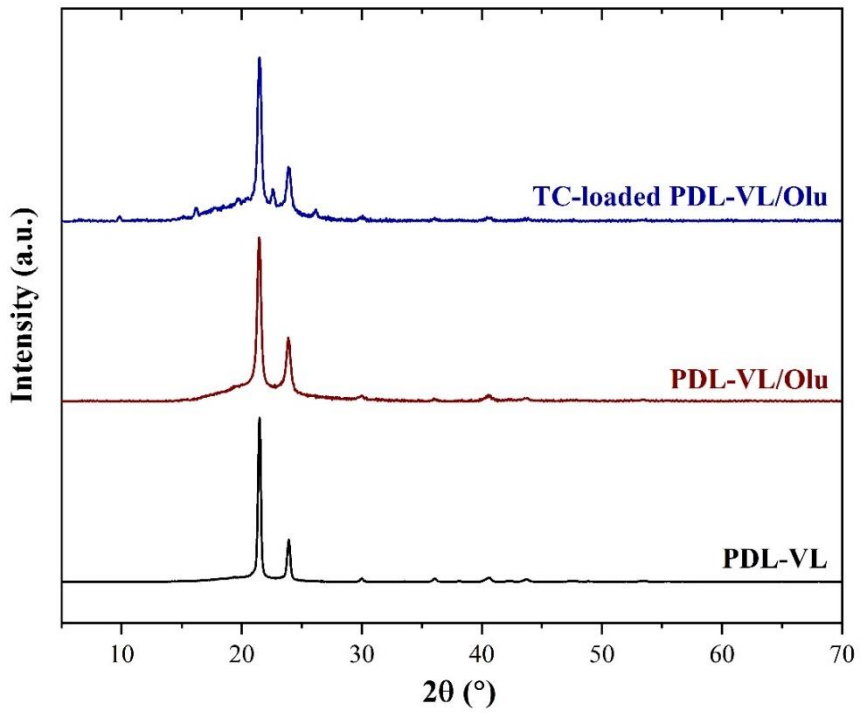

Figure 4.5 : XRD measurement of : TC-loaded PDL-VL/Olu (blue), PDL-VL/Olu (red), PDL-VL (black).

Both neat and TCH-loaded samples demonstrated two distinct diffraction peaks at 2θ = 21.4° and 23.9° which were belonged to poly(pentadecalactone-co-valerolactone) copolymer. As expected, the pure copolymer is polycrystalline, amorphism increases with the addition of oleuropein and TC. The intensity value of the crystalline peaks decreases and the spectrum becomes noisier. So crystallinity decreases. The crystalline peaks are as expected, and all of them are observed at the same value since they are crystalline polymers. Intensities of characteristic crystalline peaks were decreased after TC loading and there was no TC peak indicating that drug incorporated within the microspheres at amorphous state. Parallelly, degree of crystallinity (X_c) of drug-loaded microspheres (~41.3%) was lower than PDL-VL/Olu microspheres (X_c ~ 50.3%) and PDL-VL copolymers (X_c ~ 71.9%) which is consistent with DSC results.

4.4 Antibacterial Activity of Microspheres

Antibacterial activities of PDL-VL, PDL-VL/Olu and TC-loaded PDL-VL/Olu microspheres in 10^5 CFU/mL *S. Aureus* and *E. coli* cultures are shown in Figure 4.6. These activities were calculated using Equation 3.5 [102].

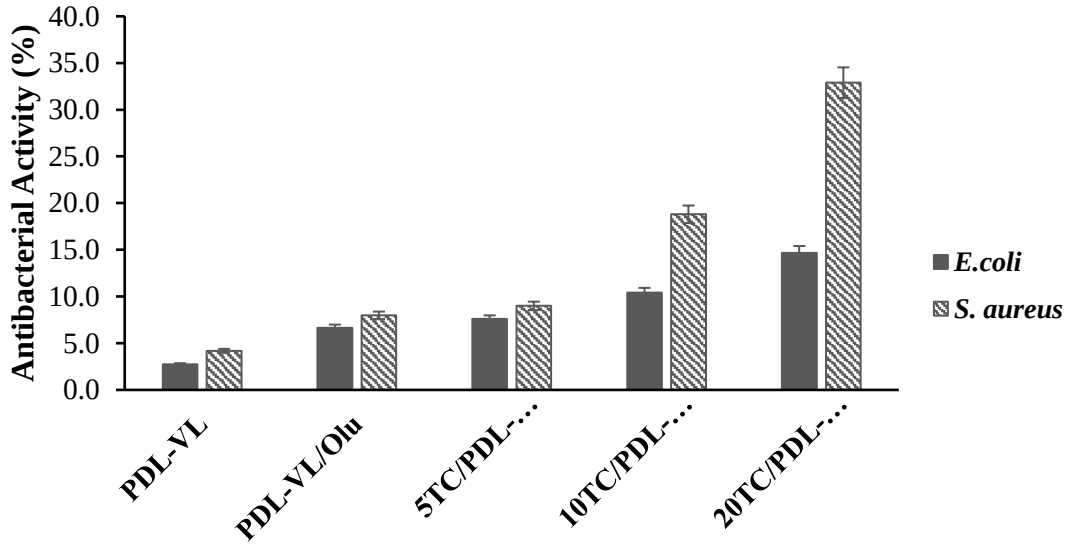

Figure 4.6 : Antibacterial activity(%) of PDL-VL, PDL-VL/Olu and TC-loaded PDL-VL/Olu microspheres in 10^5 CFU *S. aureus, E.coli* cultures.

To compare the antibacterial capabilities of PDL-VL, PDL-VL/Olu, and TC-loaded PDL-VL/Olu microspheres, one must first understand the taxonomic and morphological features of the bacteria utilized in antibacterial experiments.

Staphylococcus aureus (*S. Aureus*), was first found in the 1880s. Since then, it has been identified as a potentially pathogenic Gram-positive bacteria, causing mild skin infections and post-operative wound infections [103]. *S. Aureus*, is a well-known bacterial pathogen that causes both minor skin infections and serious, invasive infections worldwide. It is a leading cause of pneumonia, respiratory tract infections, surgical site, prosthetic joint, and cardiovascular infections, as well as nosocomial bacterialemia. Moderately severe skin infections caused by *S. aureus*, such as furuncles, abscesses, and wound infections, can cause substantial morbidity and suffering, but are often not life-threatening. They pose a significant public health burden due to their frequency (millions each year in the US) [104]. With the recent rise of antibiotic-resistant strains such as penicillin, methicillin, and vancomycin caused by diverse mutations, it has become increasingly pathogenic in nations such as Europe, the United States, and Australia. [105]. Plant-based antimicrobial drugs are

considered a significant benefit over synthetic antibiotics since they are biocompatible and bacteria cannot build resistance to them [106]. Given the previously mentioned advantages, plant-derived antibacterial compounds in microspheres are acknowledged as a potent therapeutic strategy against bacteria such as *S.aureus*, which frequently develops antibiotic resistance in academic studies [107]. Because of these characteristics, *S.aureus* is another gram-positive bacterium chosen for the antibacterial research of PDL-VL, PDL-VL/Olu and TC-loaded PDL-VL/Olu microspheres.

Escherichia coli, often known as *E. coli*, is a gram-negative bacteria that may be genetically altered both naturally and randomly. Sequenced *E. coli* genomes show diverse sizes and genetic diversity across commensals and pathogens, demonstrating a wide range within the bacterial species. These non-pathogenic bacteria can behave as commensals and are found in the normal gut microbiota of humans and animals [108]. *E.coli*, which possesses pathogenic subspecies, is responsible for the majority of food poisoning because to the release of many entretoxins [109]. *E.coli*, like *S. aureus*, are resistant to most antibiotics, including aminoglycosides and β-lactams [110]. As previously stated, it was believed that herbal extracts with antibacterial properties could also affect this pathogen due to its resistance to synthetic antibiotic groups; therefore, PDL-VL, PDL-VL/Olu and TC-loaded PDL-VL/Olu microspheres were included in the antibacterial tests alongside other bacterial species.

According to the sample codes specified in Table 4.2, actibacterial tests of the samples were carried out. Antibacterial activity test on *E. coli* and *S. aureus* cells for PDL-VL copolymer, PDL-VL/Olu microspheres containing 50 mg Olu and TC-loaded PDL-VL/Olu microspheres containing 5 mg, 10 mg and 20 mg TC, respectively, has been completed. Antibacterial activity (%) for *E. coli* and *S. Aureus* cells was calculated as for A-1 sample 2.7 and 4.2; D-1 sample 6.7 and 8.0; D-2 sample 7.6 and 9.0; D-3 sample 10.4 and 18.8; D-4 sample 14.7 and 32.9. As can be seen in Figure 4.6, *S.aureus* was more sensitive to oleuropein compared to *E.coli* species, and it was the species in which the most antibacterial activity was observed.

When the antibacterial properties of PDL-VL, PDL-VL/Olu and TC-loaded PDL-VL/Olu microspheres were examined in Figure 4.6, it was observed that the highest antibacteriality occurred at sample D-4 which has 50 mg Olu and 20 mg TC for both bacterial species. Due to its double lipid layer's antimicrobial resistance, *E. Coli*, a

Gram-negative bacterium, is assumed to have the lowest antibacterial activity of oleuropein [111]. Gram-positive Compared to E. coli, S. aureus shown less resistance to oleuropein, which led to increased antibacterial activity. This is believed to be the outcome of the taxonomic and morphological characteristics that are gram-positive. [107, 112]. Additionally, according to the scientific experiments in the literature, The compounds based on Chalcones were shown to have strong antibacterial properties and to be easily obtained by using the Claisen-Schmidt condensation approach to produce several skeletons of this group [113]. And in this experiment, it was observed that as the TC ratio increased, the antibacterial activity on both cells increased. Based on these findings, it was determined that PDL-VL/Olu and TC-loaded PDL-VL/Olu microspheres had antibacterial qualities. As a consequence, these microspheres can be employed to treat illnesses brought on by pathogens like *S. aureus* and *E. coli.*

4.5 In Vitro Cytotoxicity (WST) Test of Microspheres

In vitro cytotoxicity tests (WST) were performed by using the human breast cancer cell (MCF-7) of microspheres loaded with oleuropein at 1:1 (wt%) with copolymer concentrations also with TC 1:5 (wt%) with copolymer concentrations, where at concentrations likely to show the highest cytotoxicity was observed. Figure 4.7 shows the effects of microspheres with TC-loaded and Olu-contained concentrations. Analyzes were performed with a positive control in the presence of a substance with known toxic effects, and with a negative control in the presence of a substance that was not a sample and was only cells.

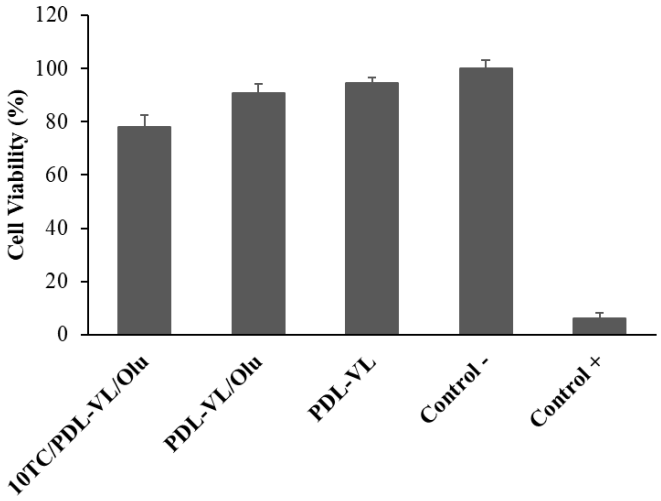

Figure 4.7 : Percentage cellular viability of MCF-7 breast cancer cells treated with TC loaded and Olu added microspheres at 72 hour periods.

According to the Figure 4.8 given above, cell viability (%) results were calculated as for TC 1:5 (wt%) loaded PDL-VL/Olu microspheres 78±4.5, for 1:1 (wt%) PDL-VL/Olu microspheres 90.7±3.5, for PDL-VL microspheres 94.4±2.2, for Control- 100±3.3 and for Control+ 6.0±2.1 by using Equation 3.6. After the 72 hours incubation, it can be said that there is slightly decrease on cell viability in onder to look at the sample of TC 1:5 (wt%) loaded PDL-VL/Olu comparing with others. In the medium containing 500 ug/ml sample concentration of PDL-VL, PDL-VL/Olu and TC-loaded PDL-VL microspheres at 72 hours, the cell viability was observed %94.4 for PDL-VL sample, %90.7 for PDL-VL/Olu sample and %78 for TC-loaded PDL-VL sample while it was %6 for Control+ sample. It can be deduced from this that TC-loaded microspheres can kill 22% of cells within 72 hours. As can be seen from this experiment, these results show that, as a result of WST cytotoxicity analyzes of microsphere samples, it leads to a reduction in the viability of human breast cancer cell lines (MCF-7), and therefore it is effective and promising for human breast cancer therapy.

4.6 pH Dependent Drug Release from Microspheres

The parameters of the release media have a substantial impact on the rate, quantity, and mechanism of drug release. One of these qualities is pH, which was examined for its implications on microsphere release.

In this work, two distinct pH values were used to imitate the circumstances of various sections of the human body and to investigate the release behavior of different amount of TC-loaded PDL-VL/Olu microspheres at pH 5.6 and 7.4 as it can be seen from Figure 4.8. (pH 7.4: level of healthy human body, pH 5.6: tumor cell microenvironment [114]). As mentioned before, microspheres containing Olu in different ratios were tested and it was observed that the optimum ratio was 100%. For this reason, this ratio was kept constant and drug release experiments were studied in PDL-VL/Olu microspheres to which different amounts of TC were loaded.

Firstly, for pH 7.4, it was observed that 'initial burst release' occurred during the first 24 hours. Initial burst release was observed as 17.4±0.1% in 20 mg TC loaded PDL-VL/Olu microspheres. In the other 2 samples, this rate is higher; 38.0±0.4% in the 5 mg TC loaded PDL-VL/Olu microsphere, and 41.7±0.2% in the 10 mg TC loaded PDL-VL/Olu microsphere. It was observed that the release profiles of 3 different PDL-

VL/Olu microspheres loaded with different amounts of TC were similar. The drug release behavior first started with an initial burst release and then continued with a gradual release. In the drug release experiments lasting 964 hours in total, it was concluded that the highest release percentage was %85.9±0.5 in the 10 mg TC loaded PDL-VL/Olu microsphere. The other two samples are as follows; %42.1±0.7 in 5 mg TC loaded PDL-VL/Olu microsphere and %47.1±0.2 in 20 mg TC loaded PDL-VL/Olu microsphere. From this, it can be deduced that in terms of drug release behavior, the most optimum TC value for PDL-VL/Olu microspheres containing 50 mg Olu with this pH and 50 mg copolymer is 10 mg.

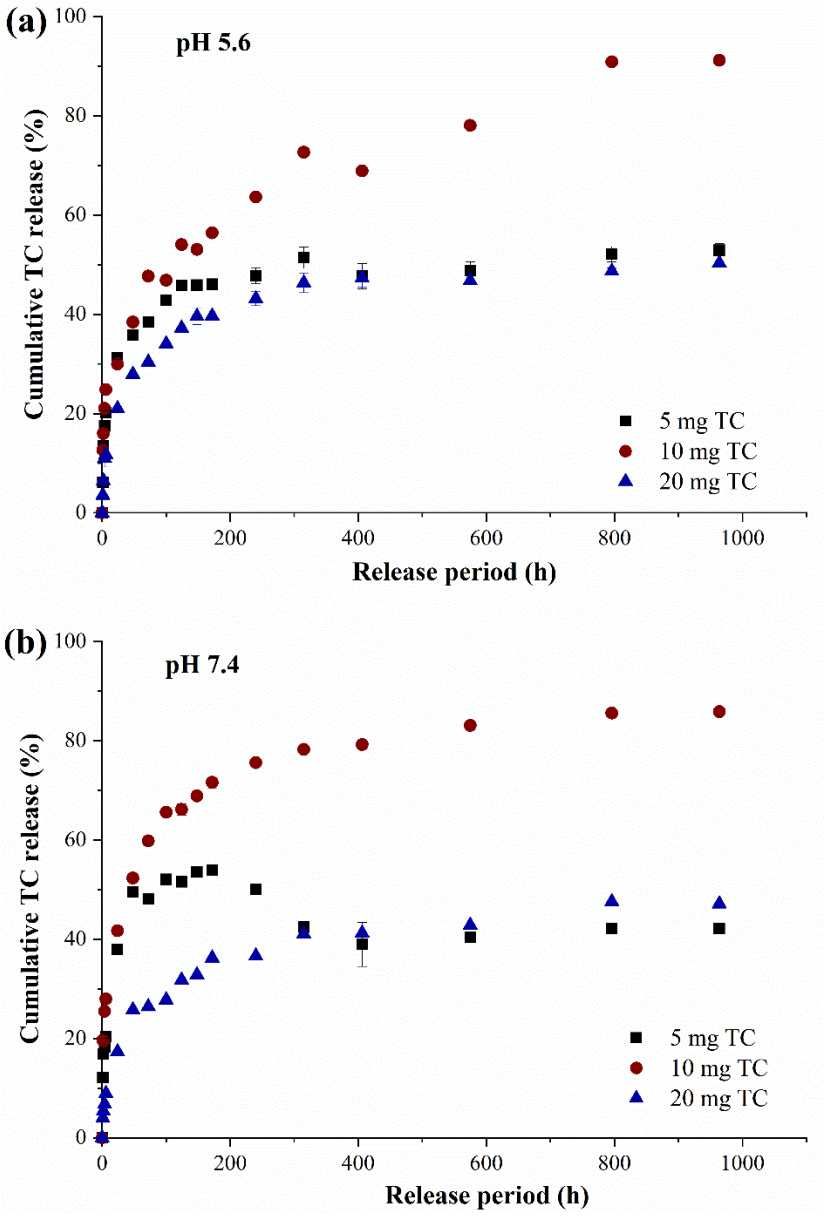

Figure 4.8 : Cumulative TC release (%) in two different pH media (pH 5.6 and pH 7.4) with different amount of TC-loaded PDL-VL/Olu microspheres.

Seconly, for pH 5.6, it was also observed that 'initial burst release' occurred during the first 24 hours. However, this time initial burst release behavior was limited to %25 for 3 different samples which are in 5 mg, 10 mg and 20 mg TC-loaded PDL-VL/Olu microspheres. Like for pH 7.4, the release profiles of 3 different PDL-VL/Olu microspheres loaded with different amounts of TC were similar. The drug release behavior first started with an initial burst release and then continued with a gradual release. In the drug release experiments lasting 964 hours in total, it was concluded that the highest release percentage was %91.2±0.3 in the 10 mg TC loaded PDL-VL/Olu microsphere. The other two samples are as follows; %52.9±1.3 in 5 mg TC loaded PDL-VL/Olu microsphere and %50.3±0.3 in 20 mg TC loaded PDL-VL/Olu microsphere. According to this values, it can again be concluded that in terms of drug release behavior, the most optimum TC value for PDL-VL/Olu microspheres containing 50 mg Olu with this pH and 50 mg copolymer is 10 mg.

When drug release behaviors at two pH values are compared, it can be concluded that the release percentages at pH 5.6 are higher than the release percentages at pH 7.4. It was observed that 5 and 10 mg TC loaded PDL-VL/Olu microspheres showed a higher burst release rate in pH 7.4 environment. It can be said that there is a more controlled release for these samples in the pH 5.6 environment. As the pH of the release medium was raised to neutral levels, cumulative release steadily reduced in order to compare acidic results. In line with this finding, a prior investigation on a hydrophobic drug found that reduced drug release in neutral or slightly basic media was due to drug molecules concentrated on the surface of the microspheres being more stable [85, 115]. The porosity of microspheres is crucial in drug release evaluations. Specifically, high porosity would result in an early burst release, whereas low porosity would result in persistent drug release [115]. To clarify the mechanism behind the initial burst and lag time, information on microsphere form and early release kinetics may be crucial. Drug release must be continuously monitored in order to get an accurate release rate profile. It can be seen from the previous study, drug release was monitored continuously by using High Pressure Liquid Chromatography (HPLC). That analysis demonstrated that the first burst was caused by a variety of causes. The first explosion has often been ascribed to the drug's quick release from the microspheres' surface in earlier accounts. But there is some ambiguity in the meaning of "surface drug." While some research defined "surface drug" as a social drug, other findings were ambiguous. These results

unequivocally demonstrated that the surface drug only contributed a portion of the first burst, regardless of how it was defined (that is, as a superficial drug or as a drug at the effective surface of microspheres) [116]. Novel drug delivery systems are a promising option for medication development in the biomedical industry because of their quick development time and affordable price. Targeted drug delivery systems, nanodrug delivery systems, slow- and controlled-release drug delivery systems, etc. are examples of new drug delivery technologies.

In order to reduce or eliminate the issues brought on by conventional medication therapy, sustained-release drug carriers are a crucial kind of drug delivery system. They also let pharmaceuticals operate more slowly in the blood, which is crucial for drug therapy. In general, a system that allows a medication to gradually enter the bloodstream to lower blood concentration and provide long-term continuous release of the drug is referred to as a "sustained release drug carrier." Slow-release drugs microspheres provide targeted therapy delivery at tumor locations while minimizing side responses. As a result, sustained-release drugs microspheres are critical to increasing the therapeutic efficacy of malignancy therapies. Sustained-release drug microspheres, as a kind of sustained-release drug carrier, have broad development prospects. There is optimism that the use of sustained-release medication microspheres in tissue engineering will grow in the future, and that their usefulness will extend as diverse fields advance [117]. For this purpose, microspheres showing controlled, gradual and long-term release behavior in this study will also be beneficial for future research.

4.7 Kinetic Modelling and Release Mechanism

The drug release profiles were fitted to two kinetic models which are Higuchi and Korsmeyer-Peppas mathematical models to better understand the process of drug release for each sample as it is described on the section 3.2.6. Figure 4.9 shows the computed parameters for the fitted kinetic model.

To compare of both kinetic models, it can be seen that the Korsmeyer-Peppas kinetic model had the higher correlation coefficient ($R^2 > 0.95$). The Korsmeyer-Peppas model was shown to have the greatest R^2 values (~0.98-0.99) for in vitro drug release profiles. This model determines the type of diffusion based on the release exponent (n) determined from the slope of the linearized equation (Equation (3.4)) [89].When drug

release is regulated mostly by Fickian diffusion, the n value for spherical geometries is less than 0.43 [118]. When the n value is between 0.43 and 0.85, the dominant release mechanism is anomalous transport or non-Fickian diffusion, which combines diffusion with polymer erosion. N values greater than 0.85 imply supercase-II transport, which is regulated by polymer chain erosion [119]. All of the microsphere formulations shown in the figure below have a n value less than 0.43.

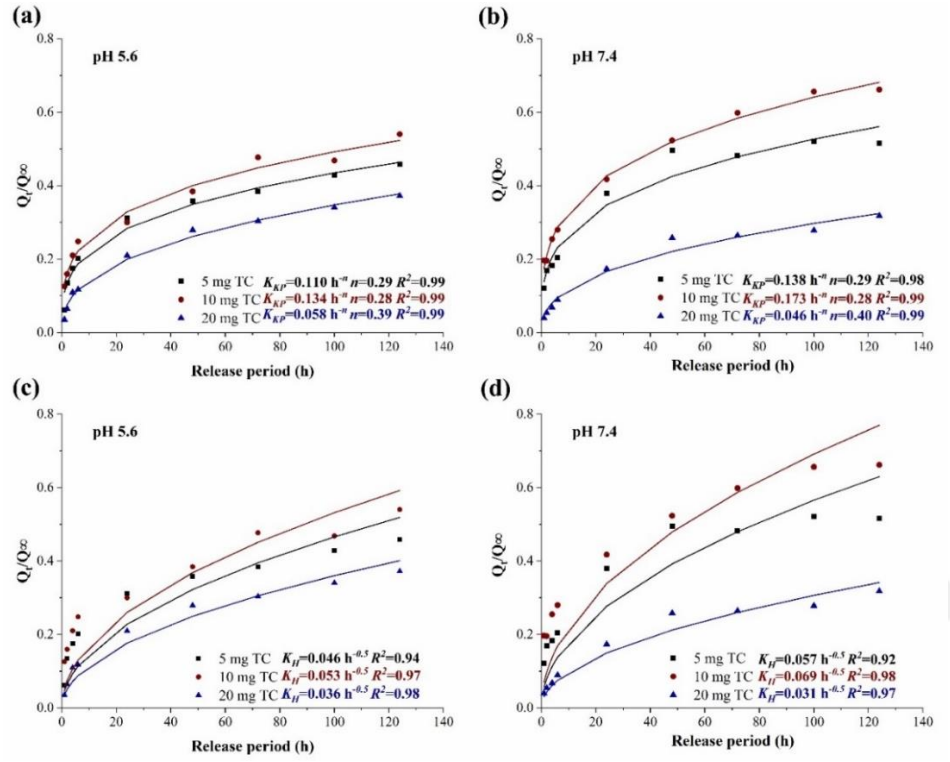

Figure 4.9 : Kinetic modelling and release mechanisms calculations in two different pH media (pH 5.6 and pH 7.4) with different amount of TC-loaded PDL-VL/Olu microspheres.

The computed n value revealed that TC release from all microsphere formulations was regulated by Fickian diffusion, and polymer erosion had no influence on the release. This data also shows that variations in the pH of the release media had no effect on the microsphere formulations' primary release mechanism. In conclusion, the Korsmeyer-Peppas model was found to be suitable for all samples and pH environments.

5. CONCLUSSION AND RECOMMENDATIONS

There are three stages to this study. The initial stage involved lipase immobilization on surface-modified RHA by physical adsorption. 3-APTES was utilized to add -NH_2 groups to the surface of the silica-based substance RHA, resulting in surface alteration. Following this process, the free form of CALB was immobilized by physical adsorption, as previously described [11]. In the second stage, a ω-pentadecalactone-co-δ-valerolactone copolymer was produced enzymatically using the monomer ratios from earlier research as a reference. The highest molecular weighted sample (M_n = 23722 g/mol) was obtained at 80°C and 24 hour reaction duration with 75% ω-pentadecalactone feed weight ratio and selected for microsphere formation. [37]. Therefore, in this work, ω-pentadecalactone-co-δ-valerolactone is synthesized utilizing these values. The sample was then determined to be employed in microsphere manufacture. In the third stage, oleuropein and transchalcone loaded microspheres were produced by O/W emulsion, and their chemical characterization, antibacterial and cytotoxic properties, the loading efficiency and in vitro release behavior. were investigated.

In the third stage of the study, oleuropein/transchalcone loaded PDL-VL microspheres was tried to be produced via O/W emulsion method. In order to determine the highest encapsulation efficiency and drug release behavior, combinations of 10, 20 and 40 percent TC, as well as 42.5, 75 and 100 percent Olu, in proportion to the copolymer mass were examined. At the same time, microsphere productions without the addition of TC or Olu and without both were also produced and examined. As can be seen in Table 4.2, it was determined that microspheres produced at 100% Olu:PDL-VL ratio and 20% TC:PDL-VL ratio (Sample D-3) had the highest encapsulation efficiency (%) which it was 81.7±0.5 (%). In experiments with other combinations, it was observed that the lowest encapsulation efficiency was 29.3±6.3 (%), and the second highest was 70.3±0.4 (%). It was observed that the encapsulation efficiency increased by increasing the Olu ratio from 42.5% to 100%, and at the same time, it was observed that the 100% Olu:PDL-VL ratio was kept constant and the TC:PDL-VL ratio increased the

encapsulation efficiency during the transition from 10% to 20%. The mean particle diameter was determined as 2.9±1.7 when TC and Olu were not present, and in the presence of 20% TC by mass, the mean particle diameter values of the microspheres increased suddenly and were seen as 8.5±4.5. On the contrary, when Olu was added at 42.5% and 75% by mass, the mean particle diameter values were found to be 2.0±2.0 and 0.5±0.2, respectively. From here, it can be concluded that TC loading significantly increases, and the addition of Olu also reduces the mean particle value. It has been observed that at lower mean particle size values, the encapsulation efficiency is higher and having a small particle size is a desired feature in microspheres. When Olu was added and TC was loaded to the microspheres, it was observed that the mean particle size value was lower comparing of they were added and loaded seperately. Zeta potential values were negative as expected. In particular, it was observed that the absolute Zeta potential value reached the highest level when 75% Olu by mass was added and 20% TC was loaded. After microspheres are made, several characterization analysis were applied such as SEM, DSC, TGA, FTIR and XRD in order to understand thermal, mechanical and morphological properties of PDL-VL, PDL-VL/Olu and TC-loaded PDL-VL/Olu microspheres.

DSC analysis was applied to observe the thermochemical changes of the copolymer and microspheres samples. Melting temperatures and enthalpy values of PDL-VL, PDL-VL/Olu and TC-loaded PDL-VL/Olu microspheres were examined according to the previous scientific studies. The fact that no melting peak was observed in both oleuropein and transchalcone samples indicates that PDL-VL/Olu and TC-loaded PDL-VL/Olu microspheres are properly dispersed into the structure as stated in the literature [96]. Additionally, based on scientific articles, it can be deduced that transchalcon can be used as a thermal stabilizer [97]. TGA analyzes were applied in order to analyze the thermal degradation behavior of TC-loaded PDL-VL/Olu and PDL-VL/Olu microspheres and compare with PDL-VL. Weight loses and decompositions were examined and explained according to the analysis obtained and from the literature. FT-IR was used as a characterization method to observe the chemical groups indicating the presence of Olu, TC, PDL-VL, PDL-VL/Olu and TC-loaded PDL-VL/Olu microspheres. All the characteristic peaks were examined and explained in the section 4.3.3. It was concluded that Olu was added to the microspheres and TC was encapsulated in the microspheres. In addition to all other analyses, the

influence of TC loading on crystallinity and crystalline structures of microspheres was examined using XRD analysis. The X_c values were determined, and distinctive crystalline peaks were investigated. The results were similar with those obtained from the DSC. It can be seen from the SEM images that spherical geometry was found in all microsphere formulations.

Antibacterial tests of PDL-VL, PDL-VL/Olu and TC-loaded PDL-VL/Olu microspheres were performed on gram positive *Staphylococcus aureus*, and gram negative *Escherichia coli* bacteria. Antibacterial activities (%) for all the samples were determined. It was observed that Olu has increased the antibacterial activity and also as the TC ratio increased, the antibacterial activity on both cells are increased. These results led to the conclusion that PDL-VL/Olu and PDL-VL/Olu microspheres loaded with TC have antibacterial properties. Consequently, diseases caused by pathogens such as S. aureus and E. coli can be treated using these microspheres.

The human breast cancer cell (MCF-7) and microspheres loaded with oleuropein at 1:1 (wt%) with copolymer concentrations and TC at 1:5 (wt%) with copolymer concentrations were used for in vitro cytotoxicity tests (WST), where the highest cytotoxicity was observed at these concentrations. And this experiment shows that as a result of WST cytotoxicity analyzes of microsphere samples, it leads to a reduction in the viability of human breast cancer cell lines (MCF-7), and therefore it is effective and promising for human breast cancer therapy.

In this study, pH dependent drug release experiments were performed with two pH values which was 5.6 and 7.4 in order to see drug release behaviour of microspheres produced with different environments. The microsphere formulations improved the total cumulative release of TC, which reached 91.2 % in pH 5.6 media and 85.9 % in pH 7.4 media. Comparing the drug release behaviors at two pH values, it can be seen that the pH 5.6 release percentages are greater than the pH 7.4 release percentages. In a pH 7.4 setting, it was shown that PDL-VL/Olu microspheres loaded with 5 and 10 mg of TC had a greater burst release rate. In the pH 5.6 condition, it might be claimed that these samples leak more subtly. The behavior of microspheres' release was based on pH; the more acidic the release medium, the greater the release. The higher solubility of TC resulting from the production of flavylium cations in acidic environments may be the reason of the increased TC release from the microspheres. In all cases, TC release was carried out for up to 964 hours. Lastly, the release kinetics

of the design points were investigated. When the release rate constants were assessed, it was discovered that the release suited the Korsmeyer-Peppas kinetic model, which had higher correlation coefficient ($R^2 > 0.95$) and the Korsmeyer-Peppas model was found to be suitable for all samples and pH environments. The computed n value revealed that TC release from all microsphere formulations was regulated by Fickian diffusion, and polymer erosion had no influence on the release. This data also shows that variations in the pH of the release media had no effect on the microsphere formulations' primary release mechanism. ($n < 0.43$)

In summary, the aim of this research is to create a novel drug delivery system by incorporating an antibacterial component into a bio-based polymeric framework. Microspheres will be created by manufacturing a biocompatible, non-toxic, high molecular weight copolymer with naturally immobilized enzymes that are compatible with the environment and the human body. The addition of an antibacterial ingredient to this product will allow for controlled drugs distribution adds durability to the material.. Thus, the drug's negative effects will be considerably decreased, while its therapeutic capabilities will be enhanced. The copolymer produced with a biocatalyst will be combined with trans-chalcone and/or oleuropein for medicinal purposes. Antibacterial and cytotoxicity tests showed that the microspheres were antibacterial due to the properties of the Olu additive and that it reduced the viability of cells on human breast cancer lines as a result of TC loading. TC-loaded PDL-VL/Olu microspheres have been shown to be attractive candidates for biomedical applications especially for human breast cancer therapy due to their high rates of drug release in inflammatory parameters. Because of its antibacterial qualities, oleuropein has been shown in the findings to be useful as a support for material durability and antibacteriality in microspheres. The utilization of diverse chemical active compounds, such as transchalcone and oleuropein in various types of carriers, has been shown to produce benefits in a variety of medical research, including anticancer trials. After all characterization analysis and drug release behaviour were obtained, it can be concluded that the the results of this study point to a potential use for microspheres in the long-term therapy of disease. And, undoubtedly, much more study will be required to assess cytotoxicity, cell survival, and in vivo pharmacokinetics.

REFERENCES

[1] **Engel, J., Cordellier, A., Huang, L., & Kara, S.** (2019). Enzymatic Ring-Opening Polymerization of Lactones: Traditional Approaches and Alternative Strategies. *ChemCatChem*, *11*(20), 4983–4997. https://doi.org/10. 1002/cctc.201900976

[2] **Yu, D., Zhang, X., Wang., T., Geng., H., Wang., L., Jiang., L., & Elfallah., W.** (2021). Immobilized Candida Antartica Lipase B (CALB) on functionalized MCM-41: Stability and catalysis of transesterification of syobean oil and phytosteral. *Food Bioscience*, 40. https://doi.org/10.1016/j.fbio.2021.100906

[3] **Ganesan, P., Johnson A. J. D., Sabapathy L., & Duraikannu, A.** (2014). *Am. J. Drug Disover. Dev*., 4(3), 153-179. https://doi.org/10.3923/ajdd.2014. 153.179

[4] **Rastogi, V., Shukla, S. S., Singh, R., Lal, N., & Yadav, P.** (2016). MICROSPHERES: A PROMISING DRUG CARRIER. *Journal of Drug Delivery and Therapeutics*, 6(3). https://doi.org/10.22270/jddt. v6i3.1196

[5] **Sharma., B., Singh I., Sharma J., Chaudhary., A., & Kumar., I.** (2022). *Ijppr.Human*, Vol. 24 (2): 47-67.

[6] **EMA** monograph, ed. Assessment report on olea europaea L., folium-. ; 2017.

[7] **Karković Marković, A., Torić, J., Barbarić, M., & Jakobušić Brala, C.** (2019). *Hydroxytyrosol, Tyrosol and Derivatives and Their Potential Effects on Human Health*. *Molecules*, *24*(10).

[8] **Huguet-casquero, A., Xu, Y., Gainza, E., Luis, J., & Beloqui, A.** (2020). Oral delivery of oleuropein-loaded lipid nanocarriers alleviates in fl ammation and oxidative stress in acute colitis. *International Journal of Pharmaceutics*, *586*(April), 119515. https://doi.org/10.1016/j.ijpharm. 2020.119515

[9] **Martinez, R. M., Pinho-Ribeiro, F. A., Vale, D. L., Steffen, V. S., Vicentini, F. T., Vignoli, J. A., Baracat, M. M., Georgetti, S. R., Verri, W. A., & Casagrande, R.** (2017). Trans-chalcone added in topical formulation inhibits skin inflammation and oxidative stress in a model of ultraviolet B radiation skin damage in hairless mice. *Journal of Photochemistry and Photobiology B: Biology*, 171, 139–146. https://doi.org/10.1016/ j.jphotobiol.2017.05.002

[10] **Piñero, J., Temporal, R. M., Silva-Gonçalves, A. J., Jiménez, I., Bazzocchi, I. L., Oliva, A., Perera, A., Leon, L. L., & Valladares, B.** (2006). New administration model of trans-chalcone biodegradable polymers for the treatment of experimental leishmaniasis. *Acta Tropica*, *98(1)*, 59–65. https://doi.org/10.1016/j.actatropica.2006.02.001

[11] **Ulker, C., Gokalp, N., and Guvenilir-Avcibasi, Y.,** (2016), "Immobilization of Candida antarctica lipase B (CALB) on surface-modified rice husk ashes (RHA) via physical adsorption and cross- linking methods", Biocatal. Biotransform., Vol 34, No. 4, 172-180.

[12] **Park, S. B., Lih, E., Park, K. S., Joung, Y. K., & Han, D. K.** (2017). Biopolymer-based functional composites for medical applications. *Progress in Polymer Science*, *68*, 77–105. https://doi.org/10.1016/j.progpolymsci.2016.12.003

[13] **Wu, S., Snajdrova, R., Moore, J. C., Baldenius, K., & Bornscheuer, U. T.** (2020). Biocatalysis: Enzymatic Synthesis for Industrial Applications. *Angewandte Chemie International Edition*, *60(1)*, 88–119. https://doi.org/10.1002/anie.202006648

[14] **Gorrasi, G., & Pantani, R.** (2013). Effect of PLA grades and morphologies on hydrolytic degradation at composting temperature: Assessment of structural modification and kinetic parameters. *Polymer Degradation and Stability*, 98(5), 1006–1014. https://doi.org/10.1016/j.polymdegradstab.2013.02.005

[15] **Smith, P. J., Wang, H. T., York, W. S., Peña, M. J., & Urbanowicz, B. R.** (2017). Designer biomass for next-generation biorefineries: leveraging recent insights into xylan structure and biosynthesis. *Biotechnology for Biofuels*, 10(1). https://doi.org/10.1186/s13068-017-0973-z

[16] **Gomes, S., Leonor, I. B., Mano, J. F., Reis, R. L., & Kaplan, D. L.** (2012). Natural and genetically engineered proteins for tissue engineering. *Progress in Polymer Science*, *37(1)*, 1–17. https://doi.org/10.1016/j.progpolymsci.2011.07.003

[17] **Kalia, S., Dufresne, A., Cherian, B. M., Kaith, B. S., Avérous, L., Njuguna, J., & Nassiopoulos, E.** (2011). Cellulose-Based Bio- and Nanocomposites: A Review. *International Journal of Polymer Science*, 1–35. https://doi.org/10.1155/2011/837875

[18] **Lisitsyn, A., Semenova, A., Nasonova, V., Polishchuk, E., Revutskaya, N., Kozyrev, I., & Kotenkova, E.** (2021). Approaches in Animal Proteins and Natural Polysaccharides Application for Food Packaging: Edible Film Production and Quality Estimation. *Polymers*, 1*3(10)*, 1592. https://doi.org/10.3390/polym13101592

[19] **Jamshidian, M., Tehrany, E. A., Imran, M., Jacquot, M., & Desobry, S.** (2010). Poly-Lactic Acid: Production, Applications, Nanocomposites, and Release Studies. *Comprehensive Reviews in Food Science and Food Safety*, *9(5)*, 552–571. https://doi.org/10.1111/j.1541-4337.2010.00126.x

[20] **Chandra, P., Enespa, Singh, R., & Arora, P. K.** (2020). Microbial lipases and their industrial applications: a comprehensive review. *Microbial Cell Factories*, *19(1)*. https://doi.org/10.1186/s12934-020-01428-8

[21] **Mendes, A. A., Freitas, L., de Carvalho, A. K. F., de Oliveira, P. C., & de Castro, H. F.** (2011). Immobilization of a Commercial Lipase from Penicillium camembertii (Lipase G) by Different Strategies. *Enzyme Research*, 1–8. https://doi.org/10.4061/2011/967239

[22] **Vanags, E., Abolins, A., & Cabulis, U.** (2022). Lipase Catalyzed Self-epoxidation of Tall Oil Fatty Acids in Batch and Continuous Flow Conditions. *Journal of Polymers and the Environment, 31(5),* 2166–2176. https://doi.org/10.1007/s10924-022-02739-0

[23] **Ulker, C.,** (2015). Immobilization of Lipase on an Inorganic Support Material and Polycaprolactone Synthesis, M.Sc. Thesis, ITU, Institute of Science and Technology, Istanbul.

[24] **Siódmiak, T., G. Haraldsson, G., Dulęba, J., Ziegler-Borowska, M., Siódmiak, J., & Marszałł, M. P.** (2020). Evaluation of Designed Immobilized Catalytic Systems: Activity Enhancement of Lipase B from Candida antarctica. *Catalysts, 10(8),* 876. https://doi.org/10.3390/catal10080876

[25] **Nguyen, H. H., & Kim, M.** (2017). An Overview of Techniques in Enzyme Immobilization. *Applied Science and Convergence Technology, 26(6),* 157–163. https://doi.org/10.5757/asct.2017.26.6.157

[26] **Maghraby, Y. R., El-Shabasy, R. M., Ibrahim, A. H., & Azzazy, H. M. E. S.** (2023). Enzyme Immobilization Technologies and Industrial Applications. *ACS Omega, 8(6),* 5184–5196. https://doi.org/10.1021/acsomega.2c07560

[27] **Mohidem, N. A., Mohamad, M., Rashid, M. U., Norizan, M. N., Hamzah, F., & Mat, H. B.** (2023). Recent Advances in Enzyme Immobilisation Strategies: An Overview of Techniques and Composite Carriers. *Journal of Composites Science, 7(12),* 488. https://doi.org/10.3390/jcs7120488

[28] **Brena, B., González-Pombo, P., & Batista-Viera, F.** (2013). Immobilization of Enzymes: A Literature Survey. *Methods in Molecular Biology,* 15–31. https://doi.org/10.1007/978-1-62703-550-7_2

[29] **Öztürk Düşkünkorur, H., Pollet, E., Phalip, V., Güvenilir, Y., & Avérous, L.** (2014). Lipase catalyzed synthesis of polycaprolactone and clay-based nanohybrids. *Polymer, 55(7),* 1648–1655. https://doi.org/10.1016/j.polymer.2014.02.016

[30] **Della, V., Kühn, I., & Hotza, D.** (2002) Rice husk ash as an alternate source for active silica production. *Materials Letters, 57(4),* 818–821. https://doi.org/10.1016/s0167-577x(02)00879-0

[31] **Rizki, K., Pranowo, D., & Joko Raharjo, T.** (2020). Immobilization of lipase in silica gel from rice husk ash and its activity assay to hydrolyze palm oil. *BIO Web of Conferences, 28,* 03005. https://doi.org/10.1051/bioconf/20202803005

[32] **Soltani, N., Bahrami, A., Pech-Canul, M., & González, L.** (2015). Review on the physicochemical treatments of rice husk for production of advanced materials. *Chemical Engineering Journal, 264,* 899–935. https://doi.org/10.1016/j.cej.2014.11.056

[33] **Spennato, M., Todea, A., Corici, L., Asaro, F., Cefarin, N., Savonitto, G., Deganutti, C., & Gardossi, L.** (2021). Turning biomass into functional composite materials: Rice husk for fully renewable immobilized biocatalysts. *EFB Bioeconomy Journal, 1,* 100008. https://doi.org/10.1016/j.bioeco.2021.100008

[34] **Mousavi, M., & Fini, E.** (2020). Silanization Mechanism of Silica Nanoparticles in Bitumen Using 3-Aminopropyl Triethoxysilane (APTES) and 3-Glycidyloxypropyl Trimethoxysilane (GPTMS). *ACS Sustainable Chemistry & Engineering, 8*(8), 3231–3240. https://doi.org/10.1021/acssuschemeng.9b06741

[35] **Sypabekova, M., Hagemann, A., Rho, D., & Kim, S.** (2022). Review: 3-Aminopropyltriethoxysilane (APTES) Deposition Methods on Oxide Surfaces in Solution and Vapor Phases for Biosensing Applications. *Biosensors, 13*(1), 36. https://doi.org/10.3390/bios13010036

[36] **Costantini, A., & Califano, V.** (2021). Lipase Immobilization in Mesoporous Silica Nanoparticles for Biofuel Production. *Catalysts, 11*(5), 629. https://doi.org/10.3390/catal11050629

[37] **Derviscemaloglu, M.,** (2023). Production of Antibacterial Biobased Blends for Biomedical Use, M.Sc. Thesis, ITU, Institute of Science and Technology, Istanbul.

[38] **de la Cruz-Martínez, F., Martínez de Sarasa Buchaca, M., del Campo-Balguerías, A., Fernández-Baeza, J., Sánchez-Barba, L. F., Garcés, A., Alonso-Moreno, C., Castro-Osma, J. A., & Lara-Sánchez, A.** (2021). Ring-Opening Copolymerization of Cyclohexene Oxide and Cyclic Anhydrides Catalyzed by Bimetallic Scorpionate Zinc Catalysts. *Polymers, 13*(10), 1651. https://doi.org/10.3390/polym13101651

[39] **Engel, J., Cordellier, A., Huang, L., & Kara, S.** (2019). Enzymatic Ring-Opening Polymerization of Lactones: Traditional Approaches and Alternative Strategies. *ChemCatChem, 11*(20), 4983–4997. https://doi.org/10.1002/cctc.201900976

[40] **Matsumura, S.** (2005). Enzymatic Synthesis of Polyesters via Ring-Opening Polymerization. *Enzyme-Catalyzed Synthesis of Polymers*, 95–132. https://doi.org/10.1007/12_030

[41] **Ulker Turan, C., & Guvenilir, Y.** (2018). Lipase-catalyzed synthesis and characterization of poly(Ω-pentadecalactone): an alternative aliphatic polyester to poly(ε-caprolactone). *New Biotechnology, 44,* S107. https://doi.org/10.1016/j.nbt.2018.05.999

[42] **Fernández, J., Etxeberria, A., Varga, A. L., & Sarasua, J. R.** (2015). Synthesis and characterization of ω-pentadecalactone-co-ε-decalactone copolymers: Evaluation of thermal, mechanical and biodegradation properties. *Polymer, 81,* 12–22. https://doi.org/10.1016/j.polymer.2015.11.001

[43] **Nuyken, O., & Pask, S.** (2013). Ring-Opening Polymerization—An Introductory Review. *Polymers, 5*(2), 361–403. https://doi.org/10.3390/polym5020361

[44] **Yu, D., Zhang, X., Wang, T., Geng, H., Wang, L., Jiang, L., & Elfalleh, W.** (2021). Immobilized Candida antarctica lipase B (CALB) on functionalized MCM-41: Stability and catalysis of transesterification of soybean oil and phytosterol. *Food Bioscience, 40*, 100906. https://doi.org/10.1016/j.fbio.2021.100906

[45] **McGinty, D., Letizia, C., & Api, A.** (2011). Fragrance material review on ω-pentadecalactone. *Food and Chemical Toxicology, 49*, S193–S201. https://doi.org/10.1016/j.fct.2011.07.026

[46] **Chang, Q., Li, L., Yang, D., Zhang, M., Ton-That, M. T., Hu, W., & Lü, S.** (2015). Synthesis and characterization of poly(ω-pentadecalactone) for its industrial-scale production. *Chemical Research in Chinese Universities, 31*(4), 640–644. https://doi.org/10.1007/s40242-015-5092-4

[47] **Letizia Focarete, M., Scandola, M., Kumar, A., & Gross, R. A.** (2001). Physical characterization of poly(ω-pentadecalactone) synthesized by lipase-catalyzed ring-opening polymerization. *Journal of Polymer Science Part B: Polymer Physics, 39*(15), 1721–1729. https://doi.org/10.1002/polb.1145

[48] **Yang, J., Jia, L., Hao, Q., Li, Y., Li, Q., Fang, Q., & Cao, A.** (2005). New Biodegradable Amphiphilic Block Copolymers of ε-Caprolactone and δ-Valerolactone Catalyzed by Novel Aluminum Metal Complexes. *Macromolecular Bioscience, 5*(9), 896–903. https://doi.org/10.1002/mabi.200500096

[49] **Harris, S. B., Tschirner, U. W., Gillespie, A., & Seeger, M. J.** (2018). Characteristic Properties of Novel Organosolv Lignin/Polylactide/Delta-Valerolactone Terpolymers. *Journal of Polymers and the Environment, 26*(8), 3262–3271. https://doi.org/10.1007/s10924-018-1212-9

[50] **Duale, K., Zięba, M., Chaber, P., Di Fouque, D., Memboeuf, A., Peptu, C., Radecka, I., Kowalczuk, M., & Adamus, G.** (2018). Molecular Level Structure of Biodegradable Poly(Delta-Valerolactone) Obtained in the Presence of Boric Acid. *Molecules, 23*(8), 2034. https://doi.org/10.3390/molecules23082034

[51] **Ulker, C., Gok, Z., & Guvenilir, Y.** (2019). Performance comparison of commercial and home-made lipases for synthesis of poly(δ-valerolactone) homopolymers. *Journal of Renewable Materials, 7*(4), 335–343. https://doi.org/10.32604/jrm.2019.03819

[52] **Harris, S. B., Tschirner, U. W., Gillespie, A., & Seeger, M. J.** (2018). Characteristic Properties of Novel Organosolv Lignin/ Polylactide/Delta-Valerolactone Terpolymers. *Journal of Polymers and the Environment, 26*(8), 3262–3271. https://doi.org/10.1007/s10924-018-1212-9

[53] **Gheorghita, R., Anchidin-Norocel, L., Filip, R., Dimian, M., & Covasa, M.** (2021). Applications of Biopolymers for Drugs and Probiotics Delivery. *Polymers, 13*(16), 2729. https://doi.org/10.3390/polym13162729

[54] **Gao, G., Wang, Y., Hua, H., Li, D., & Tang, C.** (2021). Marine Antitumor Peptide Dolastatin 10: Biological Activity, Structural Modification and Synthetic Chemistry. *Marine Drugs, 19*(7), 363. https://doi.org/10.3390/md19070363

[55] **Albro, M. B., Nims, R. J., Durney, K. M., Cigan, A. D., Shim, J. J., Vunjak-Novakovic, G., Hung, C. T., & Ateshian, G. A.** (2016). Heterogeneous engineered cartilage growth results from gradients of media-supplemented active TGF-β and is ameliorated by the alternative supplementation of latent TGF-β. *Biomaterials, 77*, 173–185. https://doi.org/10.1016/j.biomaterials.2015.10.018

[56] **Biswas, M. C., Jony, B., Nandy, P. K., Chowdhury, R. A., Halder, S., Kumar, D., Ramakrishna, S., Hassan, M., Ahsan, M. A., Hoque, M. E., & Imam, M. A.** (2021). Recent Advancement of Biopolymers and Their Potential Biomedical Applications. *Journal of Polymers and the Environment, 30*(1), 51–74. https://doi.org/10.1007/s10924-021-02199-y

[57] **He, L., Yan, X., Liang, J., Li, S., He, H., Xiong, Q., Lai, X., Hou, S., & Huang, S.** (2018). Comparison of different extraction methods for polysaccharides from Dendrobium officinale stem. *Carbohydrate Polymers, 198*, 101–108. https://doi.org/10.1016/j.carbpol.2018.06.073

[58] **Kakizawa, Y., Lee, J. S., Bell, B., & Fahmy, T. M.** (2017). Precise manipulation of biophysical particle parameters enables control of proinflammatory cytokine production in presence of TLR 3 and 4 ligands. *Acta Biomaterialia, 57*, 136–145. https://doi.org/10.1016/j.actbio.2017.01.025

[59] **Iordanidou, V., & De Potter, P.** (2004). Porous polyethylene orbital implant in the pediatric population. *American Journal of Ophthalmology, 138*(3), 425–429. https://doi.org/10.1016/j.ajo.2004.04.062

[60] **Ezike, T. C., Okpala, U. S., Onoja, U. L., Nwike, C. P., Ezeako, E. C., Okpara, O. J., Okoroafor, C. C., Eze, S. C., Kalu, O. L., Odoh, E. C., Nwadike, U. G., Ogbodo, J. O., Umeh, B. U., Ossai, E. C., & Nwanguma, B. C.** (2023). Advances in drug delivery systems, challenges and future directions. *Heliyon, 9*(6), e17488. https://doi.org/10.1016/j.heliyon.2023.e17488

[61] **Kumar, R., Saha, P., Sarkar, S., Rawat, N., & Prakash, A.** (2021). A review of drug delivery stestem. *International Journal of Research and Analytival Reviews (IJRAR) , 8*(1).

[62] **Van Gheluwe, L., Chourpa, I., Gaigne, C., & Munnier, E.** (2021) Polymer-Based Smart Drug Delivery Systems for Skin Application and Demonstration of Stimuli-Responsiveness. *Polymers, 13*(8), 1285. https://doi.org/10.3390/polym13081285

[63] **Prabahar, K., Alanazi, Z., & Qushawy, M.** (2021). Targeted Drug Delivery System: Advantages, Carriers and Strategies. *Indian Journal of Pharmaceutical Education and Research, 55*(2), 346–353. https://doi.org/10.5530/ijper.55.2.72

[64] **Jerbić, I. S..** (2018) Biodegradable Synthetic Polymers and their Application in Advanced Drug Delivery Systems (DDS). *Nano Tech Appl. 1*(1), 1-9.

[65] **Utrata-Wesołek, A., Trzebicka, B., Polaczek, J., Radecka, I., & Kowalczuk, M.** (2023). Polymeric Carriers for Delivery Systems in Biomedical Applications—In Memory of Professor Andrzej Dworak. *Indian Journal of Pharmaceutical Sciences, Polymers, 15*(8), 1810. https://doi.org/10.3390/polym15081810

[66] **Liechty, W. B., Kryscio, D. R., Slaughter, B. V., & Peppas, N. A.** (2010). Polymers for Drug Delivery Systems. *Annual Review of Chemical and Biomolecular Engineering, 1*(1), 149–173. https://doi.org/10.1146/annurev-chembioeng-073009-100847

[67] **Ravi, S., Peh, K., Darwis, Y., Murthy, B., Singh, T. R., & Mallikarjun, C.** (2008). Development and characterization of polymeric microspheres for controlled release protein loaded drug delivery system. *Indian Journal of Pharmaceutical Sciences, 70*(3), 303. https://doi.org/10.4103/0250-474x.42978

[68] **Jeong, S. Y., & Kim S., W.** (1986). Biodegradable Polymeric Drug Delivery Systems . *Arch. Pharm. Res. 9*(2), 63-73.

[69] **Deliormanli, A. M., & Yenice, A. C.** (2021). Preparation of hollow PCL microspheres by o/w single emulsion-solvent evaporation method in the presence of graphene nanopowders. *Express Polymer Letters, 15*(7), 641–653. https://doi.org/10.3144/expresspolymlett.2021.54

[70] **Raj, H., Sharma, S., Sharma, A., Verma, K. K., & Chaudhary, A.** (2021). A Novel Drug Delivery System: Review on Microspheres. *Journal of Drug Delivery and Therapeutics, 11*(2-S), 156–161. https://doi.org/10.22270/jddt.v11i2-s.4792

[71] **Yawalkar, A. N., Pawar, M. A., & Vavia, P. R.** (2022). Microspheres for targeted drug delivery- A review on recent applications. *Journal of Drug Delivery Science and Technology, 75*, 103659. https://doi.org/10.1016/j.jddst.2022.103659

[72] **K, A., Vineetha, K., Kamath K, K., & Shabaraya, A. R.** (2022). Microspheres as A Novel Drug Delivery System - A Review. *International Journal of Pharmaceutical Sciences Review and Research*, 160–166. https://doi.org/10.47583/ijpsrr.2022.v75i01.027

[73] **Freiberg, S., & Zhu, X.** (2004). Polymer microspheres for controlled drug release. *International Journal of Pharmaceutics, 282*(1–2), 1–18. https://doi.org/10.1016/j.ijpharm.2004.04.013

[74] **O'Donnell, P. B., & McGinity, J. W.** (1997). Preparation of microspheres by the solvent evaporation technique. *Advanced Drug Delivery Reviews, 28*(1), 25–42. https://doi.org/10.1016/s0169-409x(97)00049-5

[75] **Iqbal, M., Zafar, N., Fessi, H., & Elaissari, A.** (2015, December). Double emulsion solvent evaporation techniques used for drug encapsulation. International *Journal of Pharmaceutics, 496*(2), 173–190. https://doi.org/10.1016/j.ijpharm.2015.10.057

[76] **Liu, R., Ma, G., Meng, F. T., & Su, Z. G.** (2005). Preparation of uniform-sized PLA microcapsules by combining Shirasu Porous Glass membrane emulsification technique and multiple emulsion-solvent evaporation method. *Journal of Controlled Release*, *103*(1), 31–43. https://doi.org/10.1016/j.jconrel.2004.11.025

[77] **Kurrey, A., Suresh, P., & Singh, M.** (2014). Hollow microspheres as a drug carrier: An overview of fabrication and in vivo characterization techniques. *Chronicles of Young Scientists*, *5*, 1. https://link.gale.com/apps/doc/A363842861/HRCA?u=anon~a57eb1e7&sid=googleScholar&xid=9addd9a1

[78] **Kim, B. K., Hwang, S. J., Park, J. B., & Park, H. J.** (2002). Preparation and characterization of drug-loaded polymethacrylate microspheres by an emulsion solvent evaporation method. *Journal of Microencapsulation, 19*(6), 811–822. https://doi.org/10.1080/0265204021000022770

[79] **Haris Omar, S.** (2010). Oleuropein in Olive and its Pharmacological Effects. *Scientia Pharmaceutica, 78*(2), 133–154. https://doi.org/10.3797/scipharm.0912-18

[80] **Soler-Rivas, C., Espin, J.C., Wichers, H.J.** (2000). Review Oleuropein and related compounds. *Journal of the Science of Food and Agriculture, 80,* pp. 1013-1023

[81] **Omar, S. H.** (2010). Oleuropein in olive and its pharmacological effects. *Scientia Pharmaceutica*, *78*(2), 133–154. https://doi.org/10.3797/ scipharm. 0912-18

[82] **Aponte, J. C., Verástegui, M., Málaga, E., Zimic, M., Quiliano, M., Vaisberg, A. J., Gilman, R. H., & Hammond, G. B.** (2008). Synthesis, Cytotoxicity, and Anti-Trypanosoma cruzi Activity of New Chalcones. *Journal of Medicinal Chemistry, 51*(19), 6230–6234. https://doi.org/10.1021/jm800812k

[83] **Liu, H., Jiang, W., & Xie, M.** (2010). Flavonoids: Recent Advances as Anticancer Drugs. *Recent Patents on Anti-Cancer Drug Discovery, 5*(2), 152–164. https://doi.org/10.2174/157489210790936261

[84] **Kłósek, M., Kuropatnicki, A. K., Szliszka, E., Korzonek-Szlacheta, I., & Król, W.** (2017). Chalcones Target the Tumor Necrosis Factor–Related Apoptosis-Inducing Ligand (TRAIL) Signaling Pathway for Cancer Chemoprevention. *Nutrition and Functional Foods for Healthy Aging*, 233–244. https://doi.org/10.1016/b978-0-12-805376-8.00020-4

[85] **Kaptan, Y.,** (2022). Controlled delivery of Chalcone via Biopolyester Nanohybrid, *PhD. Thesis*, ITU, Institute of Science and Technology, Istanbul.

[86] **Ali, M. S., Elham, M., & Dhahiyah, M. S. I.** (2015). Spectrophometric Measurement of Solubility Test Turbidity as an Improved Diagnostic Tool for the Diagnosis of Sickle Cell Trait. *International Journal of Technical Research and Applications, 3*(1), 51–53.

[87] **Ahmad Sowhini, N., Abdullah Sani, M., Has-Yun Hashim, Y., Othman, R., Mahamad Maifiah, M., & Mohd Desa, M.** (2020). Antibacterial test and toxicity of plant seed extracts: a review. *Food Research, 4*(S1), 12–27. https://doi.org/10.26656/fr.2017.4(s1).s36

[88] **Nguyen, T. T. T., Chung, O. H., & Park, J. S.** (2011). Coaxial electrospun poly(lactic acid)/chitosan (core/shell) composite nanofibers and their antibacterial activity. *Carbohydrate Polymers*, *86*(4), 1799–1806. https://doi.org/10.1016/j.carbpol.2011.07.014

[89] **Ulker Turan, C., & Guvenilir, Y.** (2021). Fabrication and characterization of electrospun biopolyester/gelatin nanofibers. *Journal of Biomedical Materials Research - Part B Applied Biomaterials*, *109*(10), 1478–1487. https://doi.org/10.1002/jbm.b.34807

[90] **Ulker Turan, C., & Guvenilir, Y.** (2022). Electrospun poly(ω-pentadecalactone-co-ε-caprolactone)/gelatin/chitosan ternary nanofibers with antibacterial activity for treatment of skin infections. *European Journal of Pharmaceutical Sciences : Official Journal of the European Federation for Pharmaceutical Sciences*, *170*, 106113. https://doi.org/10.1016/j.ejps.2021.106113

[91] **Chiara Di Meo, M., Izzo, F., Rocco, M., Zarrelli, A., Mercurio, M., & Varricchio, E.** (2022). Mid-Infrared spectroscopic characterization: New insights on bioactive molecules of Olea europaea L. leaves from selected Italian cultivars. *Infrared Physics & Technology*, *127*, 104439. https://doi.org/10.1016/j.infrared.2022.104439

[92] **Genc, N., Yildiz, I., Chaoui, R., Erenler, R., Temiz, C., & Elmastas, M.** (2020). Biosynthesis, characterization and antioxidant activity of oleuropein-mediated silver nanoparticles. *Inorganic and Nano-Metal Chemistry*, *51*(3), 411–419. https://doi.org/10.1080/24701556.2020.1792495

[93] **Erdogan, I., Demir, M., & Bayraktar, O.** (2014). Olive leaf extract as a crosslinking agent for the preparation of electrospun zein fibers. *Journal of Applied Polymer Science, 132*(4). https://doi.org/10.1002/app.41338

[94] **Ainurofiq, A., Mauludin, R., Mudhakir, D., & Nurono Soewandhi, S.** (2018). The effect of compression on solid-state properties of desloratadine and multicomponent crystal. *Journal of Research in Pharmacy, 22*(1), 240–247. https://doi.org/10.12991/jrp.2018.99

[95] **Sena, S., Sumeyra, K. N., Ulkugul, G., Sema, A., Betul, K., Muge, S. B., Sayip, E. M., Muhammet, U., Cevriye, K., Mahir, M., Titu, M. A., Ficai, D., Ficai, A., & Gunduz, O.** (2019). Controlled Release of Metformin Hydrochloride from Core-Shell Nanofibers with Fish Sarcoplasmic Protein. *Medicina, 55*(10), 682. https://doi.org/10.3390/medicina55100682.

[96] **Chen, X., Li, H., Lu, W., & Guo, Y.** (2021). Antibacterial Porous Coaxial Drug-Carrying Nanofibers for Sustained Drug-Releasing Applications. *Nanomaterials, 11*(5), 1316. https://doi.org/10.3390/nano11051316

[97] **Olejnik, O., Masek, A., & Kiersnowski, A.** (2020). Thermal Analysis of Aliphatic Polyester Blends with Natural Antioxidants. *Polymers*, *12*(1), 74. https://doi.org/10.3390/polym12010074

[98] **Kojnoková, T., Markovičová, L., & Nový, F.** (2021). Application of thermal gravimetric analysis and comparison of polyethylene films before and after exposure in various chemical solutions. *IOP Conference Series: Materials Science and Engineering*, *1178*(1), 012029. https://doi.org/10.1088/1757-899x/1178/1/012029

[99] **Kenawy, E. R. S., Kamoun, E. A., Ghaly, Z. S., Shokr, A. B. M., El-Meligy, M. A., & Mahmoud, Y. A. G.** (2022). Novel Physically Cross-Linked Curcumin-Loaded PVA/Aloe vera Hydrogel Membranes for Acceleration of Topical Wound Healing: In Vitro and In Vivo Experiments. *Arabian Journal for Science and Engineering*, *48*(1), 497–514. https://doi.org/10.1007/s13369-022-07283-6

[100] **Erdey, L., Paulik, F., & Paulik, J.** (1954). Differential Thermogravimetry. *Nature*, *174*(4436), 885–886. https://doi.org/10.1038/174885b0

[101] **Radomska, E., Mika, L., & Sztekler, K.** (2020). The Impact of Additives on the Main Properties of Phase Change Materials. *Energies*, *13*(12), 3064. https://doi.org/10.3390/en13123064

[102] **Nguyen, T. T. T., Chung, O. H., & Park, J. S.** (2011). Coaxial electrospun poly(lactic acid)/chitosan (core/shell) composite nanofibers and their antibacterial activity. *Carbohydrate Polymers*, *86*(4), 1799–1806. https://doi.org/10.1016/j.carbpol.2011.07.014

[103] **Deurenberg, R. H., & Stobberingh, E. E.** (2008). The evolution of Staphylococcus aureus. *Infection, Genetics and Evolution*, *8*(6), 747–763. https://doi.org/10.1016/j.meegid.2008.07.007

[104] **Cheung, G. Y. C., Bae, J. S., & Otto, M.** (2021). Pathogenicity and virulence of Staphylococcus aureus. *Virulence*, *12*(1), 547–569. https://doi.org/10.1080/21505594.2021.1878688

[105] **Li, Z.** (2018). A Review of Staphylococcus aureus and the Emergence of Drug-Resistant Problem. *Advances in Microbiology*, *08*(01), 65–76. https://doi.org/10.4236/aim.2018.81006

[106] **Nazir, A.** (2020). A review: Use of plant extracts and their phytochemical constituents to control antibiotic resistance in S. aureus. *Pure and Applied Biology*, *9*(1). https://doi.org/10.19045/bspab.2020.90078

[107] **Beveridge, T. J., & Davies, J. A.** (1983). Cellular responses of Bacillus subtilis and Escherichia coli to the Gram stain. *Journal of Bacteriology*, *156*(2), 846–858. https://doi.org/10.1128/jb.156.2.846-858.1983

[108] **Braz, V. S., Melchior, K., & Moreira, C. G.** (2020). Escherichia coli as a Multifaceted Pathogenic and Versatile Bacterium. *Frontiers in Cellular and Infection Microbiology*, *10*. https://doi.org/10.3389/fcimb.2020.548492

[109] **Martín-Rodríguez, A. J., Joffré, E., & Sjöling, Å.** (2022). Bacterial Gastrointestinal Infections. In N. Rezaei (Ed.), *Encyclopedia of Infection and Immunity* (pp. 72–81). Elsevier. https://doi.org/https://doi.org/10.1016/B978-0-12-818731-9.00105-1

[110] **Galindo-Méndez, M.** (2020). Antimicrobial Resistance in Escherichia coli. https://doi.org/10.5772/intechopen.93115

[111] **Panawala, L.** (2017). Difference Between Gram Positive and Gram Negative Bacteria Stunning images of cells Discover how scientists use Main Difference – Gram Positive vs Gram Negative Bacteria. *Pediaa, 4*(April), 13.

[112] **Morão, L. G., Polaquini, C. R., Kopacz, M., Torrezan, G. S., Ayusso, G. M., Dilarri, G., Cavalca, L. B., Zielińska, A., Scheffers, D., Regasini, L. O., & Ferreira, H.** (2018). A simplified curcumin targets the membrane of Bacillus subtilis. *MicrobiologyOpen, 8*(4). https://doi.org/10.1002/mbo3.683

[113] **da Silva, L., Donato, I. A., Gonçalves, C. A. C., Scherf, J. R., dos Santos, H. S., Mori, E., Coutinho, H. D. M., & da Cunha, F. A. B.** (2022). Antibacterial potential of chalcones and its derivatives against Staphylococcus aureus. 3 *Biotech, 13*(1). https://doi.org/10.1007/s13205-022-03398-7

[114] **Gao, W., Chan, J. M., & Farokhzad, O. C.** (2010). pH-Responsive Nanoparticles for Drug Delivery. *Molecular Pharmaceutics, 7*(6), 1913–1920. https://doi.org/10.1021/mp100253e

[115] **Mamidi, N., Zuníga, A. E., & Villela-Castrejón, J.** (2020). Engineering and evaluation of forcespun functionalized carbon nano-onions reinforced poly (ε-caprolactone) composite nanofibers for pH-responsive drug release. *Materials Science and Engineering: C, 112*, 110928. https://doi.org/10.1016/j.msec.2020.110928

[116] **Wang, J., Wang, B. M., & Schwendeman, S. P.** (2002). Characterization of the initial burst release of a model peptide from poly(d,l-lactide-co-glycolide) microspheres. *Journal of Controlled Release, 82*(2–3), 289–307. https://doi.org/10.1016/s0168-3659(02)00137-2

[117] **Ruan, L., Su, M., Qin, X., Ruan, Q., Lang, W., Wu, M., Chen, Y., & Lv, Q.** (2022). Progress in the application of sustained-release drug microspheres in tissue engineering. *Materials Today Bio, 16*, 100394. https://doi.org/10.1016/j.mtbio.2022.100394

[118] **Permanadewi, I., Kumoro, A. C., Wardhani, D. H., & Aryanti, N.** (2019). Modelling of controlled drug release in gastrointestinal tract simulation. *Journal of Physics: Conference Series, 1295*(1), 012063. https://doi.org/10.1088/1742-6596/1295/1/012063

[119] **Ozsagiroglu, E., Iyisan, B., & Guvenilir, Y. A.** (2013). Comparing the in-vitro biodegradation kinetics of commercial and synthesized polycaprolactone films in different enzyme solutions. *Ekoloji, 96*(86), 90–96. https://doi.org/10.5053/ekoloji.2013.8611

APPENDICES

APPENDIX A: Calibration Curves

APPENDIX A: Calibration Curves

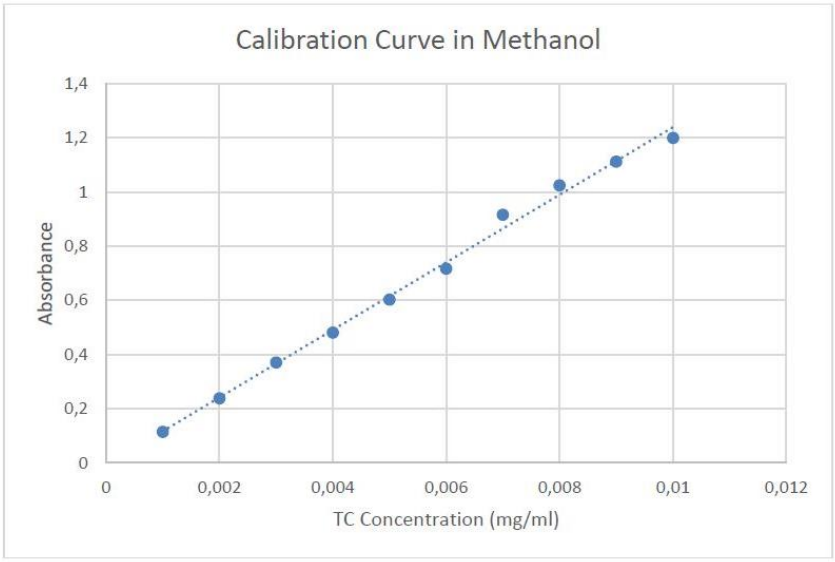

Figure A.1 : Calibration curve of TC in Methanol.

$$y = 124.72 \times x - 0.0084$$
$$R^2 = 0.9952$$

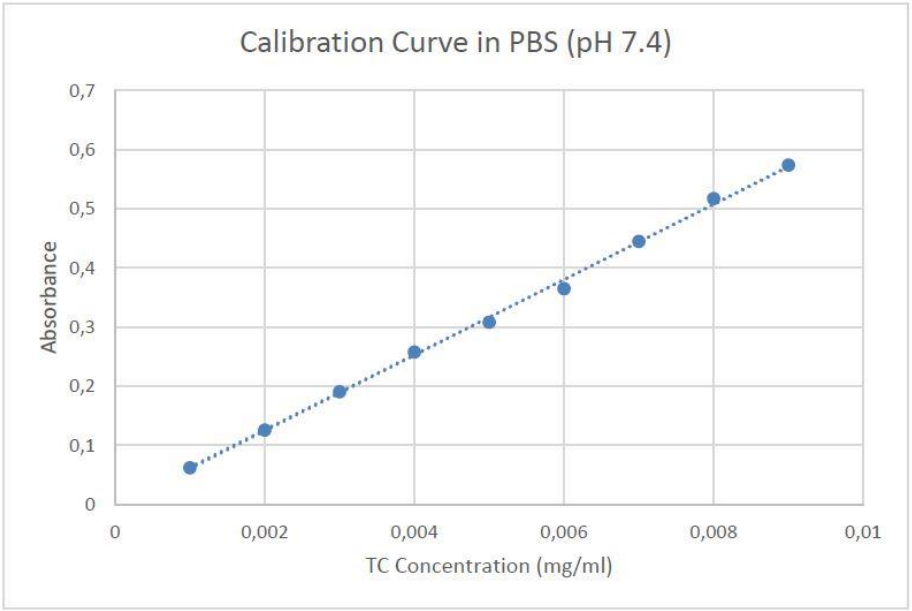

Figure A.2 : Calibration curve of TC in PBS (pH 7.4).

$$y = 63.95 \times x - 0.0036$$
$$R^2 = 0.9982$$

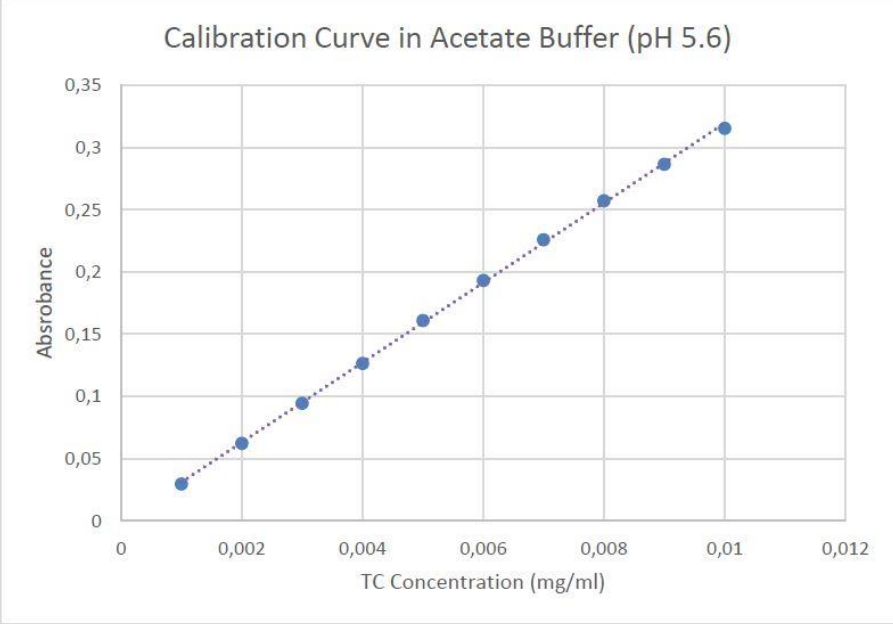

Figure A.3 : Calibration curve of TC in acetate buffer solution (pH 5.6).

$$y = 32.03 \times x - 0.0009$$
$$R^2 = 0.9995$$

CURRICULUM VITAE

Name Surname **:** Şenol BEYAZ

EDUCATION:

- **B.Sc.** **:** 2020, Kocaeli University, Faculty of Engineering, Deparment of Chemical Engineering.

PUBLICATIONS, PRESENTATIONS AND PATENTS ON THE THESIS:

- **Beyaz, S.,** Ulker Turan, C. and Guvenilir, Y. 2023: Biomedical Application of an Enzymatically Synthesized Biopolyester, International Graduate Research Symposium – IGRS'23, May 16-18, 2023, Turkey. (Abstract and Full Paper submitted, Oral presentation, Online conference)